

# DIFFUSIONAL FORMATION OF FERRITE IN IRON AND ITS ALLOYS

*H. K. D. H. Bhadeshia*

University of Cambridge, Department of Metallurgy and Materials Science,  
Pembroke Street, Cambridge CB2 3QZ, U.K.

*(Received 15 July 1985)*

## CONTENTS

NOMENCLATURE	322
ABBREVIATIONS	324
1. INTRODUCTION	324
2. CLASSIFICATION OF FERRITIC MICROSTRUCTURES	325
2.1. <i>Other Transformations in Steels</i>	327
3. MECHANISM OF DIFFUSIONAL TRANSFORMATION TO FERRITE	328
3.1. <i>The Influence of Interface Structure</i>	328
3.1.1. <i>Glissile interfaces</i>	329
3.1.2. <i>Epitaxial semi-coherency</i>	329
3.1.3. <i>Reconstructive diffusion</i>	330
3.1.4. <i>Incoherent interfaces</i>	331
3.1.5. <i>Experimental evidence on the <math>\gamma/\alpha</math> interface</i>	331
4. INTERFACE MOTION: RATE-CONTROLLING PROCESSES	332
5. DIFFUSION-CONTROLLED GROWTH	334
5.1. <i>Diffusion Coefficients</i>	334
5.1.1. <i>Diffusion in multicomponent systems</i>	335
5.1.2. <i>Diffusion in ternary Fe-X-C alloys</i>	336
5.1.3. <i>The diffusion of carbon in austenite</i>	338
5.2. <i>Diffusion-Controlled Growth of Ferrite in Fe-C Alloys</i>	339
5.3. <i>Diffusion-Controlled Growth of Ferrite in Fe-X-C Alloys: Local Equilibrium</i>	340
5.3.1. <i>Quantitative determination of the tie-line and interface velocity</i>	343
5.3.2. <i>Two- and three-dimensional growth with local equilibrium</i>	344
5.3.3. <i>Concentration dependent diffusion coefficients</i>	344
5.3.4. <i>Interface composition (IC) contours for diffusion-controlled growth</i>	345
5.3.5. <i>Interface velocity (IV) contours</i>	346
5.3.6. <i>Tie-line shifting due to soft impingement</i>	347
5.4. <i>Diffusion-Controlled Growth of Ferrite in Fe-X-C Alloys: Paraequilibrium</i>	349
5.4.1. <i>Solute and solvent trapping</i>	351
5.4.2. <i>The transition from local equilibrium to paraequilibrium</i>	352
6. INTERFACE-CONTROLLED GROWTH	353
6.1. <i>Pure Iron</i>	353
6.2. <i>Iron Alloys</i>	354
7. THE LEDGE MECHANISM OF INTERFACE MOTION	355
7.1. <i>Movement of an Isolated Ledge</i>	355
7.2. <i>Multistep Interactions</i>	358
7.3. <i>Ledge Motion in a Medium of Finite Extent</i>	359
7.4. <i>Relative Kinetics of Stepped and Continuous Growth</i>	360
8. SOLUTE-DRAG	360
8.1. <i>Conventional Solute-Drag Theories</i>	361
8.1.1. <i>Diffusion coefficients for solute-drag theory</i>	361
8.1.2. <i>Interaction free energy</i>	362
8.1.3. <i>Composition profile at the boundary</i>	362
8.1.4. <i>Drag at interphase-interfaces</i>	362

8.2. <i>Special Solute-Drag Effects</i>	363
8.2.1. <i>Interaction of carbide-forming elements with interfaces</i>	363
8.2.2. <i>The zero-segregation case</i>	363
8.2.3. <i>Special drag with segregation at the interface</i>	364
8.2.4. <i>Interaction of clusters with interfaces</i>	365
9. EXPERIMENTAL MEASUREMENTS OF GROWTH KINETICS	365
9.1. <i>The Thickening of Ferrite Allotriomorphs</i>	365
9.2. <i>The Lengthening of Ferrite Allotriomorphs</i>	369
9.3. <i>Summary</i>	369
10. MASSIVE FERRITE	370
10.1. <i>General Aspects of Massive Transformations</i>	370
10.2. <i>Massive Transformation in Iron and its Alloys</i>	372
11. ORIENTATION RELATIONSHIP BETWEEN AUSTENITE AND FERRITE	376
12. INTERPHASE PRECIPITATION	378
13. CONCLUSIONS	379
14. APPENDIX: DIFFUSION-CONTROLLED GROWTH OF WIDMANSTÄTTEN FERRITE	381
14.1. <i>Theory of Diffusion-Controlled Plate Growth</i>	381
ACKNOWLEDGEMENTS	383
REFERENCES	383

## NOMENCLATURE

Braces are used exclusively to denote functional relations;  $D\{x\}$  thus implies that  $x$  is an argument of the function  $D$ .

$a_i^\alpha$	Activity of $i$ in phase $\alpha$
$B_1$	Constant defined in eq. 5.19b
$B_2$	Constant defined in eq. 5.23
$B_3, B_4, B_5$	Mobility constants in interface-controlled growth, eq. 6.2
$c_i$	Concentration of component $i$ , moles per unit volume, also taken to be the concentration in the matrix at infinity
$\bar{c}_i$	Average concentration of $i$ in alloy, moles per unit volume
$c_i^\gamma$	Concentration of $i$ in $\gamma$ at $\gamma/\alpha$ interface, moles per unit volume
$c_i^\alpha$	Concentration of $i$ in $\alpha$ at $\alpha/\gamma$ interface, moles per unit volume
$c_{i\alpha}$	Concentration of $i$ in homogeneous phase $\alpha$ , moles per unit volume
$c_{i\gamma}$	Concentration of $i$ in homogeneous phase $\gamma$ , moles per unit volume
$c_i^{\gamma\alpha}$	Concentration of $i$ in $\gamma$ which is in equilibrium with $\alpha$ , moles per unit volume
$c_i^{\alpha\gamma}$	Concentration of $i$ in $\alpha$ which is in equilibrium with $\gamma$ , moles per unit volume
$C$	Euler's constant, 0.5772 . . .
$d$	Height of an isolated ledge or the leading ledge of a train
$d_l$	Height of trailing ledge divided by $d$
$d^*$	Critical height of ledge for successful nucleation
$\bar{D}_i$	Intrinsic diffusivity of component $i$
$D$	Chemical or interdiffusion coefficient for a binary solution
$D_{ik}$	Chemical or interdiffusion coefficient for ternary solution
$e_{ik}$	Wagner interaction parameter (eq. 5.8)
$E_1$	Function of $z$ , $D$ and $t$ , eq. 5.18c
$E_2$	Function of $z$ , $D$ and $t$ , eq. 5.20f
$E_3$	Function of $z$ , $D$ and $t$ , eq. 5.20g
$Ei$	Exponential integral function, Abramowitz and Stegun (1964)
$F, f$	Functions arising in diffusion-controlled growth theory, eq. 5.14
$f^*$	Attempt frequency for atomic jumps across interface, eq. 6.1
$f_i$	Fractional supersaturation of $i$
$F_1, F_2$	Functions of concentration, eqs 5.23e,f
$G^\alpha$	Molar Gibbs free energy of phase $\alpha$
$\Delta G^{\alpha\gamma}$	Molar Gibbs free energy change $G^\alpha - G^\gamma$ , for composition-invariant transformation
$\Delta G^*$	Molar Gibbs activation free energy
$G_i$	Molar Gibbs free energy dissipated in interface processes
$G_D$	Molar Gibbs free energy dissipated in diffusion of solute ahead of interface
$G_s$	Molar Gibbs free energy of interaction between interface and solute
$\Delta G_i^{\alpha\gamma}$	Molar Gibbs free energy change accompanying the $\gamma \rightarrow \alpha$ transformation in pure Fe
$G_i\{x, \bar{x}\}$	Molar Gibbs free energy corresponding to a point $x$ on a tangent at point $\bar{x}$ on the $\gamma$ free energy curve for Fe-C

$\Delta G' \{x, \bar{x}\}$	Molar Gibbs free energy change accompanying the transfer of a small amount of material of composition $x$ , from $\gamma$ of composition $\bar{x}$ , to $\alpha$ of composition $x$ in Fe-C
$\Delta G_v$	Gibbs free energy change per unit volume
$h$	Planck's constant
$h_1$	Separation of leading and trailing ledges in a two-step train, divided by the height of the leading ledge
$H_1$	Function arising in diffusion-controlled growth theory, eq. 5.13b
$H_2$	Function arising in diffusion-controlled growth theory, eq. 5.20c
$H_3$	Function of $p$ , arising in theory of ledge growth, eq. 7.2h
$H_4$	Function of $p$ , for ledge growth in a finite medium, eq. 7.9a
$H_5$	Function of $L$ , for ledge growth in a finite medium, eq. 7.9a
$i$	Subscript identifying element; $i = 1, 2, 3$ for C, substitutional alloying element and Fe respectively
$J_b$	Flux of solute across boundary, eq. 6.2
$\bar{J}_i$	Diffusion flux of $i$ , relative to Kirkendall frame of reference
$J_i$	Diffusion flux of $i$ , relative to the volume-fixed, number-fixed or laboratory frame of reference
$k$	Boltzmann's constant
$K_0$	Modified Bessel function of zero order
$K_{ij}$	Phenomenological coefficients of the Onsager theory, relative to the Kirkendall frame of reference
$L$	Extent of $\gamma$ in direction of interface motion
$L_{ij}$	Phenomenological coefficients of the Onsager theory
$M$	Interface mobility, eq. 7.2b
$M_s$	Martensite-start temperature
$n$	Time exponent in the relation $Z = \alpha_1 t^n$
$n_s$	Number of ledges per unit length
$p$	Péclet number, a dimensionless velocity, eq. 7.2c
$P$	Drag force in solute-drag theory
$q$	Interface mobility parameter, eq. 7.6b
$r$	Tip radius of ferrite plate
$r_c$	Critical tip radius for ferrite plate, at which $V_1 = 0$
$R$	Gas constant
$t$	Time
$t_1$	Time at the onset of carbon soft impingement, eq. 5.23c
$t_2$	Time for completion of second stage of soft impingement, eq. 5.23b
$T$	Absolute temperature
$T_a$	$T$ at which a thermal arrest is observed during continuous cooling
$T_0$	Temperature at which parent and product phases of identical composition have the same free energy
$v$	Rate at which a planar interface moves
$v_k$	Velocity of Kirkendall markers
$v_s$	Step velocity
$V_1$	Lengthening rate of Widmanstätten ferrite
$V_m$	Molar volume of ferrite
$\bar{V}_i$	Partial molar volume of component $i$
$W$	Number of nearest-neighbour octahedral interstitial sites surrounding a given octahedral interstice in $\gamma$
$x_i$	Mole fraction of component $i$
$\bar{x}_i$	Average mole fraction of component $i$ in alloy, also taken to be the concentration in the matrix at infinity
$x_i^\gamma$	Mole fraction of component $i$ in phase $\gamma$ at $\gamma/\alpha$ interface
$x_i^\alpha$	Mole fraction of component $i$ in phase $\alpha$ at $\gamma/\alpha$ interface
$x_{i\alpha}$	Mole fraction of component $i$ in homogeneous phase $\alpha$
$x_{i\gamma}$	Mole fraction of component $i$ in homogeneous phase $\gamma$
$x_i^{\gamma\alpha}$	Mole fraction of $i$ in $\alpha$ which is in equilibrium with $\gamma$
$x_i^{\alpha\gamma}$	Mole fraction of $i$ in $\gamma$ which is in equilibrium with $\alpha$
$\Delta x$	Composition difference between $\alpha$ and $\gamma$ remote from interface
$\Delta x_f$	$x_i^\alpha - x_i^\gamma$
$\Delta x_w$	$x_i^{\alpha\gamma} - x_i^{\gamma\alpha}$
$\Delta x_D$	$\bar{x}_i - x_i^\alpha$
$x_r$	Mole fraction of carbon in $\gamma$ which is in constrained equilibrium with $\alpha_w$ whose plate tip radius is $r$
$X$	Substitutional alloying element
$X_i$	Generalised force of Onsager's theory
$y$	Co-ordinate normal to step face
$y'$	Moving co-ordinate attached to step, normal to step face

$z$	Co-ordinate normal to interface plane
$z'$	Moving co-ordinate attached to step, normal to stationary part of a stepped interface
$z_{id}$	Effective diffusion distance for component $i$
$Z$	Position of interface along co-ordinate $z$
$\alpha$	Ferrite
$\alpha_w$	Widmanstätten ferrite
$\alpha_1, \alpha_2, \alpha_3$	Parabolic thickening rate constant for one, two and three dimensional growth, respectively
$\gamma$	Austenite
$\Gamma_i$	Activity coefficient of $i$
$\Gamma_m$	Activity coefficient arising in absolute reaction rate theory, eq. 5.11
$\eta$	Function of carbon concentration in $\gamma$ , eq. 5.11
$\eta_i$	Rate constant for growth controlled by diffusion of $i$
$\theta$	Interstitial to substitutional atom ratio $x_1/(1-x_1)$
$\delta_b$	Thickness of interface
$\lambda$	Spacing of $\{002\}_\gamma$ planes
$\phi$	Ensemble average interstitial site exclusion parameter
$\sigma$	Interface energy per unit area
$\mu_i^\alpha$	Chemical potential of $i$ in phase $\alpha$
$\omega_\gamma$	Nearest-neighbour carbon-carbon interaction energy in austenite

### ABBREVIATIONS

BCC	Body-centred cubic
FCC	Face-centred cubic
IPS	Invariant-plane strain
IC	Interface composition contour
IV	Interface velocity contour
KS	Kurdjumov-Sachs orientation relationship
NPLe	Negligible partitioning, local equilibrium
NW	Nishiyama-Wasserman orientation relationship
PLE	Partitioning, local equilibrium
THEEM	Thermionic electron emission microscope
TTT	Time-temperature-transformation
Ae3	Upper temperature limit of the $\alpha + \gamma$ phase field
Ae1	Lower temperature limit of the $\alpha + \gamma$ phase field

## 1. INTRODUCTION

At atmospheric pressure and at temperatures between 1185 K and 1655 K, pure iron exists as a face-centred cubic (FCC) arrangement of iron atoms. Unlike other FCC metals, lowering the temperature leads to the formation of a less dense, body-centred cubic (BCC) allotrope of iron. This change in crystal structure can occur in at least two different ways. Given sufficient atomic mobility, the FCC lattice can undergo complete *reconstruction* into the BCC ferrite form, with considerable unco-ordinated, diffusive mixing-up of atoms at the transformation interface. On the other hand, if the FCC phase is rapidly cooled to a very low temperature, well below 1185 K, there may not be enough time or atomic mobility to facilitate diffusional transformation. The driving force for transformation nevertheless increases with undercooling below 1185 K, and the diffusionless formation of BCC martensite eventually occurs, by a *displacive* or 'shear' mechanism involving the systematic and co-ordinated transfer of atoms across the interface. This formation of BCC martensite is indicated by a very special change in the shape of the transformed region, a change of shape which is beyond that expected on the basis of a volume change effect alone. The shape change is in fact an invariant-plane strain (IPS) with a significant shear component.

When interstitial and substitutional alloying additions are made to pure iron, many subtle variations of the displacive and diffusional mechanisms arise, together with the possibility of

other phases and morphological variations. The versatility of steels depends to a large extent on this wide variety of microstructures that can be obtained by transformation from austenite ( $\gamma$ ). The microstructure varies not just in morphology, but in phase composition, defect structure, stored energy and thermodynamic stability. This review deals specifically with the ferrite ( $\alpha$ ) which forms from  $\gamma$  by a diffusional transformation mechanism. The aim is to present a reasonably complete account of the theory and experimental data on the diffusional formation of ferrite in low-alloy steels. It is hoped that this work complements and updates the classical reviews of Aaronson (1962), Aaronson *et al.* (1970), Coates (1973b), Honeycombe (1976) and De Hoff (1981).

## 2. CLASSIFICATION OF FERRITIC MICROSTRUCTURES

Ferrite which grows by a diffusional mechanism can be classified into two main forms: allotriomorphic ferrite and idiomorphic ferrite (Dubé, 1948; Aaronson, 1955; Dubé *et al.*, 1958). The term 'allotriomorphic' means that the phase is crystalline in internal structure but not in outward form. It implies that the limiting surfaces of the crystal are not regular and do not display the symmetry of its internal structure (Christian, 1975). Thus, allotriomorphic ferrite (Fig. 1a) which nucleates at prior austenite grain boundaries tends to grow along the  $\gamma$  boundaries at a rate faster than in the direction normal to the boundary plane, so that its shape is strongly influenced by the presence of the boundary and hence does not necessarily reflect its internal symmetry. Of course, allotriomorphic ferrite need not form just at  $\gamma$  boundaries, but it invariably does so, presumably because there are no other suitable (two-dimensional) heterogeneous nucleation sites in austenite.

The term idiomorphic implies that the phase concerned has faces belonging to its crystalline form; in steels, idiomorphic ferrite is taken to be that which has a roughly equiaxed morphology (Fig. 1b). Idiomorphic ferrite usually forms intragranularly (Dubé, 1948), presumably at inclusions or other heterogeneous nucleation sites.

Both of these morphological definitions are subject to the condition that neither hard impingement (physical impingement between adjacent grains) nor soft impingement (overlap of diffusion or temperature fields of nearby grains) effects exist. The definitions also have to be loosely interpreted. In particular, they refer to a macroscopic scale of observation, such as by optical microscopy. For example, allotriomorphic ferrite is sometimes crystallographically faceted even though this may not be apparent on an optical scale. Similarly, with idiomorphic ferrite we do not really know whether the morphology reflects the internal form of ferrite—it is more likely to reflect the symmetry of the  $\gamma$ - $\alpha$  bicrystal (Cahn and Kalonji, 1981). In fact, the ability of any growing precipitate to form facets depends not just on the orientation dependence of interface energy but also on the driving force for transformation (Cahn, 1960). In principle,  $\alpha$  formed at high temperatures (low supersaturations) could appear faceted while that formed at lower temperatures may not.

Since both idiomorphic and allotriomorphic ferrite grow by a diffusional transformation mechanism, their growth is not restricted by austenite grain boundaries. The extent of penetration into particular grains may vary since interface mobility can change with the  $\alpha/\gamma$  orientation relationship. Massive ferrite, which also grows by a diffusional transformation mechanism, has the distinction that it inherits the composition of the parent austenite. The ability to cross parent austenite grain boundaries is particularly pronounced during massive transformation; the final ferrite grain size can be larger than the initial grain size of the  $\gamma$ . The lack of a composition change allows the transformation to proceed until all of the austenite is consumed. These factors combine to give a single-phase microstructure of large

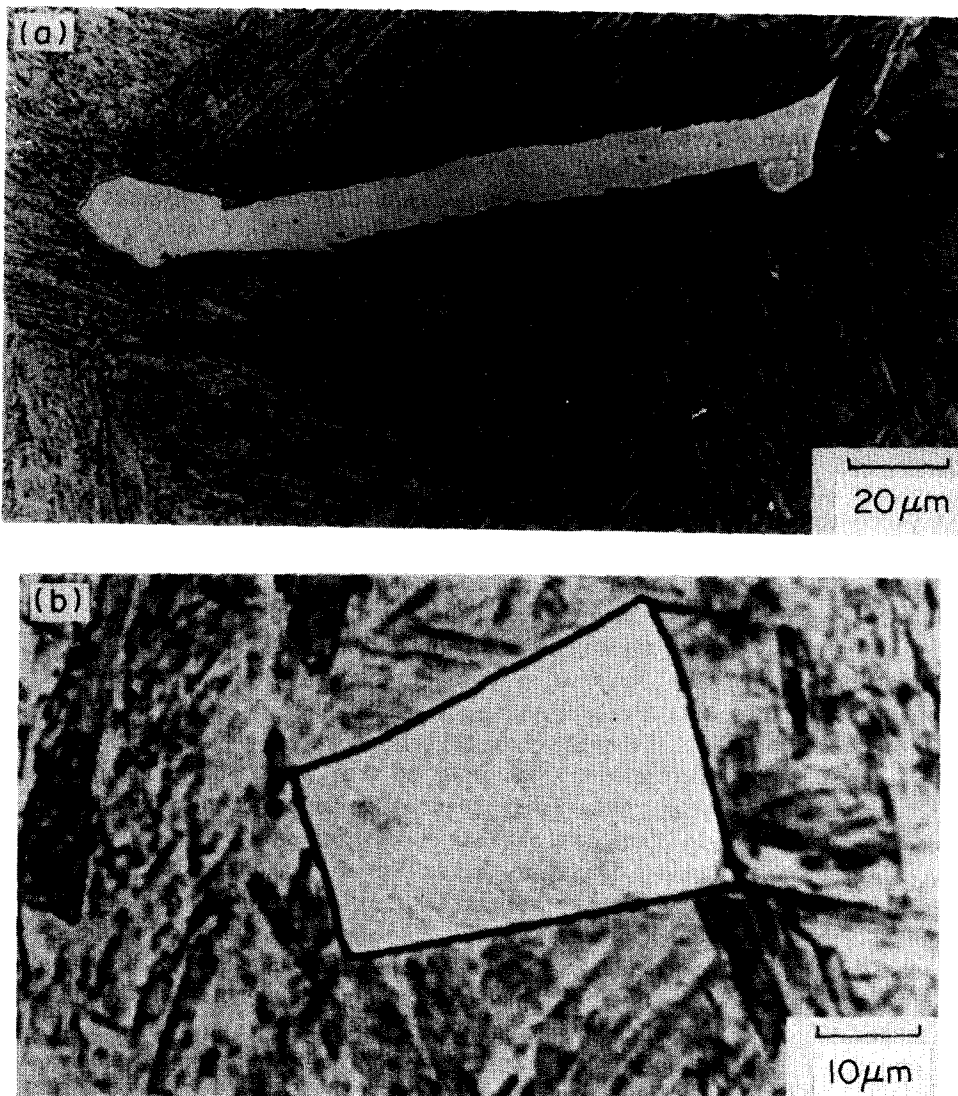


FIG. 1. Optical micrographs of allotropic ferrite (a) and idiomorphic ferrite (b) in Fe-5.0W-0.23C wt.% alloy, partially transformed at 800°C before water quenching (after Sahay, 1985).

grains of ferrite which have an approximately equiaxed morphology due to impingement between neighbouring grains. The transformation may begin with the growth of idiomorphs or allotriomorphs and massive ferrite cannot strictly be regarded as a separate morphology in the classification scheme. Ferrite growth without a change in composition can only occur below the  $T_0$  temperature at which  $\alpha$  and  $\gamma$  of identical composition have equal free energy. The  $T_0$  temperature lies between the  $Ae_3$  and  $Ae_1$  temperatures which in turn define the upper and lower limits respectively of the two-phase  $\alpha + \gamma$  field. For the range  $Ae_3 \rightarrow T_0$ , growth is only possible if the  $\alpha$  has a different composition from the  $\gamma$  whereas between  $T_0$  and  $Ae_1$ ,

growth of ferrite of equilibrium or unchanged composition is in principle possible. Below the  $Ae_1$  temperature, only massive growth is possible if the transformation mechanism is diffusional.

The original Dubé classification was for plain carbon steels, but is also applicable to alloy steels; in such cases, the ferrite sometimes contains carbide dispersions (e.g. Honeycombe, 1976). Due to the high rates of transformation in pure iron, the Dubé classification has not been established for pure iron. In spite of these difficulties, morphological classifications serve a useful purpose in the investigation of structure–property relationships.

### 2.1. *Other Transformations in Steels*

Allotriomorphic, idiomorphic and massive ferrite can only be fully appreciated in the context of the other microstructural constituents which also arise in steels. The formation of pearlite in steels involves the co-operative, diffusional growth of ferrite and cementite from austenite. In two-dimensional sections, this eutectoid mixture appears to consist of alternate lamellae of ferrite and cementite, which together form a pearlite colony. In reality, the cementite and ferrite within a given colony are single crystals, the lamellae of each phase being connected in three dimensions (Hillert, 1962). With the exception of the ferrite found within pearlite, all other ferrite morphologies involve plate or lath shapes. If a plate or lath is idealized as a rectangular parallelepiped with sides of length  $a$ ,  $b$  and  $c$ , then  $a = b \gg c$  for a plate, and  $a \gg b \gg c$  for a lath.

Martensite is a product of diffusionless transformation and can occur in the form of thin, lenticular plates which often extend right across the parent  $\gamma$  grains, or as packets of approximately parallel, fine laths whose size is generally less than that of the  $\gamma$  grains. In both cases, the parent and product crystals are related by an atomic correspondence and the formation of martensite causes the shape of the transformed region to change; this shape change is macroscopically an invariant-plane strain, the invariant-plane being the habit plane of the martensite. The nucleation of martensite is generally athermal (but can be isothermal) and is believed to be diffusionless in nature. Martensite can occur at very low temperatures and its interface with the parent phase necessarily has to be glissile. Martensite forms at high undercoolings where the chemical free energy change for transformation is generally very large, well in excess of that required to accomplish diffusionless transformation even when the stored energy of the martensite is taken into account.

Widmanstätten ferrite ( $\alpha_w$ ) can form at low undercoolings below the  $Ae_3$  temperature where the driving force for transformation is small, so that the partitioning of carbon during transformation is a thermodynamic necessity. On an optical scale, Widmanstätten ferrite has the shape of a thin wedge, the actual shape being somewhere between that of a plate and a lath (Watson and McDougall, 1973; King and Bell, 1974). The formation of Widmanstätten ferrite is also accompanied by a change in the shape of the transformed region; the shape change due to a single wedge of Widmanstätten ferrite consists of two adjacent and opposing invariant-plane strain deformations. These IPS deformations each have large shear components ( $\sim 0.4$ ) and imply the existence of an atomic correspondence between the parent and product phases as far as the iron and substitutional solute atoms are concerned. Interstitial atoms, like carbon can diffuse during growth without affecting the shape change or the displacive character of the transformation. The co-operative growth of a pair of adjacent mutually-accommodating crystallographic variants allows the elastically accommodated strain energy accompanying plate formation to be rather small, of the order of 50 J/mole. This is consistent with the low undercoolings at which Widmanstätten ferrite forms and with the

wedge morphology which arises because the adjacent variants have slightly different habit planes. The shape change indicates that the  $\alpha_w/\gamma$  interface is glissile and the plates therefore grow at a constant rate controlled by the diffusion of carbon in the  $\gamma$  ahead of the plate tip. Widmanstätten ferrite clearly cannot be regarded as a product of diffusional transformation since there is no diffusion involved in the actual lattice change; iron and substitutional atoms do not diffuse during transformation. A discussion of the growth kinetics of  $\alpha_w$  is nevertheless included as an appendix to this review, on the grounds that it provides an interesting example of diffusion-controlled linear growth. Finally, we note that when  $\alpha_w$  nucleates from grain boundary allotriomorphs of ferrite, it is called a 'Widmanstätten ferrite side-plate' but when it nucleates directly from  $\gamma$  boundaries, it is referred to as a 'Widmanstätten ferrite primary side-plate'.

Bainite occurs at a higher undercooling relative to Widmanstätten ferrite and grows in the form of sheaves originating from  $\gamma$  grain boundaries. The sheaves consist of much smaller platelets ('sub-units') of ferrite. The sheaf itself has a wedge shaped plate morphology on a macroscopic scale (Bhadeshia and Edmonds, 1980). When carbon is present, cementite precipitation occurs from the austenite between the sub-units in the case of upper bainite; in lower-bainite, the cementite (or  $\epsilon$  carbide) can also precipitate from within the bainitic ferrite. Unlike tempered martensite, the carbides within lower bainitic ferrite usually precipitate in a single crystallographic variant. Lower bainite occurs at a lower temperature compared with upper bainite. In both cases, the formation of a sub-unit is accompanied by an IPS shape change of the transformed region. The sub-units within a given sheaf have the same habit plane, orientation relationship with the  $\gamma$ , and shape deformation.

There is little evidence on the nucleation of Widmanstätten ferrite and bainite, but the nucleation is isothermal and should involve the partitioning of carbon during the nucleation event (Bhadeshia, 1981). There is some evidence to suggest that the activation energy for nucleation is directly proportional to the chemical free energy change accompanying nucleation, and this can be interpreted to imply that the nucleation is displacive in character (Bhadeshia, 1981).

### 3. MECHANISM OF DIFFUSIONAL TRANSFORMATION TO FERRITE

#### 3.1. *The Influence of Interface Structure*

The Ehrenfest (1933) classification of phase transformations is based on the successive differentiation of a thermodynamic potential (e.g. Gibbs free energy) with respect to an external variable such as temperature or pressure. The order of the transformation is given by the lowest derivative to exhibit a discontinuity. In a first order transformation, the partial derivative of the Gibbs free energy with respect to temperature is discontinuous at the transition temperature. There is thus a latent heat of transformation evolved at a 'sharp' transformation interface which separates the co-existing parent and product phases. In a first order transformation, the phase change occurs at a well defined interface, the interface separating perfect forms of the parent and product phases. In these circumstances, interface structure must dominate the mechanism of transformation and the formation of a new phase involves a nucleation and growth process†.

The  $\gamma \rightarrow \alpha$  transformation is a first order transformation which occurs by the motion of well defined interfaces. The structure of the interface influences the way in which the atoms

†In a second order transformation the parent and product phases do not co-exist; when such a transformation involves a lattice change, the change occurs continuously throughout the parent phase until its lattice is gradually changed into that of the product. There is no identifiable interface.

of the parent lattice move in order to generate the  $\alpha$  lattice. It can be shown (Christian, 1975) that two arbitrary crystals can be joined by a stress-free coherent interface only if one of the crystals can be generated from the other by a homogeneous transformation strain which is an invariant-plane strain (IPS). This condition in turn requires that two of the principal strains of the pure strain part of the transformation strain be of opposite sign, the third being zero. By the addition of a suitable rigid body rotation, a pure strain like this can be converted into an IPS. The pure deformation which converts a FCC crystal to a BCC crystal, and which seems to involve the smallest atomic displacements, is the Bain strain (Bain, 1924). In steels, all of the principal strains of the Bain strain have finite values, two of them being positive and the third negative. Combination of the Bain strain with a rigid body rotation cannot therefore give a transformation strain which is an IPS. It follows that  $\alpha/\gamma$  interfaces must be semi-coherent or incoherent, except at the nucleation stage where the  $\alpha$  may be forced into coherence. For larger areas of contact, the structure of the interface will in general consist of coherent patches separated periodically by discontinuities which prevent the misfit in the interface from accumulating over large distances.

### 3.1.1. *Glissile interfaces*

There are two kinds of semi-coherency (Christian, 1965, 1969, 1975)—if the discontinuities discussed above consist of a single set of screw dislocations,† or dislocations whose Burgers vectors do not lie in the interface plane, then this semi-coherency is of the kind associated with glissile interfaces. A glissile interface also requires that the glide planes (of the misfit dislocations) associated with the  $\alpha$  lattice meet the corresponding glide planes in the  $\gamma$  lattice edge to edge in the interface, along the dislocation lines (Christian and Crocker, 1980). A glissile  $\alpha/\gamma$  interface can move conservatively and when it does so, the interface dislocations inhomogeneously shear the volume of material swept by the interface in such a way that the macroscopic shape change accompanying transformation is an IPS even though the homogeneous lattice transformation strain is an invariant-line strain. Conservative motion of a glissile interface leads to martensitic transformation.

### 3.1.2. *Epitaxial semi-coherency*

If the intrinsic interface dislocations have Burgers vectors which lie in the interface plane, not parallel to the dislocation line, then the interface is said to be 'epitaxially semi-coherent' (Fig. 2). The normal displacement of such an interface necessitates the thermally activated climb of the misfit dislocations, so that the interface can only move in a non-conservative manner with relatively restricted mobility at low temperatures.

The nature of the shape change that accompanies the motion of an epitaxially semi-coherent interface is difficult to assess. As discussed by Christian (1965, 1969, 1975), the upwards non-conservative motion of the boundary AB (Fig. 2) to a new position C'D' should change the shape of a region ACDB of the parent crystal to a shape AC'D'B of the product phase. The shape change thus amounts to a uniaxial distortion normal to AB together with a shear component parallel to the interface plane (i.e. an IPS). Because of the dislocation climb implicit in the process, the total number of atoms in regions ACDB and AC'D'B will not be equal, the difference being removed by diffusion normal to the interface plane. Atom movements are therefore necessary over a distance (at least) equal to that moved by the

†If the transformation strain is an invariant-line strain (consisting of the Bain strain and an appropriate rigid body rotation), and if the invariant-line lies in the interface, then the latter need only contain a single set of misfit dislocations. For martensitic transformations, the transformation strain has to be an invariant-line strain in order to ensure a glissile interface.

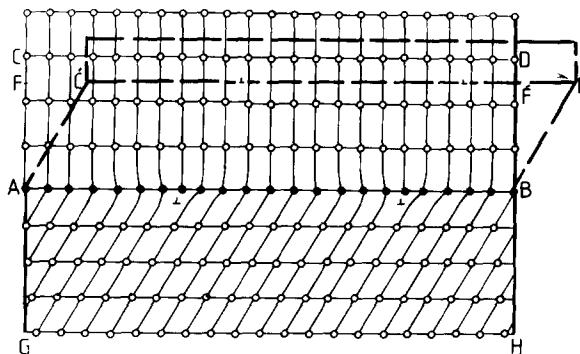


FIG. 2. Diagram illustrating the nature of the shape change accompanying the movement of an epitaxially semi-coherent interphase interface (after Bhadeshia, 1982a).

boundary, corresponding to the thickness of the transformed region. If this constitutes the only diffusional flux that accompanies interface motion, then the shear component of the shape change will not be destroyed, and the transformation will exhibit surface relief effects (and corresponding strain energy) normally associated with displacive transformations. The mobility will, of course, be limited by the climb process. A situation like this in effect amounts to an orderly removal of atoms as the interface migrates (i.e. removal of the extra half-planes of the misfit dislocations) so that a partial atomic correspondence is still maintained between the parent and product phases.

However, Christian (1965) has pointed out that since atoms have to migrate over large distances when an epitaxially semi-coherent interface moves, they should also be able to produce a net flow parallel to the interface, thus eliminating the shear component of the shape change and its associated strain energy. Referring to Fig. 2, this would involve the diffusion of matter contained in the region  $BF'D'$  to region  $AFC'$ , in a direction parallel to the interface. Hence, it has been considered improbable that atomic correspondence can be maintained during non-conservative interface motion. Bhadeshia (1982a) has suggested that this may not be true if the flow parallel to the interface has to occur through a distance much larger than that normal to the interface—after all, the length to thickness ratio of plates is always large. This argument would fail if the dislocation climb process draws vacancies from a large distance normal to the interface.

### 3.1.3. *Reconstructive diffusion*

From the above discussion it is evident that diffusion both parallel and normal to the interface plane is necessary if the migration of an epitaxially semi-coherent interface is to produce diffusional transformation. The diffusion processes have been described phenomenologically, but in reality, they should occur as the interface moves. Such diffusion is henceforth referred to as 'reconstructive diffusion', to describe the atomic mixing necessary to accomplish the lattice change without causing the macroscopic displacements characteristic of martensitic transformations in steels. It is emphasized that in diffusional transformations, reconstructive diffusion is necessary even if the parent and product phases have identical composition, or if the transformation occurs in a pure element. Diffusional transformation in effect represents transformation and recrystallisation occurring simultaneously, and reconstructive diffusion is the recrystallisation part of the process.

During the formation of martensite, much of the driving force is used up in accommodating the elastic strains due to the shape change. Such strains are absent for diffusional

transformations which can consequently occur at lower driving forces. The conservative motion of a glissile interface leads to martensitic transformation. If circumstances arise where a glissile interface exists but only diffusional reaction is possible, then the interface can move if reconstructive diffusion accompanies its motion (Bhadeshia, 1984). The displacive formation of bainite from austenite stops when the carbon-enriched austenite can no longer support such transformation; Bhadeshia (1982a) has shown that continued holding at isothermal transformation temperature causes the interfaces which initially led to displacive bainite growth to move at a much slower rate, as the residual austenite continues to diffusively transform.

During diffusion-controlled growth, the compositions of the two phases in contact are approximately in equilibrium; it is sometimes assumed (e.g. De Hoff, 1981) that deviations from this equilibrium can only occur if the kinetic process by which solute is transferred across the interface is slow in comparison with its diffusion in the matrix ahead of the interface. This ignores the existence of reconstructive diffusion since the transfer of solvent (Fe) atoms can also be restrictive.

#### 3.1.4. *Incoherent interfaces*

As the misfit between adjacent crystals increases, the dislocations in the connecting interface become more closely spaced. They eventually coalesce so that the boundary consists of closely spaced 'vacancies' or 'dislocation cores'. Such a boundary is said to be incoherent; there is little correlation of atomic positions across the boundary. The motion of incoherent boundaries can only cause diffusional transformation, with no atomic correspondence between the parent and product phases. For incoherent boundaries, the free volume and diffusivity within the boundary may be sufficiently high to confine reconstructive processes to the close proximity of the boundary itself (unlike semi-coherent interfaces).

Incoherent, coherent and semi-coherent boundaries can co-exist around a particle which has grown diffusively; only semi-coherent and coherent boundaries can exist around a particle which has grown displacively. This is because if an atomic correspondence exists across a particular interface of a particle, then it necessarily does so across any other interface (Christian, 1975; Christian and Edmonds, 1983).

#### 3.1.5. *Experimental evidence on the $\gamma/\alpha$ interface*

Experimental evidence on the structure of interfaces responsible for the diffusional growth of  $\alpha$  from  $\gamma$  simply does not exist, but evidence on the reverse transformation points towards the interface being semi-coherent. Rigsbee (1979) has studied the diffusional formation of  $\gamma$  by intercritically annealing a low-alloy steel in the  $(\alpha + \gamma)$  phase field; subsequent cooling to ambient temperature led to the retention of austenite. High-resolution transmission electron microscopy of the retained- $\gamma/\alpha$  interfaces revealed regularly spaced linear discontinuities in the interface. The spacing of these discontinuities varied as a function of interface orientation. The results are consistent with the interfaces being partially coherent, although no detailed identification of the discontinuities or the  $\gamma/\alpha$  orientation relationship was presented.

Howell *et al.* (1981) examined  $\gamma/\alpha$ -ferrite interfaces in a duplex stainless steel, in which the  $\gamma$  was diffusively precipitated from supersaturated  $\delta$ -ferrite. The interfaces examined were suggested to be at equilibrium, the orientation relationship being:

$$(111)_{\gamma} \parallel (110)_{\delta}$$

$$[01\bar{1}]_{\gamma} \parallel [\bar{1}11]_{\delta}$$

Howell *et al.* claimed that an interface parallel to  $(102)_\gamma$  contained at least two sets of intrinsic dislocations, with Burgers vectors parallel to  $[110]_\gamma$  and  $[10\bar{1}]_\gamma$ , respectively, making the semi-coherent interface sessile.

In an earlier study also on a duplex stainless steel, Howell *et al.* (1979a) tentatively concluded that for  $\gamma$  and  $\delta$ -ferrite related approximately by the above orientation relationship, interfaces parallel to  $(111)_\gamma$  contained no dislocation structure and this was confirmed by the absence of certain electron diffraction effects, associated with periodic strain fields due to interface dislocations. However, the evidence presented is weak since such diffraction effects were not found at some other interface orientations where dislocation arrays were clearly resolved. The implied fully-coherent  $(111)_\gamma$  interface extending over approximately  $1 \mu\text{m}$  is unlikely; since the two lattices cannot be related by a transformation strain which is an IPS, only forced coherence is possible. This should in turn lead to characteristic strain field contrast in the transmission electron microscope, contrast which does not seem to have been detected by Howell *et al.* (1979).

#### 4. INTERFACE MOTION: RATE-CONTROLLING PROCESSES

The rate at which an interface moves depends both on its intrinsic mobility (related to the process of atom transfer across the interface) and on the ease with which any alloying elements partitioned during transformation diffuse ahead of the moving interface. The two processes are in series so that interface velocity as calculated from the interface mobility always equals the velocity calculated from the diffusion of solute ahead of the interface. Both of these processes dissipate the free energy ( $\Delta G'$ ) available for interface motion; when  $\Delta G'$  is primarily used up in driving the diffusion of solute ahead of the interface, growth is said to be diffusion-controlled. Interface-controlled growth occurs when most of  $\Delta G'$  is dissipated in the process of atom transfer across the interface.

These concepts can be illustrated in terms of the formation of  $\alpha$  from supersaturated  $\gamma$  in a Fe-C alloy isothermally transformed in the  $\alpha + \gamma$  phase field at a temperature  $T$ . The notation used is defined as follows: the mole fraction of an element  $i$  ( $i = 1, 2, 3$  for C, X, Fe respectively, where X is a substitutional alloying element) in a phase  $\alpha$  at the  $\alpha/\gamma$  interface is written  $x_i^\alpha$ , with  $x_i^{\alpha\gamma}$  representing the mole fraction of  $i$  in  $\alpha$ , when  $\alpha$  is in equilibrium with  $\gamma$ .  $\bar{x}_i$  refers to the average mole fraction of  $i$  in the alloy concerned.

For isothermal growth of ferrite of composition  $x_i^{\alpha\gamma}$  involving the movement of a flat  $\alpha/\gamma$  interface, the total composition difference between the ferrite and austenite remote from the interface may be written:

$$\Delta x = \Delta x_\infty + \Delta x_I + \Delta x_D \quad (4.1a)$$

where

$$\Delta x_\infty = x_1^{\gamma\alpha} - x_1^{\alpha\gamma}$$

$$\Delta x_I = x_1^\gamma - x_1^{\gamma\alpha}$$

$$\Delta x_D = \bar{x}_1 - x_1^\gamma.$$

$\Delta x_I$  and  $\Delta x_D$  are related to the free energies  $G_I$  and  $G_D$  dissipated in the interface and diffusion processes respectively, such that  $G_D = 0$  when  $\Delta x_D = 0$  and  $G_I = 0$  when  $\Delta x_I = 0$ . Similarly,  $\Delta G'$  is related to  $(\Delta x_\infty - \Delta x)$  and is zero when  $x_1^{\gamma\alpha} = \bar{x}_1$ .

It is emphasized that the rate of interface motion is always under mixed control (since the two processes are in series) but is said to be diffusion controlled if  $|\Delta x_D| \gg |\Delta x_I|$  and because

variations in interface parameters have virtually no effect on velocity. Similarly, interface-control implies that  $|\Delta x_D| \ll |\Delta x_I|$  and variations in diffusion parameters then have a negligible effect. True mixed control implies that  $\Delta x_D$  and  $\Delta x_I$  are of comparable magnitude.

The diffusional growth of  $\alpha$  during transformation in the  $\alpha + \gamma$  phase field involves the partitioning of carbon and we consider a case where the interface moves at a rate which is under mixed diffusion- and interface-control. A possible carbon concentration profile developed at the  $\alpha/\gamma$  interface is illustrated in Fig. 3, where  $x_I^\alpha \neq x_I^\gamma$  and  $x_I^\alpha$  need not equal  $x_I^\gamma$ . Displacement of a flat  $\alpha/\gamma$  interface to produce  $\alpha$  is phenomenologically equivalent to taking a small amount of material of composition  $x_1^\alpha$  from  $\gamma$  of composition  $\bar{x}_1$ , and after transformation at constant composition, adding it to  $\alpha$  of composition  $x_1^\alpha$ . The molar Gibbs free energy change  $\Delta G' \{x_1^\alpha, \bar{x}_1\}$  for this process is the driving force for interface motion and is given by (see for example, Hillert, 1969; or Baker and Cahn, 1969):

$$\begin{aligned} \Delta G' \{x_1^\alpha, \bar{x}_1\} &= x_3^\alpha [\mu_3^\alpha \{x_3^\alpha\} - \mu_3^\gamma \{\bar{x}_3\}] + x_1^\alpha [\mu_1^\alpha \{x_1^\alpha\} - \mu_1^\gamma \{\bar{x}_1\}] \\ &= x_3^\alpha (\Delta G_3^{\gamma\alpha} + RT \ln \{a_3^\alpha \{x_3^\alpha\} / a_3^\gamma \{\bar{x}_3\}\}) \\ &\quad + x_1^\alpha RT \ln \{a_1^\alpha \{x_1^\alpha\} / a_1^\gamma \{\bar{x}_1\}\} \end{aligned} \quad (4.1b)$$

where  $\mu_i^\alpha$  and  $a_i^\alpha$  represent the chemical potential and activity respectively, of component  $i$  in the  $\gamma$  phase.

$a_3^\alpha$  and  $a_3^\gamma$  are defined with respect to pure  $\alpha$ -iron and pure  $\gamma$ -iron as the respective standard states while the activities of carbon are defined relative to pure graphite as the standard state.  $\Delta G_3^{\gamma\alpha}$  is the molar Gibbs free energy for the  $\gamma \rightarrow \alpha$  transformation in pure iron.

$\Delta G'$  is irreversibly dissipated in driving the diffusion of carbon ahead of the interface and in the process of transferring atoms across the interface. If  $G_D$  and  $G_I$  are the dissipations due to diffusion and interface processes respectively, then

$$\begin{aligned} G_I &= \Delta G' - G_D \\ &= x_3^\alpha (\Delta G_3^{\gamma\alpha} + RT \ln \{a_3^\alpha \{x_3^\alpha\} / a_3^\gamma \{x_3^\gamma\}\}) \\ &\quad + x_1^\alpha RT \ln \{a_1^\alpha \{x_1^\alpha\} / a_1^\gamma \{x_1^\gamma\}\}. \end{aligned} \quad (4.2)$$

It follows that when  $x_I^\alpha \cong \bar{x}_1$  (so that  $|\Delta x_D| \gg |\Delta x_I|$ ), most of  $\Delta G'$  is dissipated in interface processes and the reaction is interface-controlled; if  $x_I^\alpha \cong x_I^\gamma$  then most of  $\Delta G'$  is dissipated in driving the diffusion of C ahead of the interface which moves at a rate controlled by the diffusion of carbon in the  $\gamma$  ahead of the interface.

A reasonable approximation for diffusion-controlled growth is that the compositions of the phases in contact at the interface are in equilibrium. This is because  $\Delta x_I$  is relatively small for diffusion-controlled growth. Subject to this approximation, local equilibrium is said to exist at the interface. This involves the assumption that the whole of the concentration gradient can be divided up into a large number of thin slices (or sub-systems), each of which has a definite concentration, so that each of the sub-systems can be considered as if it were in local equilibrium, even though free energy dissipation occurs in the diffusion process itself (there are gradients of the thermodynamic variables). These assumptions are valid if perturbations from equilibrium are not too large (Miller, 1960) and they allow the application of classical equilibrium thermodynamics to steady-state situations like the irreversible process of diffusion which actually arises due to the lack of equilibrium. It is a common assumption that we may apply equilibrium thermodynamics locally (Darken and Gurry, 1953).

Another interesting consequence of the assumption of local equilibrium is that the diffusion-controlled growth and dissolution of a precipitate must proceed at the same rate.

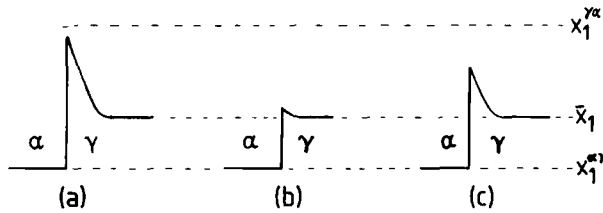


FIG. 3. Carbon concentration profile at a  $\alpha/\gamma$  interface moving under: (a) diffusion-control; (b) interface-control; and (c) mixed interface and diffusion-control.

The principle of detailed balance implies that for a reaction proceeding in the environs of equilibrium, the forward rate along any one reaction path must equal the reverse rate along that path (Purdy and Kirkaldy, 1962; Christian, 1975, p. 81).

## 5. DIFFUSION-CONTROLLED GROWTH

### 5.1. Diffusion Coefficients

The problem of representing diffusion during the growth of ferrite in steels does not lend itself to simple treatments because elements like carbon and nitrogen diffuse interstitially while Fe and substitutional alloying elements diffuse by a vacancy mechanism. The diffusion coefficients are often concentration dependent. Most steels are usually higher than binary alloys so that several diffusion coefficients have to be known and the interdependence of fluxes also has to be taken into account. In certain circumstances, the composition gradients of solute in the matrix ahead of the interface can be very large, in which case the dependence of the diffusion coefficient on the gradient itself may be significant. We therefore briefly consider the nature of and relations between diffusion coefficients before embarking on the treatment of diffusion-controlled growth.

In a binary system, an empirically defined diffusion coefficient is simply the proportionality constant relating the rate of transfer of a diffusing substance through a unit area of a section, and the concentration gradient measured normal to the section (Fick, 1855). Because the chemical potentials of the two components of a binary system are related by the Gibbs–Duhem equation, the flux of any element can be described in terms of just one empirical diffusion coefficient if the latter is defined in a volume-fixed frame (Miller, 1960); the significance of the frame of reference will be discussed later.

The tracer diffusion coefficient represents the diffusivity of radioactively labelled isotopes in an otherwise chemically homogeneous solution. When the tracer atoms are of the same species as the non-tracer atoms, the tracer diffusion coefficient is called the self-diffusion coefficient.

Tracer and self-diffusion coefficients do not properly represent diffusion in concentration gradients, since in the presence of a chemical composition gradient, an additional virtual force acts on the diffusing species. This virtual force is due to the chemical potential gradient associated with the composition gradient. An intrinsic diffusion coefficient  $\bar{D}_A$  takes account of this and hence represents the flux of component  $A$  of a binary  $A$ – $B$  substitutional solution in a concentration gradient of  $A$  (and hence of  $B$ ). However, when the two species in an interdiffusion experiment have unequal intrinsic diffusion coefficients and when diffusion occurs by a vacancy mechanism, there is a net flux across any plane in the diffusion zone.

If one end of the specimen is chosen as a reference plane, then inert markers within the specimen move relative to this reference plane—this is the Kirkendall effect (Kirkendall, 1942). This bulk flow obviously contributes to composition change at any point, but is not accounted for in the definition of intrinsic coefficients.

The chemical or interdiffusion coefficient  $D$  does take account of the Kirkendall effect and represents the rate at which free energy gradients in the solution level out, or the rate at which mixing or unmixing occurs (Crank, 1975; Christian, 1975). If  $\bar{D}_A = \bar{D}_B$ , there is no Kirkendall effect and  $\bar{D}_A = \bar{D}_B = D$ . We have thus separated bulk flow from true diffusion resulting from the random motion of non-uniformly distributed  $A$  atoms. Intrinsic coefficients account for true diffusion only, whereas interdiffusion coefficients also account for bulk flow.

Because intrinsic diffusion coefficients do not take account of bulk flow arising due to the Kirkendall effect, the substitution of these coefficients into Fick's first law defines fluxes  $\bar{J}_i$  relative to the 'lattice-fixed' or 'Kirkendall' frame of reference. In other words, the fluxes  $\bar{J}_i$  occur through a section fixed so that no bulk flow occurs through it. The Kirkendall frame thus moves (with the velocity of the inert markers) relative to the laboratory frame (to which the specimen is fixed).  $D$ , on the other hand, is defined with respect to the laboratory frame.

It is often convenient to define  $D$  relative to other frames of reference. In the volume-fixed frame, the fluxes  $J_i$  occur across a section defined such that the total volume on either side of the section remains constant as diffusion proceeds. It follows that  $\sum J_i \bar{V}_i = 0$ , where  $\bar{V}_i$  refers to the partial molar volume of component  $i$  in an  $n$  component solution. If  $\bar{V}_i/\bar{V}_n = 1$  for all  $i$ , then the volume-fixed frame coincides with the laboratory frame. Miller (1960) states that with few exceptions, most experimental determinations of interdiffusion coefficients assume constant volume, and hence refer to the volume-fixed frame.

$D$  relative to a number-fixed frame is such that the fluxes  $J_i$  occur across a section defined such that the total number of atoms on either side of the section remains constant, so that  $\sum J_i = 0$ .

Diffusion data for steels have been reviewed by Fridberg *et al.* (1969).

### 5.1.1. Diffusion in multicomponent systems

Fick's law for a binary system can be formally stated as:

$$J_i = -D \text{ grad } c_i, \quad (5.1)$$

where  $c_i$  is the concentration of  $i$  in moles per unit volume, and the flux is referred to a volume-fixed frame of reference and  $D$  is the chemical diffusion coefficient. For a system of  $n$  components, where the flux of  $i$  may also depend on the concentration gradients of other components, Fick's law may be generalized as follows (Onsager, 1945; Kirkaldy, 1970):

$$J_i = - \sum_{k=1}^{n-1} D_{ik} \text{ grad } c_k \quad (5.2)$$

the flux again being defined with respect to the volume-fixed frame of reference;  $D_{ik}$  form a matrix of empirical chemical diffusion coefficients. Fick's law is based on a hypothesized relation between the flux and chemical concentration gradient and this is why the diffusion coefficient is sometimes called empirical. The form of the equation is nevertheless convenient and is historically well established. If the flux actually depends on the chemical potential gradient rather than the concentration gradient, then the failure of the law is prevented by making  $D$  concentration dependent. It is on this basis that Darken's equations (Darken, 1948) relating activity and diffusion are derived. The virtual force ( $X_i$ ) acting on a diffusing species should really depend on the negative gradient of its chemical potential (Einstein, 1905;

Hartley, 1931); in a multicomponent system this force is also a function of the chemical potential gradients of the other species.

To find a relation between  $J_i$  and  $X_i$  we rely on the assumptions of the thermodynamics of irreversible processes (reviewed by Miller, 1960; Christian, 1975), the major results of which were obtained by Onsager (1931). The theory assumes that if there is more than one irreversible process occurring (and diffusion in a multicomponent system is such a case), then each 'flow'  $J_i$  is not only linearly related to its conjugate 'force'  $X_i$ , but it is also linearly related to all the other forces which lead to dissipation (or entropy production). For the case of diffusion in an isotropic medium, referred to a volume-fixed frame, and for an  $n$ -component system, this may be expressed mathematically as:

$$J_i = \sum_{k=1}^{n-1} L_{ik} X_k \quad (5.3a)$$

and if the forces are taken to be chemical potential gradients (obeying the Gibbs–Duhem equation) then the  $n-1$  independent forces are given by (Kirkaldy, 1970):

$$X_k = -\text{grad} [\mu_k - (\bar{V}_k/\bar{V}_n)\mu_n] \quad (5.3b)$$

where the  $L_{ik}$  are phenomenological coefficients of the various linear 'force–flux' relations. Comparison of eq. 5.3 with eq. 5.2 gives (Kirkaldy, 1970):

$$D_{ik} = \sum_j L_{ij} \eta_{jk}, \quad (5.4)$$

with

$$\eta_{jk} = \partial[\mu_j - (\bar{V}_j/\bar{V}_n)\mu_n]/\partial c_k.$$

The on-diagonal diffusion coefficients have always been found to be positive, although Kirkaldy (1970) has shown that this need not be the case. Onsager's theory also states that as long as the  $J_i$  and  $X_i$  which contribute to dissipation are independent, then for diffusion processes,  $L_{ij} = L_{ji}$ .

### 5.1.2. Diffusion in ternary Fe–X–C alloys

For a ternary Fe–X–C alloy,

$$J_1 = L_{11}X_1 + L_{12}X_2 \quad (5.5a)$$

$$J_2 = L_{22}X_2 + L_{21}X_1 \quad (5.5b)$$

where the fluxes are referred to a volume-fixed frame of reference. Using the Gibbs–Duhem relations, and assuming that  $\bar{V}_1/\bar{V}_3 = 0$  and  $\bar{V}_2/\bar{V}_3 = 1$ , we get (for diffusion in one dimension along a co-ordinate  $z$ ):

$$X_1 = -\partial\mu_1/\partial z \quad (5.5c)$$

$$X_2 = -(1 + [x_2/x_3]) (\partial\mu_2/\partial z) - (x_2/x_3) (\partial\mu_1/\partial z). \quad (5.5d)$$

The assumptions concerning the partial molar volumes are considered reasonable (Kirkaldy, 1970) as long as the volume change of mixing is insufficient to significantly influence the diffusion profiles. It follows that:

$$D_{11} = L_{11}(\partial\mu_1/\partial c_1) + L_{12}(x_1/x_3) (\partial\mu_1/\partial c_1) + L_{12}(1 + [x_2/x_3]) (\partial\mu_2/\partial c_1) \quad (5.5e)$$

$$D_{12} = L_{11}(\partial\mu_1/\partial c_2) + L_{12}(1 + [x_2/x_3]) (\partial\mu_2/\partial c_2) \\ + L_{12}(x_1/x_3) (\partial\mu_1/\partial c_2) \quad (5.5f)$$

$$D_{22} = L_{21}(\partial\mu_1/\partial c_2) + L_{22}(x_1/x_3) (\partial\mu_1/\partial c_2) \\ + L_{22}(1 + [x_2/x_3]) (\partial\mu_2/\partial c_2) \quad (5.5g)$$

$$D_{21} = L_{21}(\partial\mu_1/\partial c_1) + L_{22}(x_1/x_3) (\partial\mu_1/\partial c_1) \\ + L_{21}(1 + [x_2/x_3]) (\partial\mu_2/\partial c_1). \quad (5.5h)$$

Values of  $D_{11}$  and  $D_{22}$  are readily available and eqs 5.5e–h can be used to obtain the ratios  $D_{12}:D_{11}$  and  $D_{21}:D_{22}$ ; with certain approximations, these ratios can be expressed in terms of accessible thermodynamic parameters (Purdy and Kirkaldy, 1962; Brown and Kirkaldy, 1964; Kirkaldy, 1970). To illustrate the approximations involved, it is necessary to obtain a relation between the coefficients  $L_{ij}$  defined in the laboratory frame and the corresponding Onsager coefficients  $K_{ij}$  defined in the Kirkendall frame. Kirkaldy (1970) has shown that for dilute solutions ( $x_1, x_2 \ll x_3$ ) where all components diffuse independently in one dimension along a co-ordinate  $z$ ,

$$L_{11} = K_{11} - x_1^2 K_{33} \quad (5.6a)$$

$$L_{12} = x_1 K_{22} - x_1 x_2 K_{33} = L_{21} \quad (5.6b)$$

$$L_{22} = (1 - 2x_2)K_{22} - x_2^2 K_{33}. \quad (5.6c)$$

Assuming that interstitials do not significantly contribute to the Kirkendall effect, the velocity of the Kirkendall markers ( $v_k$ ) is then given by (Kirkaldy, 1970):

$$v_k = (RT/[c_2 + c_3]) \{[(K_{22}/x_2) - K_{33}] [\partial x_2/\partial z] - K_{33} [\partial x_1/\partial z]\}.$$

If  $\partial x_1/\partial z$  is small, then the Kirkendall effect vanishes when  $K_{22} = x_2 K_{33}$  or  $L_{12} = 0$ ; in this limit,

$$D_{12}/D_{11} = (\partial\mu_1/\partial x_2)/(\partial\mu_1/\partial x_1), \quad (5.7a)$$

$$D_{21}/D_{22} = \frac{[x_1(\partial\mu_1/\partial x_1) + x_3(\partial\mu_2/\partial x_1) + x_2(\partial\mu_2/\partial x_1)]}{[x_1(\partial\mu_1/\partial x_2) + x_3(\partial\mu_2/\partial x_2) + x_2(\partial\mu_2/\partial x_2)]}. \quad (5.7b)$$

For dilute solutions, these equations may be expressed in terms of the Wagner interaction parameters  $e_{ik}$  (Wagner, 1952):

$$e_{ik} = \partial \ln \Gamma_i / \partial x_k = e_{ki} \quad (5.8)$$

where  $\Gamma_i$  is the activity coefficient of  $i$  relative to the standard state at infinite dilution. Equations 5.7a, b can thus be simplified as follows:

$$D_{12}/D_{11} = e_{12}x_1/(1 + e_{11}x_1) \quad (5.9a)$$

$$D_{21}/D_{22} = x_2(1 + e_{12})/2. \quad (5.9b)$$

Equations 11a, b differ slightly from those quoted by Kirkaldy (1970); they are better approximations to eq. 5.7. Equation 5.9a is in exact agreement with the work of Kirkaldy and Purdy (1962) and Brown and Kirkaldy (1964). Brown and Kirkaldy (1964) have experimentally verified the validity of eq. 5.9a for ternary steels containing Mn, Co, Cr, Ni or Si as the substitutional addition.

Kirkaldy (1970) has shown that for dilute ternary iron alloys containing two substitutional alloying elements, similar simplification of the diffusion matrix can only be made if the

diffusivity of one of the solutes is relatively large. Since this is usually not the case, Kirkaldy suggests that the direct measurement of the chemical diffusion matrix is the easiest approach.

### 5.1.3. The diffusion of carbon in austenite

The diffusion coefficient of carbon in austenite is known to be strongly concentration dependent (Wells *et al.*, 1950; Smith, 1953) and this causes complications in the kinetic analysis of carbon diffusion-controlled reactions in steels. The existence of substantial carbon concentration gradients at the transformation interfaces involved in such reactions makes it imperative to account for the variation of  $D_{11}$  with  $x_1$ , and it has been demonstrated (Trivedi and Pound, 1967) that, for most purposes, a weighted average diffusivity  $D_{11}$  can adequately represent the effective diffusivity of carbon that is needed for the application of the theory of diffusion-controlled growth. Trivedi and Pound (1967) first considered this problem in detail and found that for diffusion-controlled growth occurring at a constant rate, the weighted average diffusivity is given by:

$$D_{11} = \int_{x_1^?}^{\bar{x}_1} D_{11} dx_1 / (\bar{x}_1 - x_1^?) \quad (5.10)$$

Although this equation is strictly only valid for steady-state growth, Coates (1973c) has suggested that it should be a reasonable approximation for parabolic growth as well, although no detailed justification was presented.

It is clearly necessary to know  $D_{11}\{x_1\}$  at least over the range  $\bar{x}_1 \rightarrow x_1^?$ , although experimental determinations of  $D_{11}\{x_1\}$  do not extend beyond  $x_1 = 0.06$ . Kaufmann *et al.* (1962) attempted to overcome this difficulty by assuming a relationship between the activation energy for the growth of a ferrite plate in austenite and that for the diffusion of carbon in  $\gamma$ . It was additionally assumed that the pre-exponential factor of the diffusion coefficient can be satisfactorily extrapolated beyond the range of experimental observations. This empirical extrapolation of  $D_{11}$  cannot in general be taken to be satisfactory.

Siller and McLellan (1969, 1970) have developed a theoretical representation of  $D_{11}$  which is compatible with both the kinetic and thermodynamic behaviour of carbon in austenite. The model takes account of two important factors: the concentration dependence of the activity of carbon in austenite (Smith, 1946) and the existence of a finite repulsive interaction between nearest neighbouring carbon atoms situated in octahedral sites (McLellan and Dunn, 1969). Smith (1953) has demonstrated that the composition dependence of activity cannot alone account for  $D_{11}$ . Siller and McLellan realized that the repulsive forces between neighbouring carbon atoms should effect diffusivity by acting to reduce the probability of interstitial site occupation in the vicinity of a site already containing a carbon atom. In a concentration gradient, a carbon atom attempting random motion therefore 'sees' an exaggerated difference in the number of available sites in the forward and reverse direction, so that diffusion down the gradient is enhanced. Using these ideas, Siller and McLellan obtained:

$$D_{11}\{x_1, T\} = (kT/h) (\exp\{-\Delta F^*/kT\}) (\lambda^2/3\Gamma_m)\eta\{\theta\} \quad (5.11)$$

with

$$\eta\{\theta\}/a_1^? = 1 + [W(1+\theta)/(1-(0.5W+1)\theta + (0.25W^2 + 0.5W)(1-\phi)\theta^2] \\ + (1/a_1^?)(1+\theta)(da_1^?/d\theta)$$

where  $k$  and  $h$  are the Boltzmann and Planck constants respectively,  $W$  is the number of octahedral interstices around a single such interstice,  $\Delta F^*$  is an activation free energy,

$\Gamma_m$  is an activity coefficient and  $\lambda$  is the distance between (002) austenite planes.  $\phi = 1 - \exp(-\omega_\gamma/kT)$ ;  $\omega_\gamma$  is the nearest neighbour carbon-carbon interaction energy in austenite, taken to be 8250 J/mole (Dunn and McLellan, 1970).  $\theta$  is the ratio of the number of carbon atoms to the total number of solvent atoms, given by  $\theta = x_1/(1 - x_1)$ . Bhadeshia (1981) found  $\Delta F^*/k = 21230$  K and  $\ln(\Gamma_m/\lambda^2) = 31.84$ .

5.2. Diffusion-Controlled Growth of Ferrite in Fe-C Alloys

The simplest treatment for the growth of ferrite from austenite is a one-dimensional growth model, involving the movement of a planar  $\alpha/\gamma$  interface; if  $\alpha$  growth occurs at a rate controlled by the diffusion of carbon in the  $\gamma$  ahead of the moving interface then it is a good approximation† that local equilibrium exists in the phases in contact at the interface. It follows that  $c_1^\alpha \cong c_1^{\gamma\alpha}$  and  $c_1^\gamma = c_1^{\alpha\gamma}$ ; it is assumed that the concentration of carbon in the  $\gamma$  far away from the interface remains  $\bar{c}_1$ , so that the austenite effectively has a semi-infinite extent in the region normal to the interface.

Since  $c_1^\alpha < c_1^\gamma$ , carbon is partitioned during the formation of ferrite and the excess carbon progressively builds up in the  $\gamma$  ahead of the interface, subject to the constraint that the maximum level of C in the  $\gamma$  at the interface is  $c_1^{\gamma\alpha}$ . The extent of the carbon diffusion field thus increases with the volume fraction of ferrite so that the growth rate of the  $\alpha$  must decrease with time. From dimensional arguments (Christian, 1975) it can be demonstrated that the thickness  $Z$  of the layer of ferrite is related to time  $t$  as follows:

$$Z = \alpha_1 t^{0.5} \tag{5.12a}$$

where  $Z = 0$  at  $t = 0$  and  $Z$  defines the position of the interface along the co-ordinate  $z$  which is normal to the interface (and is positive in the  $\gamma$ ).  $\alpha_1$  is called the parabolic-thickening rate constant (for one-dimensional growth) and can be deduced by applying Fick's laws of diffusion and the principle of conservation of mass. From Fick's laws, the differential equation for the matrix is given by:

$$\partial c_1/\partial t = \partial(D_{11}\{c_1\}(\partial c_1/\partial z))/\partial z \tag{5.12b}$$

subject to the boundary conditions  $c_1 = c_1^{\gamma\alpha}$  at  $z = Z\{t\}$ ;  $t = t$  and  $c_1 = \bar{c}_1$  at  $t = 0$ . Conservation of mass at the interface requires that

$$(c_1^{\alpha\gamma} - c_1^{\gamma\alpha})(\alpha_1 t^{0.5}/2) = D_{11}\{c_1^{\gamma\alpha}\}(\partial c_1/\partial z)_{z=Z} \tag{5.12c}$$

Equation 5.12c simply states that the amount of solute partitioned from the  $\alpha$ , per unit time, equals the solute flux away from the  $\alpha/\gamma$  interface.

If the diffusion coefficients do not depend on concentration, eq. 5.12 can be solved (Zener, 1949; Dubé, 1948; Atkinson, 1967) to give an implicit relation for  $\alpha_1$  as follows:

$$f_1 = H_1\{D_{11}\} \tag{5.13a}$$

where

$$H_1\{D_{11}\} = (0.25\pi/D_{11})^{0.5}\alpha_1 [\operatorname{erfc}\{0.5\alpha_1/(D_{11})^{0.5}\}] \exp\{\alpha_1^2/(4D_{11})\} \tag{5.13b}$$

†We emphasized earlier that all interfaces strictly move under mixed-control, but that  $|\Delta x_\gamma| \ll |\Delta x_\alpha|$  for diffusion-controlled growth so that the assumption of local equilibrium is reasonable. In all subsequent treatments we assume the existence of local equilibrium at the interface during diffusion-controlled growth, bearing in mind that this is an approximation since  $\Delta x_\gamma$  is never zero.

where  $f_1$  is a fractional supersaturation given by,

$$f_1 = (\bar{c}_1 - c_1^{\gamma\alpha}) / (c_1^{\alpha\gamma} - c_1^{\gamma\alpha}). \quad (5.13c)$$

When  $D_{11}$  is a function of concentration, Atkinson (1967) has shown that the following equation can be used to approximately define  $\alpha_1$  when growth is diffusion-controlled:

$$f_1 = H_1 \{ D_{11} \{ \bar{c}_1 \} \} [ D_{11} \{ \bar{c}_1 \} / D_{11} \{ c_1^{\gamma\alpha} \} ]. \quad (5.13d)$$

Atkinson (1967), following a method due to Philip (1960a, b) has shown that when one-dimensional diffusion-controlled growth is parabolic with respect to time, and when the diffusion coefficient is concentration dependent, it is possible to obtain exact solutions to eq. 5.12 subject to the boundary conditions stated earlier. However, such solutions only arise for special forms of  $D_{11} \{ c_1 \}$ . The solution to eq. 5.12b subject to the boundary conditions of eq. 5.12 can be written (Atkinson, 1967):

$$z/t^{0.5} = F \{ [(c_1 - \bar{c}_1) / (c_1^{\gamma\alpha} - \bar{c}_1)] f \{ \alpha_1 \} \} \quad (5.14a)$$

where  $F$  is any single-valued function of  $c_1$  such that

$$D_{11} \{ c_1 \} = 0.5 (dF/dc_1) \int_0^{c_1} F dc_1 \quad (5.14b)$$

and

$$c_1 = f \{ z/t^{0.5} \},$$

where  $F = f^{-1}$ . Exact solutions like eq. 5.14a can only be obtained if corresponding pairs of the functions  $D_{11}$  and  $F$  can be found which satisfy eq. 5.14b. While this is not difficult to do (Philip, 1969), the functions  $D_{11}$  obtained are in general complex and are not well adapted to fitting experimental data on  $D_{11}$  (Crank, 1975).

Atkinson (1968) has circumvented this problem by presenting a numerical method for solving eq. 5.12, a method which will work for any given diffusion coefficient represented as a function or as a graph or table. Grain boundary allotriomorphs sometimes have an initial shape which approximates that of an oblate ellipsoid, and Atkinson (1969) has developed a similar numerical method for this morphology, given that the shape is preserved during growth. An analytical solution to the same problem, for a constant diffusion coefficient, has been given by Horvay and Cahn (1961).

### 5.3. Diffusion-Controlled Growth of Ferrite in Fe-X-C Alloys: Local Equilibrium

The diffusion-controlled growth of ferrite in Fe-X-C alloys is complicated by the fact that both interstitial and substitutional diffusion occurs during transformation; the respective diffusion coefficients differ substantially and this combined with the assumption of local equilibrium at the interface leads to a variety of possible growth modes (Hillert, 1953; Kirkaldy, 1958; Purdy *et al.*, 1964; Coates, 1973c).

If it is assumed that local equilibrium exists during the diffusion-controlled growth of  $\alpha$  from  $\gamma$ , the compositions of the phases at the interface are connected by a tie-line of the  $\alpha + \gamma$  phase field in the equilibrium Fe-X-C phase diagram. For the discussion that follows, we choose  $X = \text{Mn}$  (identified in concentration terms by the subscript  $i = 2$ ); Mn is an austenite stabilizing element but the concepts discussed are general to all substitutional alloying elements which dissolve in austenite.

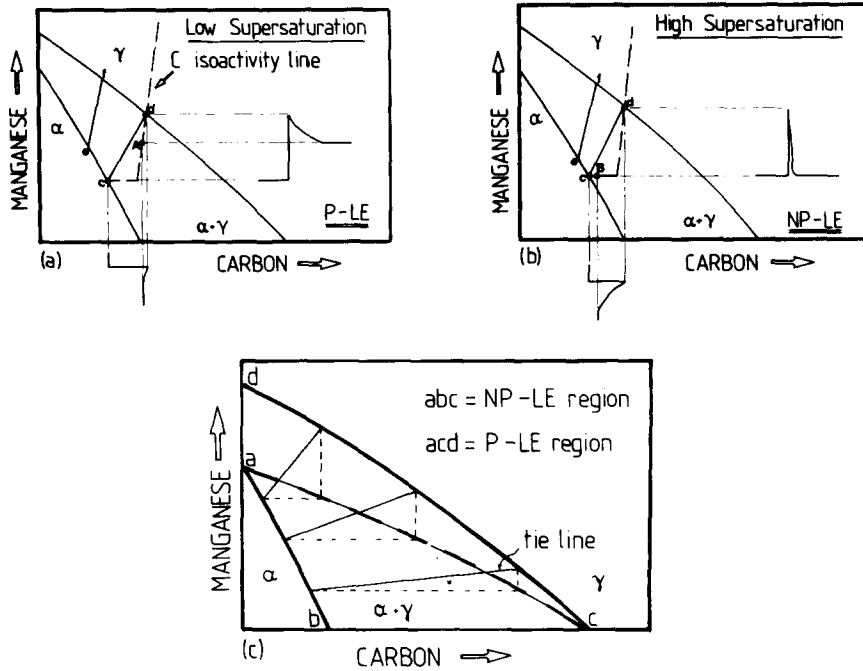


FIG. 4. Schematic isothermal sections of the Fe-Mn-C system, illustrating ferrite growth occurring with local equilibrium at the  $\alpha/\gamma$  interface. (a) Growth at low supersaturations (PLE) with bulk redistribution of Mn, and (b) growth at high supersaturations (NP-LE) with negligible partitioning of Mn during transformation. The bulk alloy compositions are designated "A" and "B" in Figs 4a and b respectively, and (c) division of the  $\alpha + \gamma$  phase field into domains where either the PLE or the NP-LE mechanisms can operate.

Schematic isothermal sections of the Fe-Mn-C phase diagram are presented in Fig. 4. For an alloy of composition  $\bar{c}_1, \bar{c}_2$ , it might seem that the tie-line defining interface compositions should pass through the point  $\bar{c}_1, \bar{c}_2$ , but this is not correct because Mn and C diffuse at very different rates. Conservation of mass at a planar interface moving with a speed  $v$  in the direction  $z$  (normal to the interface plane) requires that

$$(c_1^{\gamma\alpha} - c_1^{\alpha\gamma}) v = -D_{11} \text{grad } c_1 - D_{12} \text{grad } c_2 \tag{5.15a}$$

$$(c_2^{\gamma\alpha} - c_2^{\alpha\gamma}) v = -D_{22} \text{grad } c_2 - D_{21} \text{grad } c_1, \tag{5.15b}$$

where all the concentration gradients are in the austenite and are evaluated at the position of the interface ( $z = Z$ ). Since  $D_{12}$  and  $D_{21}$  are relatively small, these equations reduce to:

$$(c_1^{\gamma\alpha} - c_1^{\alpha\gamma}) v = -D_{11} \text{grad } c_1 \tag{5.15c}$$

$$(c_2^{\gamma\alpha} - c_2^{\alpha\gamma}) v = -D_{22} \text{grad } c_2. \tag{5.15d}$$

Because  $D_{11} \gg D_{22}$ , these equations cannot in general be simultaneously satisfied for the tie-line passing through the alloy composition  $\bar{c}_1, \bar{c}_2$ . It is however possible to choose other tie-lines which satisfy eq. 5.15; if the tie-line is such that  $c_1^{\gamma\alpha} \cong \bar{c}_1$  (e.g. line cd for alloy A of Fig. 4a), then  $\text{grad } c_1$  will become very small, the driving force for carbon diffusion in effect being reduced, so that the flux of carbon atoms is forced to slow down to a rate consistent

with the diffusion of Mn. Ferrite growing by this mechanism is said to grow by a 'Partitioning, Local Equilibrium' (or PLE) mechanism, in recognition of the fact that  $c_2^{\gamma}$  can significantly differ from  $\bar{c}_2$ , giving considerable partitioning of Mn into  $\gamma$ , with consequent long-range diffusion of Mn in  $\gamma$  (Coates, 1973c).

An alternative choice of tie-line could allow  $c_2^{\gamma} \rightarrow \bar{c}_2$  (e.g. line cd for alloy B of Fig. 4b), so that grad  $c_2$  is drastically increased since only very small amounts of Mn are partitioned into the  $\gamma$ . The flux of Mn atoms at the interface correspondingly increases and Mn diffusion can then keep pace with C, satisfying the mass conservation conditions of eq. 5.15. Growth of  $\alpha$  in this manner is said to occur by a 'Negligible Partitioning, Local Equilibrium' (or NPLE) mechanism, in recognition of the fact that the Mn content of  $\alpha$  approximately equals  $\bar{c}_2$ , so that little if any Mn partitions into  $\gamma$  (Coates, 1973c).

The exact choice of tie-line will be discussed quantitatively at a later stage; we first consider some general points concerning tie-line choice. In a Fe-Mn-C alloy, both C and Mn are austenite stabilizers and tend to partition into  $\gamma$ . It follows that  $c_1^{\gamma\alpha}$  and  $c_2^{\gamma\alpha}$  must always be greater than or equal to  $\bar{c}_1$  and  $\bar{c}_2$  respectively.  $c_1^{\alpha\gamma}$  and  $c_2^{\alpha\gamma}$  will always be less than or equal to  $\bar{c}_1$  and  $\bar{c}_2$  respectively. Tie-lines such as 'ef' (Fig. 4a, b) are therefore inappropriate and this leads to the division of the  $\gamma + \alpha$  phase field into regions where either the PLE or NPLE mechanism can operate (Fig. 4c) in a mutually exclusive manner.

These restrictions additionally imply that for an alloy lying close to the  $\gamma/\gamma + \alpha$  phase boundary (i.e. transforming at a low degree of supersaturation),  $c_2^{\alpha\gamma}$  will be significantly lower than  $\bar{c}_2$  so that the alloy can only transform by the PLE mechanism. Similarly, for an alloy lying close to the  $\alpha/\alpha + \gamma$  phase boundary (i.e. transforming at a high degree of supersaturation),  $c_1^{\gamma\alpha}$  will be significantly higher than  $\bar{c}_1$ , so that only the NPLE mechanism can operate.

In summary, given that the growth of  $\alpha$  from ternary  $\gamma$  occurs at a rate which is diffusion-controlled, with local equilibrium at the moving interface, the tie-line of the  $\alpha + \gamma$  phase field which defines the interface compositions does not in general pass through the point in the  $\alpha + \gamma$  phase field which identifies the alloy composition. This is because the diffusivities of interstitial and substitutional alloying elements in  $\gamma$  are significantly different. The appropriate tie-line must be chosen to satisfy mass conservation conditions at the moving interface and must be consistent with the partitioning behaviour of the alloying elements. Hence, the tie-line for an alloy transforming at a low supersaturation is such that there is considerable partitioning and long-range diffusion of substitutional alloying element, while the driving force for carbon diffusion is reduced to a level which allows the substitutional element flux to keep up with the carbon flux at the interface. This is the PLE mode of transformation.

At higher supersaturations, the determining tie-line causes negligible partitioning of substitutional alloying element between the  $\alpha$  and  $\gamma$  lattices, so that the gradient of the  $X$  element in the  $\gamma$  near the interface is very large. This drastically increases the driving force for  $X$  diffusion in  $\gamma$  and allows the flux of  $X$  to keep pace with the long-range diffusion of C in  $\gamma$ . This is the NPLE mode of transformation, where the diffusion of  $X$  in  $\gamma$  is short-range, being confined to the immediate vicinity of the interface.

We note that both of these modes of transformation involve local equilibrium at the interface and are therefore equally favoured on thermodynamic considerations alone. Both C and  $X$  diffuse during growth and their fluxes satisfy the equations for conservation of mass at the interface; it follows that  $v$  calculated from the diffusion of C in  $\gamma$  will be identical to that calculated from the diffusion of Mn in  $\gamma$ . Both elements control the growth rate and neither can be said to restrict the interface motion on its own.

5.3.1. *Quantitative determination of the tie-line and interface velocity*

For Fe-X-C alloys it seems reasonable to assume that the distribution of carbon in  $\gamma$  has an insignificant effect on the flux of X in  $\gamma$  (Coates, 1973a, b). This is because  $D_{11} \gg D_{22}$ , so that  $|\text{grad } c_2| \gg |\text{grad } c_1|$ . The  $D_{21}$  term of eq. 5.2 can thus be neglected, so that:

$$J_1 = -D_{11} \text{grad } c_1 - D_{12} \text{grad } c_2 \tag{5.16a}$$

$$J_2 = -D_{22} \text{grad } c_2. \tag{5.16b}$$

From eq. 5.16 and Fick's second law of diffusion it can be shown (Coates, 1973c) that for one-dimensional growth along a co-ordinate  $z$ , the differential equations for the matrix are:

$$(\partial c_1 / \partial t) = D_{11} (\partial^2 c_1 / \partial z^2) + D_{12} (\partial^2 c_2 / \partial z^2) \tag{5.17a}$$

$$(\partial c_2 / \partial t) = D_{22} (\partial^2 c_2 / \partial z^2) \tag{5.17b}$$

assuming that the diffusion coefficients are concentration independent.

Kirkaldy (1958) has given solutions of the multicomponent diffusion eq. 5.17 for the growth of linear, cylindrical and spherical precipitates (1, 2 and 3 dimensional growth, respectively) of uniform composition in an infinite medium, for constant diffusion coefficients. For the boundary conditions corresponding to the one-dimensional, diffusion-controlled growth of ferrite of uniform composition along the co-ordinate  $z$ , Kirkaldy's solutions show (see Coates, 1973a) that provided  $D_{11}$  does not equal  $D_{22}$ , the concentrations in the matrix as a function of time and distance are given by:

$$c_1 \{z, t\} = \bar{c}_1 + D_{12} (c_2^{\gamma\alpha} - \bar{c}_2) E_1 \{z, D_{22}\} / (D_{22} - D_{11}) \\ + [(c_1^{\gamma\alpha} - \bar{c}_1) - [D_{12} (c_2^{\gamma\alpha} - \bar{c}_2) / (D_{22} - D_{11})]] E_1 \{z, D_{11}\} \tag{5.18a}$$

and

$$c_2 \{z, t\} = \bar{c}_2 + (c_2^{\gamma\alpha} - \bar{c}_2) E_1 \{z, D_{22}\} \tag{5.18b}$$

where

$$E_1 \{z, t, D_{ii}\} = [\text{erfc} \{z / (4D_{ii}t)^{0.5}\}] / [\text{erfc} \{Z / (4D_{ii}t)^{0.5}\}] \tag{5.18c}$$

where  $z = Z$  defines the position of the interface, so that

$$Z = \alpha_1 t^{0.5} = \eta_1 (D_{11} t)^{0.5} = \eta_2 (D_{22} t)^{0.5} \tag{5.18d}$$

where  $\eta_1$  are growth constants, related to  $\alpha_1$ , the parabolic rate constant for one-dimensional growth. Equation 5.18a can be applied to Fe-C alloys if  $D_{12}$  is set to zero.

On combining eq. 5.18a-d with the mass conservation conditions (eq. 5.15a, b with  $D_{21} = 0$ ), Coates (1973b) shows that:

$$f_1 = H_1 \{D_{11}\} - [B_1 D_{12} / (D_{11} - D_{22})] [H_1 \{D_{22}\} - H_1 \{D_{11}\}] \tag{5.19a}$$

where

$$B_1 = (c_2^{\gamma\alpha} - c_2^{\alpha\gamma}) / (c_1^{\gamma\alpha} - c_1^{\alpha\gamma}) \tag{5.19b}$$

$$f_2 = H_1 \{D_{22}\}. \tag{5.19c}$$

We note that if  $D_{12} = 0$ , then eq. 5.19a becomes equivalent to eq. 5.13a.

For transformations occurring under conditions of local equilibrium at the interface, only one of  $c_1^{\alpha\gamma}$ ,  $c_1^{\gamma\alpha}$ ,  $c_2^{\alpha\gamma}$ ,  $c_2^{\gamma\alpha}$  is independent, since they are all linked by a tie-line of the  $\alpha + \gamma$  phase

field of the equilibrium phase diagram. The equations (5.19) therefore contain only two unknowns and can be simultaneously solved to determine the growth velocity and the tie-line governing interface compositions during growth.

### 5.3.2. Two- and three-dimensional growth with local equilibrium

Coates (1972), using the general solutions of Kirkaldy (1958), has solved the diffusion equations for two-dimensional and three-dimensional growth (radial growth of cylinders and growth of spheres, respectively) involving local equilibrium at the  $\gamma/\alpha$  interface in Fe-X-C alloys. The assumptions involved are the same as those used in the analysis of one-dimensional growth, with the additional approximation that capillarity effects may be neglected. Coates found that for two-dimensional growth,

$$f_1 = H_2\{D_{11}\} - [B_1 D_{12}/(D_{11} - D_{22})][H_2\{D_{22}\} - H_2\{D_{11}\}] \quad (5.20a)$$

$$f_2 = H_2\{D_{22}\} \quad (5.20b)$$

where

$$H_2\{D_{ii}\} = (0.25\alpha_2^2/D_{ii}) (\exp\{0.25\alpha_2^2/D_{ii}\}) Ei\{0.25\alpha_2^2/D_{ii}\} \quad (5.20c)$$

where  $Ei$  is the (tabulated) exponential integral function (Abramowitz and Stegun, 1964).

For three-dimensional growth,

$$f_1 = (0.5\alpha_3^2/D_{11}) [1 - H_1\{D_{11}\}] - 0.5B_1(D_{12}/(D_{11} - D_{22}))\alpha_3^2[(1 - H_1\{D_{22}\})/D_{22}] \\ - ((1 - H_1\{D_{11}\})/D_{11}) \quad (5.20d)$$

$$f_2 = (0.5\alpha_3^2/D_{22}) [1 - H_1\{D_{22}\}], \quad (5.20e)$$

$\alpha_2$  and  $\alpha_3$  are the parabolic rate constants for two- and three-dimensional growth respectively.

The concentration distributions in  $\gamma$  during two- and three-dimensional growth can be obtained by substituting the functions  $E_2$  or  $E_3$  (respectively) for  $E_1$  into eq. 5.18a, b where

$$E_2\{z, t, D_{ii}\} = [Ei\{z^2/(4D_{ii}t)\}]/[Ei\{Z^2/(4D_{ii}t)\}] \quad (5.20f)$$

and

$$E_3\{z, t, D_{ii}\} = [\exp\{z^2/(4D_{ii}t)\}/z \\ - (4\pi)^{0.5} \operatorname{erfc}\{z/(4D_{ii}t)^{0.5}\}]/[\exp\{Z^2/(4D_{ii}t)\}/Z \\ - (4\pi)^{0.5} \operatorname{erfc}\{Z/(4D_{ii}t)^{0.5}\}]. \quad (5.20g)$$

Equations 5.20a, 5.20d and all the equations giving the concentration distributions in the matrix can also be used to calculate two- and three-dimensional growth rates in binary alloys (e.g. Fe-C), if  $D_{12}$  is set to zero. The equations for binary growth were first obtained by Zener (1949) and Frank (1950).

### 5.3.3. Concentration dependent diffusion coefficients

The above theory for diffusion-controlled growth is based on the assumption that the diffusion coefficients are concentration independent and this is recognised to be an unrealistic assumption. Coates (1973c) has suggested that the concentration dependence of  $D_{11}$  can be taken into account by substituting the weighted average diffusivity  $D_{11}$  (eq. 5.10) for  $D_{11}$ , even though eq. 5.10 is strictly only valid for steady-state growth situations.

The ratio  $D_{12}/D_{11}$  is also concentration dependent, but the numerical calculations of Bolze *et al.* (1969) suggest that the use of a constant  $D_{12}/D_{11}$ , evaluated at the composition  $(c_1^{\gamma\alpha}, c_2^{\gamma\alpha})$  gives an adequate approximation to the problem (Coates, 1973c).

5.3.4. *Interface composition (IC) contours for diffusion-controlled growth*

The interface compositions  $(c_1^{\alpha\gamma}, c_2^{\alpha\gamma}, c_1^{\gamma\alpha}, c_2^{\gamma\alpha})$  for a ternary alloy of composition  $(\bar{c}_1, \bar{c}_2)$  are connected by a tie-line of the equilibrium phase diagram when ferrite growth occurs under conditions of diffusion-control with local equilibrium at the interface. When  $D_{11} = D_{22}$ , all alloys which lie on a given tie-line transform at different rates, but with identical compositions at the moving interface. If an ‘interface-composition contour’ (Coates, 1973b) is defined as a curve straddling the two phase  $\alpha + \gamma$  phase field, identifying all alloys which transform with the same compositions at the interface, then the tie-line corresponds to an interface-composition (IC) contour for all binary alloys and also for ternary alloys where  $D_{11} = D_{12}$ . When  $D_{11}$  does not equal  $D_{22}$ , the tie-line determining the interface compositions does not in general pass through the point defining the average alloy composition and IC contours no longer coincide with tie-lines. The derivation of an IC contour depends on the ratio  $D_{11}/D_{22}$  and on the nature of interactions between components 1 and 2.

By substituting eq. 5.18d and eq. 5.13d into eq. 5.19a, b the following functions can be derived:

$$\bar{c}_1 = \bar{c}_1 \{ \eta_1 \} \tag{5.21a}$$

$$\bar{c}_2 = \bar{c}_2 \{ \eta_1 \}. \tag{5.21b}$$

Elimination of  $\eta_1$  gives

$$\bar{c}_2 = \bar{c}_2 \{ \bar{c}_1 \}. \tag{5.22}$$

Equation 5.22 defines an IC contour joining the points  $(c_1^{\alpha\gamma}, c_2^{\alpha\gamma})$  and  $(c_1^{\gamma\alpha}, c_2^{\gamma\alpha})$ ; the straight line joining these points is the tie-line defining interface compositions during the local equilibrium growth of  $\alpha$  from  $\gamma$  whose composition lies on the IC contour. With these interface compositions, the flux balance equations (5.15) are automatically satisfied for all alloys on the IC contour. Every point lying on this IC contour represents a bulk composition which transforms with the same interface compositions. The functional relation of eq. 5.22 will in general be complex but can be numerically solved to yield IC contours (Coates, 1973b). Figure 5 illustrates some IC contours (Coates, 1973b) for various ratios  $D_{11}/D_{22}$  and  $B_1 D_{12}/D_{11}$ , for a given tie-line.

We note from Fig. 5 that as the ratio  $(D_{11}/D_{22})$  becomes large, the IC contour essentially consists of two straight segments which, together with the tie-line, form a triangle within the two-phase field. In the horizontal segment,  $f_2 = 1$  whereas in the near vertical segment,  $f_1 = -B_1 D_{12}/D_{11}$  with  $f_2 \cong 0$ . For all alloys lying on the vertical segment, the fast diffuser has its driving force for diffusion reduced to nearly zero, so that it is forced to slow down to the pace of the slow diffuser; there is also considerable partitioning of component 2, giving PLE growth.

On the other hand, for all alloy compositions falling on the horizontal segment, the amount of partitioning of component 2 is reduced to negligible levels so that growth occurs by the NPLE mode. The transition between these two modes of growth is logically taken to be the point  $(f_2 = 1, f_1 = -B_1 D_{12}/D_{11})$ , the vertex of the triangle formed by the tie-line and the two segments of the IC curve. This is of course, an approximation, since the vertex is not sharp, but rounded. By joining all such points on the phase diagram, the latter can be divided into

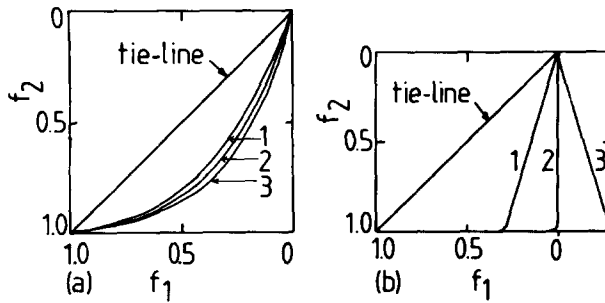


FIG. 5. Typical IC contours for a substitutionally alloyed steel, given that the tie-line slope  $B_1$  is unity (after Coates, 1973c). (a) IC contours for a system where  $D_{11}/D_{22} = 10$ ,  $D_{12}/D_1 = -0.1, 0, 0.1$  for curves 1, 2 and 3 respectively, and (b) IC contours for a system where  $D_{11}/D_{22} = 10^6$ ,  $D_{12}/D_1 = 0.3, 0, 0.3$  for curves 1, 2 and 3 respectively.

two regions, one involving growth with negligible partitioning of 2 (NPLE), and the other in which the fast diffuser is forced to keep pace with the slow diffuser (PLE).

Given that  $D_{12}/D_{11}$  is evaluated at  $c_2 = c_2^{\gamma\alpha}$ , and assuming that eq. 5.7a applies, Coates (1973b) has shown that the line  $f_1 = -B_1 D_{12}/D_{11}$  corresponds to the carbon isoactivity line passing through  $(c_1^{\gamma\alpha}, c_2^{\gamma\alpha})$ ; this was first deduced by Hillert (1953) on the basis of qualitative arguments. We note, however, that the model of Kirkaldy and Coates is quite general and is not restricted to cases where  $D_{11} \gg D_{22}$ , as is that of Hillert.

### 5.3.5. Interface velocity (IV) contours

Coates (1973b) has also defined interface velocity contours; every point on an IV contour defines a bulk composition for which precipitate growth proceeds at the same rate. The  $\alpha/\alpha + \gamma$  and  $\gamma/\gamma + \alpha$  phase boundaries represent two such contours since the interface velocity will be infinite and zero respectively for all alloys falling on these boundaries, assuming that interface motion remains diffusion-controlled under all circumstances.

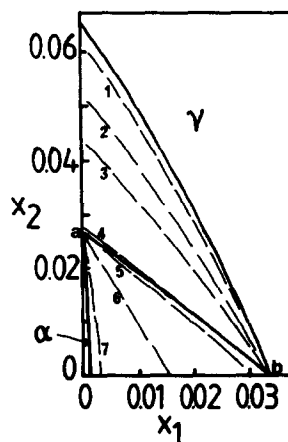


FIG. 6. Typical IV contours for the Fe-Mn-C (after Coates, 1973c). Curves 1, 2, 3, 4, 5, 6 and 7 correspond to  $100\eta_i = 0.01, 0.05, 0.1, 10, 100$  and  $500$  respectively.

For large  $D_{11}/D_{22}$ , the boundary between the PLE and NPLE regions is also an IV contour. All other contours in the  $\alpha + \gamma$  phase field can be derived using eq. 5.19. Of course, the velocity is a function of time, so that the contours really represent say lines with a constant  $\alpha_1$  values from which the velocity may be derived for any given value of time.

The contours are in general curves, which for  $D_{11} \cong D_{22}$ , follow roughly parallel paths to the two phase boundaries. As the ratio  $D_{11}/D_{22}$  increases, there is a progressively increased tendency for the IV contours to radiate from the point  $f_1 \cong 0$  on the  $c_1$  axis in the PLE region, and from the point  $f_2 = 1$  on the  $c_2$  axis in the NPLE region. Typical IV contours are illustrated in Fig. 6.

### 5.3.6. Tie-line shifting due to soft impingement

In the kinetic treatments presented earlier, the austenite was assumed to have a semi-infinite extent in the region beyond the  $\alpha/\gamma$  interface, so the composition of the  $\gamma$  at a large enough distance from the interface does not change with precipitate size or with time during isothermal transformation. The boundary conditions for diffusion-controlled growth therefore remain constant; it follows that the composition of the ferrite also remains constant during transformation and there is no diffusion within the ferrite (since  $x_i^*$  do not change with time).

The assumption of constant boundary conditions is not valid for real systems where the  $\gamma$  has a finite extent, since the diffusion fields of particles growing from different points must eventually interfere. Even if transformation involves the growth of just one precipitate, its diffusion field must eventually collide with the limiting surfaces of the finite specimen. This interference is called 'soft impingement' and leads to changing boundary conditions with time. The tie-line appropriate for local equilibrium growth must therefore also shift as a function of time. As discussed earlier, the tie-line representing interface compositions during transformation does not pass through the bulk alloy composition in Fe-X-C alloys, but the effect of soft impingement is to gradually shift the operative tie-line closer to the bulk composition, until it eventually passes through the latter, causing reaction to cease. This also implies that the  $\alpha$  composition at the interface changes with time and the resulting concentration gradients formed within the ferrite (extending from the interface in the  $-z$  direction) cause diffusion within the ferrite. The diffusion-controlled growth problem then has to be treated by setting up diffusion equations (like eq. 5.16, 5.17) for both  $\alpha$  and  $\gamma$ ; the mass conservation eq. 5.15 also has to take account of the additional flux at  $z = Z$ , due to diffusion in  $\alpha$  (Tanzilli and Heckel, 1968; Randich and Goldstein, 1975; Goldstein and Randich, 1977).

Goldstein and Randich (1977) have used numerical methods to study tie-line shifting during isothermal transformation as a function of precipitate size in Fe-Ni-P alloys (P = 1, Ni = 2, Fe = 3). In this alloy,  $D_{11} \cong 100D_{22}$ . Their results indicate that the major part of the precipitate growth occurs during the initial stages of transformation, prior to significant soft impingement of the faster diffusing P. During this period, the interface tie-line remains constant, and does not significantly alter even after the onset of P impingement. Furthermore, precipitate growth is parabolic with respect to time, prior to the beginning of Ni impingement. Growth slows down considerably with the onset of Ni impingement and the tie-line shifts towards the tie-line passing through the bulk composition. The precipitate hardly grows during this stage, and the phases tend to homogenize during this process. When the interface tie-line actually passes through the bulk composition, growth ceases. Goldstein and Randich point out that in a real system, where impingement distances may vary, it should not be surprising to find precipitates which have different compositions in the same alloy for the

same growth time; this implies lack of equilibrium, but equilibrium in this sense may take too long in practice.

Goldstein and Randich's numerical treatment becomes extremely expensive in terms of computing time, when  $D_{11} \gg 100D_{22}$ . Gilmour *et al.* (1972b) have presented an approximate but analytical treatment (for  $\alpha$  formation by the NPLE mechanism) of the soft impingement problem in Fe-X-C alloys. Gilmour *et al.* consider the movement of a planar  $\alpha/\gamma$  interface in a direction  $z$  which is normal to the interface plane;  $z$  is positive in the austenite, and  $z = Z$  defines the position of the interface at any time  $t$ , with  $Z = 0$  at  $t = 0$ . The austenite has a finite size  $L$  in the  $z$  direction, and the one-dimensional growth of  $\alpha$  is assumed to begin by the NPLE mechanism. Any diffusion fields in the  $\gamma$  should follow an error function relation (eq. 5.18a, b) but the field can be approximated by assuming the concentration to vary linearly with  $z$ . The concentration profile is approximated as a straight line, whose end point lies a distance  $z_{id}$  ahead of the interface. The concentration gradient in  $\gamma$  is therefore assumed to be uniform, given by  $(c_1^{\gamma\alpha} - \bar{c}_1)/z_{id}$ , where  $z_{id}$  is an effective diffusion distance for component  $i$ , defining the region of the austenite in which the concentration differs from  $\bar{c}_i$ . This is the Zener (1949) linearised gradient approximation and implies that the diffusion field (of element  $i$ ) extends only a finite distance  $z_{id}$  into the  $\gamma$ , instead of the infinite distance implied by an error function.

Gilmour *et al.* considered the soft impingement process to occur in three fairly distinct stages (Fig. 7). In the first stage, the interface moves as if there is no soft impingement, with  $z_{id} < (L - Z)$  and  $c_1\{L\} = \bar{c}_1$ , and  $Z$  varying parabolically with time (eq. 5.18d). The parabolic rate constant  $\alpha_1$  during this stage is obtained by solving eqs 5.19a, d.

During the second stage, impingement of the carbon diffusion field with the boundary at  $z = L$  occurs since  $z_{id} > (L - Z)$ . The position of the interface at the onset of carbon impingement is defined by  $Z = Z_1$ , and the second stage begins at  $t = t_1$ . During this stage, the carbon concentration rises everywhere in the  $\gamma$  ahead of the interface and  $c_1\{L\} > \bar{c}_1$ , although  $c_2\{L\} = \bar{c}_2$  since impingement of component 2 has not occurred. When the carbon reaches uniform activity (i.e. when  $Z = Z_2$ ,  $t = t_2$ ) in the austenite,  $c_1\{L\} = c_1^{\gamma\alpha}$ . By balancing the amount of carbon enrichment of the austenite against the carbon depletion of the ferrite (assuming  $c_1^{\alpha\gamma} = 0$ ), it can be demonstrated that for  $Z_2 > Z > Z_1$ ,

$$c_1\{L\} \cong [2L\bar{c}_1 - c_1^{\gamma\alpha}(L - Z)]/(L - Z). \quad (5.23a)$$

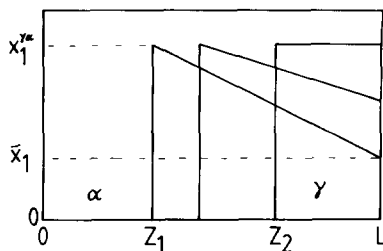


FIG. 7. Diagram illustrating the soft-impingement process described by Gilmour *et al.* (1972b). The carbon concentration of the ferrite is assumed to be zero, and  $x_1^{\gamma\alpha}$  refers to the paraequilibrium carbon concentration of the  $\gamma$ . Since Mn does not redistribute during the first two stages of soft-impingement.

The first stage is completed when  $Z = Z_1$ , and the second when  $Z = Z_2$ .

On combining this with eq. 5.15c, and integrating the resulting differential equation gives the interface position as a function of time, during stage 2:

$$t - t_1 \cong D_{11}[(Z_1^2 - Z^2) + (4B_2 + 2Z_2) - 2B_2^2 \ln((Z_2 - Z)/(Z_2 - Z_1))], \quad (5.23b)$$

where  $B_2 = L\bar{c}_1/c_1^{\gamma\alpha}$  and  $Z > Z_1$ . We note that eq. 5.23b does not represent a parabolic relation between  $Z$  and  $t$ , and is in this sense inconsistent with the results of the finite element method of Goldstein and Randich (1977). Gilmour *et al.* also derived  $t_1$  by a similar procedure:

$$t_1 \cong L^2\bar{c}_1c_1^{\gamma\alpha}/[D_{11}(c_1^{\gamma\alpha} - \bar{c}_1)^2]. \quad (5.23c)$$

For both of the above equations,  $D_{11} = D_{11}\{c_1^{\gamma\alpha}\}$ ;  $t_2$  can be obtained by substituting say  $Z = 0.99Z_2$  into eq. 5.23b.

For an Fe-Mn-C alloy, Gilmour *et al.* found  $t_1 + t_2$  to be relatively small compared with the time required for subsequent Mn diffusion, and hence suggested that the tie-line governing interface compositions does not shift at all during the first two stages.

At the end of the second stage, the chemical potential of the carbon is uniform throughout; the third stage involves the slow partitioning of  $X$  from  $\alpha$  to  $\gamma$ . Gilmour *et al.* dealt specifically with the Fe-Mn-C system, and since Mn diffuses much faster in  $\alpha$  than in  $\gamma$ , they assumed that concentration gradients in  $\alpha$  are negligible. During the third stage, the interface tie-line shifts such that the rapidly adjusting carbon distribution remains very close to the conditions of uniform activity. Using similar methods to those used in deriving eq. 5.23b, they showed that the time  $(t - t_2)$  taken for  $c_2^{\alpha\gamma}$  to change from  $c_2^{\alpha\gamma}\{t_2\}$  to any subsequent value  $c_2^{\alpha\gamma}\{t\}$ , is given by

$$(t - t_2) = (L^2/D_{22}) \int_{F_1\{c_2^{\alpha\gamma}\{t\}\}}^{F_1\{c_2^{\alpha\gamma}\{t_2\}\}} d[F_1\{c_2^{\alpha\gamma}\{t\}\}]^2/F_2\{c_2^{\alpha\gamma}\{t_2\}\}, \quad (5.23d)$$

where

$$F_1\{c_2^{\alpha\gamma}\} = (c_1^{\gamma\alpha} - \bar{c}_1)/c_1^{\gamma\alpha} \quad (5.23e)$$

and

$$F_2\{c_2^{\alpha\gamma}\} = (c_2^{\gamma\alpha} - \bar{c}_2)^2/[(\bar{c}_2 - c_2^{\alpha\gamma})(c_2^{\gamma\alpha} - c_2^{\alpha\gamma})]. \quad (5.23f)$$

We note that  $F_1$  and  $F_2$  can be defined to be functions of just  $c_2^{\alpha\gamma}$  because the other three interface compositions are not independent, being specified by a tie-line. The maximum time for the third stage depends on the equilibrium  $X$  content of the  $\alpha$ , as determined by the equilibrium tie-line passing through the bulk composition. Gilmour *et al.* have shown that their model is in reasonable agreement with experimental evidence on Fe-Mn-C alloys. Finally, we note that eqs 5.23a-c can be used to treat soft impingement in Fe-C alloys after making appropriate substitutions for the various concentration terms.

#### 5.4. Diffusion-Controlled Growth of Ferrite in Fe-X-C Alloys: Paraequilibrium

Kinetic factors often prevent transformations from occurring under equilibrium conditions; Gibbs (1961), Darken (1949), Darken and Gurry (1953), Baker and Cahn (1971) and Cahn (1980) have discussed the different kinds of kinetically constrained equilibria that arise naturally. One example of a constrained phase equilibrium is when a phase change is so rapid that one or more of the components cannot redistribute among the phases in the time scale of the experiment. For transformations in steels, the diffusion coefficients of substitutional and interstitial components differ so greatly that it is possible to imagine circumstances where

the sluggish substitutional alloying elements may not have sufficient time to redistribute during transformation of  $\gamma$  to  $\alpha$  (Hultgren, 1951; Hillert, 1952; Rudberg, 1952; Aaronson *et al.*, 1966), even though carbon may partition into the austenite.

Hultgren introduced the term 'paraequilibrium' to describe the constrained equilibrium between two phases which are forced to have the same substitutional to iron atom ratio, but which (subject to this constraint) achieve equilibrium with respect to carbon.

We first consider the thermodynamic definition of paraequilibrium for a Fe-X-C alloy. Equilibrium between austenite and ferrite (of homogeneous compositions  $x_{i\alpha}$  and  $x_{i\gamma}$  respectively, with  $i = 1, 2, 3$ ) is said to exist when

$$\mu_i^\alpha \{x_{1\alpha}, x_{2\alpha}, x_{3\alpha}\} = \mu_i^\gamma \{x_{1\gamma}, x_{2\gamma}, x_{3\gamma}\} \quad (5.24)$$

for  $i = 1, 2, 3$ . When eq. 5.24 is satisfied,  $x_{i\alpha} = x_i^{\alpha\gamma}$  and  $x_{i\gamma} = x_i^{\gamma\alpha}$ . Austenite and ferrite are said to be in paraequilibrium when

$$x_{2\alpha}/x_{3\alpha} = x_{2\gamma}/x_{3\gamma} = \bar{x}_2/\bar{x}_3 \quad (5.25a)$$

and

$$\mu_1^\alpha = \mu_1^\gamma. \quad (5.25b)$$

The Gibbs free energy change  $\Delta G$  per mole reacted for reactions in a closed system, when an infinitesimal amount of material of composition  $x_{i\alpha}$  is transferred from  $\gamma$  of composition  $x_{i\gamma}$  to  $\alpha$  of composition  $x_{i\alpha}$  is given by:

$$\Delta G = x_{1\alpha}(\mu_1^\alpha - \mu_1^\gamma) + x_{2\alpha}(\mu_2^\alpha - \mu_2^\gamma) + x_{3\alpha}(\mu_3^\alpha - \mu_3^\gamma), \quad (5.25c)$$

where the chemical potentials in the  $\gamma$  and  $\alpha$  are evaluated at the compositions  $x_{i\gamma}$  and  $x_{i\alpha}$  respectively.

$\Delta G$  clearly equals zero when  $\alpha$  and  $\gamma$  are in equilibrium, since the chemical potential differences are zero (eq. 5.24). The paraequilibrium state is also specified by setting  $\Delta G = 0$  (subject to the constraint of eq. 5.25a), so that on combining eq. 5.25a, b with eq. 5.25c we get:

$$\mu_2^\gamma - \mu_2^\alpha = (\mu_3^\alpha - \mu_3^\gamma) (\bar{x}_3/\bar{x}_2). \quad (5.25d)$$

Equation 5.25c is another description of the paraequilibrium state and was first derived by Gilmour *et al.* (1972a).

We note that during the equilibrium formation of  $\alpha$  from  $\gamma$ , the chemical potential of carbon is identical in both phases at the interface, and this remains the case when  $\alpha$  forms from  $\gamma$  by a paraequilibrium mechanism. However, the equilibrium and paraequilibrium concentrations of carbon in  $\alpha$  or in  $\gamma$  will in general differ because the chemical potential of carbon is a function of all elements in solution. The substitutional element concentrations are different for the two cases. The equilibrium phase diagram cannot be used to specify interface tie-line compositions for paraequilibrium. The paraequilibrium phase diagram is constructed on the basis of eq. 5.25 rather than eq. 5.24 and Hillert (1952) has shown that the paraequilibrium phase boundaries lie within the  $\alpha + \gamma$  phase field of the equilibrium phase diagram. Furthermore, the tie-lines of the paraequilibrium  $\alpha + \gamma$  phase field all satisfy eq. 5.25a, and hence represent lines along which the substitutional to iron atom ratio is constant. Typical paraequilibrium and equilibrium Fe-Mn-C diagrams are illustrated in Fig. 8. It is clear that for any given alloy, a critical undercooling below the equilibrium transformation temperature is necessary before paraequilibrium transformation becomes feasible. This is

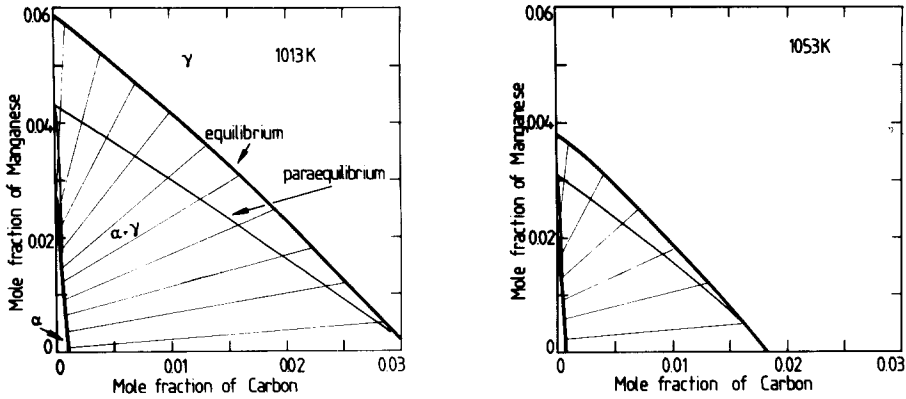


FIG. 8. Typical calculated isothermal sections of the equilibrium and paraequilibrium phase diagrams of the Fe-Mn-C system (after Bhadeshia, 1983b). The tie-lines for the paraequilibrium diagram are virtually horizontal since the Fe/Mn ratio is constant everywhere during paraequilibrium transformation.

simply a reflection of the fact that a relatively lower free energy change accompanies the formation of ferrite which is forced to accept a non-equilibrium substitutional alloy content.

Ferrite formation under conditions of paraequilibrium essentially implies that the substitutional lattice is configurationally frozen and the transformation occurs at a rate controlled by the diffusion of carbon in the austenite; the driving force for paraequilibrium transformation is dissipated in this process alone. The substitutional alloying elements influence kinetics only through their effect on the limiting carbon concentrations at the interface, since they alter the thermodynamics of the  $\gamma \rightarrow \alpha$  transformation (i.e. the phase diagram). There may also be a smaller effect on the diffusion coefficient of carbon through the influence of  $X$  elements on the activity of carbon in  $\gamma$  (eq. 5.11). Having established the paraequilibrium phase diagram, the diffusion-controlled growth rate for ferrite can be calculated using the theory relevant for Fe-C alloys, after substituting the paraequilibrium carbon concentrations for  $x_1^{\gamma\alpha}$  and  $x_1^{\alpha\gamma}$ . This involves the assumption that paraequilibrium exists locally at the interface.

#### 5.4.1. Solute and solvent trapping

Considering paraequilibrium transformation in Fe-Mn-C alloys, with the substitutional lattice configurationally frozen, the chemical potential of Mn in the ferrite that forms is higher than in the parent austenite (Mn is an austenite stabilizer). Ferrite formation therefore leads to an increase in the chemical potential of the Mn (and, by eq. 5.25d, to a decrease in the chemical potential of Fe); the Mn is therefore passively trapped in the  $\alpha$  by the advancing  $\alpha/\gamma$  interface. Baker and Cahn (1969) called this effect 'Solute-Trapping', where a component is said to be trapped when it experiences an increase in chemical potential due to the passage of the transformation interface.

If a Fe-Si-C alloy undergoes paraequilibrium transformation to  $\alpha$ , then Si is a ferrite stabilizer and its chemical potential decreases on entering the  $\alpha$  lattice, while that of the major component Fe increases; this amounts to 'Solvent-Trapping'.

Equilibrium transformation involves no solute or solvent trapping.

As a general rule (Baker and Cahn, 1971),

$$\Delta\mu_i = \mu_i^\alpha - \mu_i^\gamma = RT \ln [(x_{i\alpha}x_i^{\gamma\alpha})/(x_{i\gamma}x_i^{\alpha\gamma})]. \quad (5.26)$$

Component  $i$  is said to be trapped when  $\Delta\mu_i$  is positive—i.e. when  $[(x_{i\alpha}x_i^{\gamma\alpha})/(x_{i\gamma}x_i^{\alpha\gamma})] > 1$ . Although ferrite growth is usually considered to occur by either paraequilibrium or equilibrium transformation, an infinite number of other possibilities exist. All compositions of  $\alpha$  which allow  $\Delta G$  of eq. 5.25c to be zero or negative constitute possible  $\alpha$  compositions that can in principle form from  $\gamma$  (Baker and Cahn, 1971).

For a binary alloy, this implies that  $\alpha$  formation can involve: (1) equilibrium transformation; (2) transformation in which one of the species is trapped (with  $\Delta\mu = 0$  for the other element); and (3) non-equilibrium transformation in which neither solute nor solvent is trapped (with  $\Delta\mu < 0$  for both elements). For a ternary alloy, the following possibilities arise: (1) equilibrium transformation; (2) transformation in which one of the species is trapped, with another species having equal chemical potential in both phases (e.g. paraequilibrium); (3) transformation in which one of the species is trapped, with no species having equal chemical potential in both phases; (4) transformation in which two components are trapped; and (5) non-equilibrium transformation in which none of the components are trapped.

Finally, Baker and Cahn (1971) have pointed out that in circumstances where some components are trapped, the transfer of components across the interface cannot be independent if there is to be a net reduction in free energy.

#### 5.4.2. *The transition from local equilibrium to paraequilibrium*

When  $D_{11} \gg D_{22}$ , ferrite growth with local equilibrium at the interface can occur in two fairly distinct ways. At low supersaturations, there is bulk partitioning of the slow diffuser, the activity gradient of the fast diffuser (in the  $\gamma$ ) being reduced to a negligible level. At high supersaturations, there is negligible partitioning of the slow diffuser, so that its activity gradient in the  $\gamma$  is large enough to allow it to keep pace with the faster diffusing element.

Paraequilibrium transformation involves zero partitioning of substitutional elements during transformation, the ratio  $x_2/x_3$  being constant across the interface, even on the finest conceivable scale.

Hillert (1969), and Coates (1973b) have considered the conditions leading to the onset of paraequilibrium transformation. Coates has shown that for one-dimensional growth occurring at high supersaturations, with local equilibrium at the interface, the approximate extent ( $z_{2d}$ ) of the diffusion field of component 2 in the austenite ahead of the interface is given by:

$$z_{2d} \cong 2D_{22}/v, \quad (5.27)$$

$z_{2d}$  is therefore a function of temperature, driving force and particle size  $Z$ . As  $z_{2d}$  decreases, either due to an increase in  $v$  or a decrease in  $D_{22}$ , the composition perturbation in the  $\gamma$  ahead of the interface becomes smaller in extent until  $z_{2d}$  becomes small compared with atomic dimensions and loses physical significance. Indeed, Coates (1973b) has suggested that the perturbation then becomes a part of the interface, since the dependence of the diffusivity on concentration gradient becomes significant, giving rise to a soft-interface energy term as in spinodal decomposition. These considerations led Coates to suggest that when  $z_{2d} \cong 1$  nm, growth switches from local equilibrium to the paraequilibrium mode†. Since  $z_{2d}$  increases with particle size, Coates suggests that under suitable conditions, the particle may begin isothermal

†Karlyn *et al.* (1969) used a similar criterion to define the onset of the massive transformation in binary alloys.

growth by a paraequilibrium mechanism and then given way to growth by the local equilibrium mechanism.

Hillert (1969) has applied similar reasoning to the problem and has concluded that with increasing undercooling below the equilibrium transformation temperature, local equilibrium growth gives way to paraequilibrium; this depends on the unlikely assumption that interface velocity increases monotonically with decreasing temperature. Bhadeshia (1983a) has pointed out that because of this assumption, Hillert's attempt at explaining the bay in steel time-temperature-transformation (TTT) curves is also not correct.

—While it seems intuitively reasonable that deviations from local equilibrium must arise when  $z_{2d}$  becomes comparable to atomic dimensions, Hillert (1981) has pointed out that this reasoning fails in the case of pearlite and massive transformations. A large amount of data on the effect of alloying elements on pearlite growth can be understood by assuming the existence of local equilibrium during transformation, even though calculated values of  $z_{2d}$  are in most cases less than 0.1 nm (Hillert, 1981). It seems therefore that the criteria governing the transition to paraequilibrium are not well established. Coates (1973b) first raised the possibility that gradient energy terms may become significant when  $z_{2d}$  becomes small. The gradient energy coefficient, which has prominence in the theory of spinodals (Cahn, 1961, 1962), only becomes significant in diffusion theory when composition gradients are established over very short distances. In the present context, the influence of the gradient energy coefficient should be to reduce interface velocity, thereby leading to an increase in  $z_{2d}$ . This may be an important factor in the apparent failure of the present criteria for the breakdown of local equilibrium, although a detailed analysis is not yet available.

## 6. INTERFACE-CONTROLLED GROWTH

### 6.1. Pure Iron

In pure iron, the only factor limiting the growth of  $\alpha$  by the continuous motion of a flat  $\alpha/\gamma$  interface is the transfer of atoms across the interface. If the activation free energy (per mole) for this process is  $\Delta G^*$ , absolute reaction rate theory can be used (Christian, 1975) to show that

$$v = \delta_b f^* \exp\{-\Delta G^*/RT\} [1 - \exp\{-\Delta G_3^{\alpha\gamma}/RT\}] \quad (6.1a)$$

where  $\delta_b$  is the thickness of the interface, and  $f^*$  is an attempt frequency for atomic jumps across the interface. For small undercoolings below the equilibrium transformation temperature, this equation simplifies to

$$v = (\delta_b f^*/R) \exp\{-\Delta G^*/RT\} [\Delta G_3^{\alpha\gamma}/T], \quad (6.1b)$$

so that the velocity is proportional to  $\Delta G_3^{\alpha\gamma}$ ; the free energy is entirely dissipated in interface processes, since  $\Delta G_3^{\alpha\gamma} = G_I$  according to eq. 4.2 for pure iron. If the interface is curved then the net free energy change accompanying interface motion is reduced in proportion to the increase in interface area due to the growth process (Machlin, 1969), leading to a reduction in growth rate.

We note that for the more general case of mixed interface and diffusion-controlled growth, eq. 6.1b becomes

$$v = (\delta_b f^*/R) \exp\{-\Delta G^*/RT\} [G_I/T] \quad (6.1c)$$

where

$$G_I = \Delta G' - G_D = \Delta G_3^{\alpha\gamma} - G_D.$$

$G_D$  being the free energy dissipated in driving the diffusion in the matrix ahead of the interface.

Equation 6.1a has been derived on the basis of a specific model for the interface, but Christian has pointed out that there is in general no fundamental justification for expecting a linear relation between driving force and the interface velocity.

## 6.2. Iron Alloys

Local equilibrium does not exist at the interface during interface-controlled growth in alloys, the transport of atoms across the boundary being the rate-controlling factor. Growth occurs with virtually no concentration gradient in the matrix at the interface since solute can diffuse at a rapid rate compared with interface velocity. It follows that the chemical potential of one or more element is discontinuous at the phase boundary and the flux  $J_b$  of solute across the boundary is some function of the chemical potential discontinuity  $\Delta\mu_i$  (Nolfi *et al.*, 1969). For binary alloys, the simplest assumption takes this flux to be directly proportional to the chemical potential difference. Considering interface-controlled growth of  $\alpha$  from metastable  $\gamma$  in a Fe-C alloy,

$$J_b = B_3 \Delta\mu_1 = B_3 (\mu_1^\alpha \{c_1^\alpha\} - \mu_1^\gamma \{c_1^\gamma\}) \quad (6.2a)$$

where  $B_3$  is a proportionality constant. If the  $\alpha$  grows with its equilibrium composition, then it follows that

$$J_b = B_3 (\mu_1^\alpha \{c_1^{\alpha\gamma}\} - \mu_1^\gamma \{c_1^\gamma\}) = B_3 (\mu_1^\gamma \{c_1^{\alpha\gamma}\} - \mu_1^\gamma \{c_1^\gamma\}) \cong B_4 (c_1^{\alpha\gamma} - c_1^\gamma). \quad (6.2b)$$

If  $v$  is taken to be linearly related to  $J_b$ , then

$$v = M (c_1^{\alpha\gamma} - c_1^\gamma) \quad (6.2c)$$

where  $M$  is called the interface mobility. When growth is interface-controlled,  $c_1^\gamma \cong \bar{c}_1$  and eq. 6.2c becomes

$$v = M (c_1^{\alpha\gamma} - \bar{c}_1). \quad (6.2d)$$

Given that the various assumptions made above can be justified experimentally, eq. 6.2c implies that  $v$  is proportional to the deviation of the concentration in the matrix at the interface, from the equilibrium concentration. Since the chemical potentials of the two species in a binary alloy are related by the Gibbs-Duhem relation, eq. 6.2c can also be written in terms of the concentration difference of iron atoms. For higher order alloys in which the elements diffuse at significantly different rates, it would be necessary to identify the particular element controlling interface velocity.

Other models (Hillert, 1975) of interface-controlled growth in steels assume that the velocity is some function of the free energy  $G_I$  (eq. 4.2) dissipated in interface processes. If the latter is assumed to be proportional to velocity, then

$$v = B_5 G_I \quad (6.2e)$$

where  $B_5$  is a proportionality constant. For dilute Fe-C alloys in which the ferrite grows with the equilibrium composition,  $G_I$  is approximately proportional to  $(c_1^{\alpha\gamma} - \bar{c}_1)$  so that eq. 6.2e is similar to eq. 6.2d.

## 7. THE LEDGE MECHANISM OF INTERFACE MOTION

## 7.1. Movement of an Isolated Ledge

An interface can move in two ways: atoms may cross all parts of the interface, causing it to move as a whole, or they may attach themselves to the product phase only at favourable sites such as steps, in which case only the steps move. The normal displacement of the stationary part of the boundary then occurs by the passage of such steps across the boundary, the amount of displacement depending on the step height.

It has long been recognised that interfaces whose orientations correspond to sharp minima in interfacial free energy (i.e. singular interfaces) will tend to move by a step mechanism, rather than by the continuous displacement of every element of the interface (Gibbs, 1961; Burton *et al.*, 1950; Aaronson, 1962). Cahn (1960) has presented a general condition for predicting whether growth will be continuous or stepped; the occurrence of stepped growth depends on the existence of periodic equilibrium interface configurations whose spacing determines the height of the steps. Cahn showed that the existence of equilibrium interface configurations also depends on the driving force for transformation, so that stepped growth becomes less likely at high undercoolings.

In this section, we consider the rate of motion of an isolated step, noting that theory has only been formulated for binary diffusion; it follows that for steels, the theory can only be applied to Fe-C and Fe-X alloys and also Fe-X-C alloys which transform by the paraequilibrium mechanism.

If the steps are linear then they are called ledges; Cahn *et al.* (1964) have shown that for a series of ledges of height  $d$ , the velocity  $v$  with which the stationary part of the interface is normally displaced (by the motion of steps) is given by:

$$v = d n_s v_s \quad (7.1)$$

where  $n_s$  is the number of steps per unit length and  $v_s$  is the mean step velocity. Equation 7.1 assumes the absence of soft-impingement between the diffusion fields of neighbouring ledges.

Jones and Trivedi (1971) first considered the problem of determining  $v_s$  for solid-state transformations. They considered the steady-state motion of a square ended ledge (moving in the direction  $y$ , the normal to the interface being in the direction  $z$ , Fig. 9). Their method involves the approximation that the concentration gradient in the matrix at the step face is constant; although this is inconsistent with the steady-state growth assumption (both the concentration and its gradient should vary along the step face), the approximation is not too severe (Atkinson, 1981).

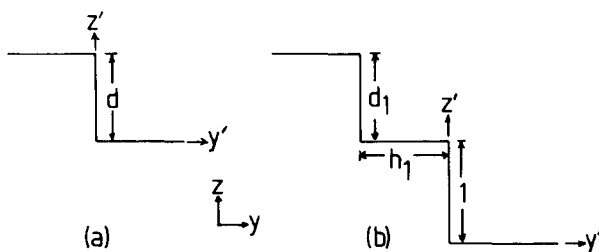


FIG. 9. Diagram illustrating the step geometry: (a) single step; and (b) two-step train.

For solid-state transformations, step motion can be controlled by the diffusion of atoms to the step or by the transfer of atoms across the step or by some combination of the two processes. The dependence of  $v_s$  on diffusion in the parent phase can be obtained by performing a flux balance across the step face (cf. eq. 5.15):

$$v_s = D_{11} (\partial c_1 / \partial y)_{\text{step}} (c_1^\alpha - c_1^\gamma)^{-1}. \quad (7.2a)$$

If growth occurs under interface-control, then  $c_1^\gamma \neq c_1^{\gamma\alpha}$  and if it is assumed that  $v_s$  is linearly proportional to the deviation of  $c_1^\gamma$  from equilibrium, then:

$$v_s = M (c_1^{\gamma\alpha} - c_1^\gamma). \quad (7.2b)$$

Since the step is assumed to move at a constant speed, the concentration ( $c_1\{y', z'\}$ ) distribution with respect to a moving co-ordinate system ( $y', z'$ , Fig. 9) attached to the step cannot change with time,  $c_1\{y', z'\}$  must therefore obey a time-independent diffusion equation in two-dimensions. By analogy with Rosenthal's (1946) work on the temperature distribution around a moving heat source, the normalised diffusion equation is given by:

$$\text{div}(D_{11} \text{grad } c_1\{y', z'\}) + 2p \partial c_1 / \partial y' = 0 \quad (7.2c)$$

where  $p$  is the Péclet number (a dimensionless velocity), given by

$$p = v_s d / 2D_{11} \quad (7.2d)$$

and the normalised, moving co-ordinates are defined by

$$y' = (y - v_s t) / d \quad (7.2e)$$

$$z' = z / d, \quad (7.2f)$$

$c_1'$  is a dimensionless solute concentration in the matrix, given by

$$c_1' = [c_1\{y', z'\} - \bar{c}_1] / (c_1^\gamma - \bar{c}_1). \quad (7.2g)$$

Using eq. 7.2g, a function  $H_3\{p\}$  can be defined as follows:

$$H_3\{p\} = -(\partial c_1' / \partial y')_{\text{step}}^{-1} = (\bar{c}_1 - c_1^\gamma) / [d(\partial c_1 / \partial y)_{\text{step}}]. \quad (7.2h)$$

By combining eqs 7.2a, b and 7.2h, Trivedi and Jones derived the following relation for  $v_s$ :

$$v_s = M(\bar{c}_1 - c_1^{\gamma\alpha}) [1 + M(c_1^{\alpha\gamma} - c_1^{\gamma\alpha}) (d/D_{11}) H_3\{p\} - 2p H_3\{p\}]^{-1}. \quad (7.3)$$

The equation takes account of both matrix diffusion and interface kinetics effects and it remains to obtain the function  $H_3$  (which is the negative of the reciprocal of the concentration gradient at the step), by solving the differential equation 7.2a subject to boundary conditions which allow the concentration gradient at the step face to be constant, and which include the condition that the step progresses without change of shape. Equations expressing these boundary conditions are (Jones and Trivedi, 1971; Atkinson, 1981):

$$\partial c_1' / \partial z' = 0 \text{ on } z' = 1, y' < 0 \quad (7.4a)$$

$$\partial c_1' / \partial z' = 0 \text{ on } z' = 0, y' > 0 \quad (7.4b)$$

$$\partial c_1' / \partial z' = -(H_3)^{-1} \text{ on } y' = 0, 0 < z' < 1. \quad (7.4c)$$

The first two boundary conditions ensure that the isoconcentration contours around the ledge (in the matrix) are always normal to the stationary parts of the interface. Equation 7.4c specifies a constant concentration gradient at the step face. Trivedi and Jones (1971)

determined  $H_3$  by using numerical techniques, but their calculations do not seem to be correct (Atkinson, 1981). Atkinson used two methods to solve for  $H_3$ : the more rigorous method was based on the numerical solution of eqs 7.2, 7.4. The other method involved a singular perturbation technique (valid for  $p \ll 1$ ) in which an 'outer' solution is obtained for the region where step geometry is unimportant and an 'inner' solution is obtained for the region near the step where details of step geometry are all important. The two solutions are then matched to provide a complete solution. Atkinson's solutions for  $H_3$  are shown in Fig. 10, but for  $p < 0.01$ , singular perturbation theory gives:

$$H_3\{p\} = (1/\pi)[1 - C - \ln(4\pi/p)] \tag{7.4d}$$

where  $C$  is the Euler constant approximately equal to 0.5772.

Both Atkinson, and Jones and Trivedi found the concentration distribution around the ledge to be assymetrical in  $y'$ , the type of assymetry differing in detail, since in Jones and Trivedi's treatment  $c'_1$  becomes zero at some finite distance from the ledge. According to Atkinson,  $c'_1$  should only be zero at infinity, the concentration distribution (in the 'outer' region) being defined by:

$$c'\{y', z'\} = [1/(H_3\pi)] \exp\{-py'\} K_0\{p[(y')^2 + (z')^2]^{0.5}\} \tag{7.5}$$

where  $K_0$  is a modified Bessel function of zero order.

The diffusion profile decays exponentially to zero in front of the step, but decays as  $p[(y')^2 + (z')^2]^{0.5}$  behind the step. The fact that the extent of the field is larger behind the ledge contradicts the results of Jones and Trivedi. Equation 7.5 is obtained using the singular perturbation method and is valid for  $p < 0.01$ . A diagram illustrating the diffusion field of an isolated step has been published by Enomoto *et al.* (1981), but it seems inconsistent with eqs 7.4a, b since the isoconcentration contours do not end normally on the stationary parts of the stepped interface.

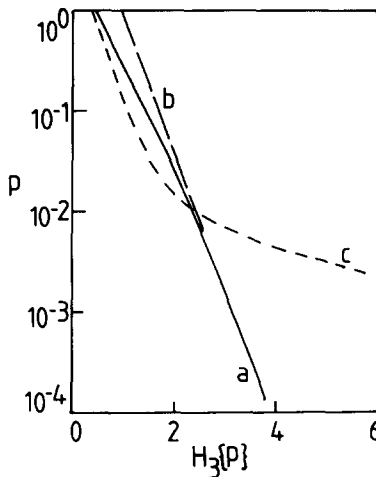


FIG. 10. The functions  $H_3\{p\}$ ; curves (a) and (b) represent a numerical solution, and an approximate solution using singular perturbation theory (after Atkinson, 1981) respectively and curve (c) is due to Trivedi and Jones (1971).

A useful form of eq. 7.3, relating  $f_1$  to  $p$ , has been given by Jones and Trivedi:

$$f_1 = 2pH_3 + (p/q)[1 - 2pH_3] \quad (7.6a)$$

$$q = M(c_1^{\gamma\beta} - c_1^{\gamma\alpha})/(2D_{11}/d). \quad (7.6b)$$

As interface mobility tends to infinity, eq. 7.6a reduces to

$$f_1 = 2pH_3 \quad (7.6c)$$

while if  $M \rightarrow 0$ , then

$$v_s \rightarrow M(c_1^{\gamma\alpha} - \bar{c}_1). \quad (7.6d)$$

## 7.2. Multistep Interactions

An analysis of the growth characteristics of trains of steps was first considered by Jones and Trivedi (1975), but because it was based on an incorrect evaluation of  $H_3$ , Atkinson (1982a) re-analysed the problem for the case where volume diffusion in the parent phase is assumed to be rate-controlling.

If trains of steps exist in which the steps all have equal heights, then they cannot have identical speeds. In a two-step train, the leading step always advances into fresh parent phase, whereas the trailing step moves in a region influenced by the back diffusion field of the leading step. Hence, for steady-state motion, the trailing step has to have a smaller height in order to keep up with the leading step (Atkinson, 1982a).

For the purposes of kinetic theory, a two-step train can be characterised in terms of dimensions normalised relative to the height  $d$  of the leading ledge. The normalised height of the leading ledge is then unity. The height of the trailing step divided by  $d$  is its normalised height  $d_1$  and the normalised separation of the ledges is written  $h_1$ . When  $h_1 \gg 1$ , the diffusion field of a two-step train, in the 'outer' region can be approximated by considering the steps as line sources located at  $(y' = -h_1, z' = 0)$  and  $(y' = 0, z' = 0)$ . For diffusion-controlled growth, eqs 7.6c and 7.5 give:

$$c'\{y', z'\} = [2p/(\pi f_1)] [\exp\{-py'\} K_0\{p[(y')^2 + (z')^2]^{0.5}\} + d_1 \exp\{-py' + ph_1\} K_0\{p[(y' + h_1)^2 + (z' - 1)^2]^{0.5}\}]. \quad (7.7)$$

If the ledges in a two-step train are to move with the same speed, then their heights must differ; for a specified separation  $h_1$ , a value of  $d_1$  and  $p$  consistent with the two-step train moving with constant speed can be obtained by the simultaneous solution of:

$$d_1 \exp\{-ph_1\} K_0\{-ph_1\} + [1 - C - \ln\{p/4\pi\}] = f_1 \pi / 2p, \quad (7.8a)$$

$$\exp\{ph_1\} K_0\{-ph_1\} + d_1 [1 - C - \ln\{pd_1/4\pi\}] = f_1 \pi / 2p. \quad (7.8b)$$

The equations show that for a pair of widely spaced steps moving at the same speed, the size of the trailing step is smaller than the leading step for a given value of  $p$ . For  $h_1 \gg 1$ ,  $d_1$  decreases as  $h_1$  decreases. Extension of the analysis to include closely spaced steps shows that  $d_1$  goes through a minimum as  $h_1$  decreases; the value of  $d_1$  at the minimum decreases as  $p$  increases (Fig. 11). The form of the curves in Fig. 11 implies that for values of  $d_1$  above the minimum, there are two spacings for which the steps travel at the same speed, the larger spacing corresponding to the stable configuration of the train. If  $d_1$  becomes lower than the minimum value, then the train is unstable, the trailing ledge catches up and merges with the leading ledge.

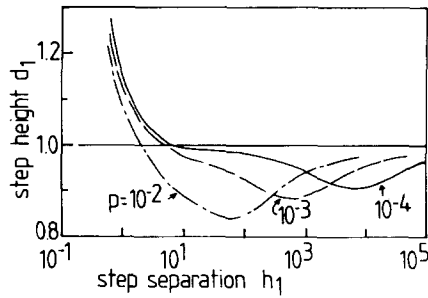


FIG. 11. Plots of normalised height ( $d_1$ ) of trailing ledge vs. normalised ledge separation ( $h_1$ ) for a two-step train in which the normalised height of the leading ledge is unity (after Atkinson, 1982a).

Equations 7.8 can also be used to show that if the height of the two-steps is forced to be equal, then the concentration gradient at the trailing step will be reduced due to the dumping of solute from the diffusion field of the leading step. The trailing step will then have a smaller velocity.

Atkinson has generalised these results to trains containing many steps, and in all cases where  $h_1 \gg 1$ , he finds that  $v_s$  is reduced as the number of steps in the train increases. Other results can be summarised as follows: (i) for closely spaced pairs of steps travelling with equal speed,  $d_1$  increases as  $h_1$  decreases (Fig. 11); (ii) as the separation of steps moving with equal speed decreases, so does their velocity; (iii) steps of equal height tend to separate when  $h_1$  is large, but tend to coalesce when  $h_1$  is small, the changeover occurring at a smaller value of  $h_1$  as  $p$  increases.

### 7.3. Ledge Motion in a Medium of Finite Extent

Atkinson (1982b) considered the problem of steady-state ledge motion during solid-state, diffusion-controlled transformation in a phase whose extent is limited to a finite length  $L$  in the  $z'$  direction. The concentration gradient at an isolated step moving at a constant speed is in such circumstances a function of  $L$  and for  $p \ll 1, L/d \gg 1$ , is given by:

$$-(\partial c'_i / \partial y')^{-1} = H_4\{p\} = (1/\pi) [1 - C + H_5 + \ln(4\pi/p)] \tag{7.9a}$$

where  $H_5$  is a complicated function of  $L/d$  and  $p$  such that  $H_5 \rightarrow 0$  as  $L/d \rightarrow \text{infinity}$ .  $H_5$  is positive as  $L/d$  becomes finite and for  $pL/d \ll 1$ , is approximately given by:

$$H_5 \cong \pi d / 2pL. \tag{7.9b}$$

It follows that  $H_4 \rightarrow H_3$  as  $L/d \rightarrow \text{infinity}$  (cf. eqs 7.9a, 7.4d). The concentration gradient (and velocity) at a step moving in a finite medium is therefore smaller relative to that moving in an infinite medium; the concentration distribution around such a ledge, in the 'outer' region, is given by:

$$c'\{y', z'\} = [1/(H_4\pi)] \exp\{-py'\} [K_0\{p[(y')^2 + (z')^2]^{0.5}\} + H_5]. \tag{7.9c}$$

The concentration at any point in the matrix is therefore higher relative to the case where an infinite medium is involved. Atkinson showed that as  $L/d$  increases,  $v_s$  increases but that for  $p > 0.1, L/d > 10, v_s$  becomes insensitive to further increase in  $L/d$ .

A surprising result is that  $v_s = 0$  if  $f_1 = d/L$ , because the movement of a ledge in these circumstances would force the concentration in the matrix behind the ledge to a level higher than  $c_1^{\text{eq}}$ .

#### 7.4. Relative Kinetics of Stepped and Continuous Growth

Because atoms are only attached to the product phase at a fraction of the boundary, the piecewise displacement of the boundary by step motion must initially be slower than continuous growth, in which every element of the interface is displaced simultaneously. However, for diffusion-controlled growth in the absence of soft-impingement effects, the rate of continuous growth decreases with time (eq. 5.2) whereas  $v_s$  is independent of time. It has been argued that for this reason, ledged motion must eventually overtake continuous growth (Atkinson *et al.*, 1973b; Enomoto *et al.*, 1981). On the other hand, the movement of a step across an interface causes a build up of solute along the interface so that the boundary conditions governing the motion of any succeeding step must be altered (i.e. the supersaturation reduced). There should therefore be a progressive change in the boundary conditions of successive steps and hence a progressive reduction in their velocity (Christian, 1975). In these circumstances, stepped growth may never give a larger growth rate than that for continuous growth, as predicted by the respective linear and parabolic growth laws.

Another problem with the application of such ideas is the absence of information on factors governing the rate of ledge nucleation and ledge height. These determine the geometry of the stepped interface and hence the rate of interface motion.

Bhadeshia (1982b) has considered the problem of ledge nucleation. According to Cahn (1960), the occurrence of stepped growth depends on the existence of periodic equilibrium interface configurations; the spacing of such configurations should presumably correspond to that of the lattice planes parallel to the plane of the interface, so that the steps which accomplish growth would be expected to be of atomic height. However, it is now well established that the diffusional formation of ferrite in steels often occurs by the movement of 'superledges' whose heights can reach several hundreds of lattice spacings (e.g. Honeycombe, 1976). Bhadeshia suggested that this may happen due to the difficulty of nucleating smaller ledges, the minimum ledge height  $d^*$  being given by:

$$d^* = \sigma / \Delta G_v, \quad (7.10)$$

where  $\sigma$  is the interfacial energy per unit area of the stationary part of the stepped interface and  $\Delta G_v$  is the Gibbs free energy change (per unit volume) for the nucleation process. The equation does not set an upper limit to the ledge height, but does seem to correctly predict the temperature dependence of  $d$  (Bhadeshia, 1982b).

While nucleation processes must be of importance in determining  $d$ , Atkinson's work on the stability of ledge trains may provide other clues to this problem.

## 8. SOLUTE-DRAG

Experiments in recrystallisation have convincingly demonstrated the existence of solute-induced diffusional drag on grain boundary motion. The addition of small quantities of 'impurities' can be shown to lead to large changes in the recrystallisation temperatures of deformed materials. Such results can be qualitatively rationalised in terms of the association of solute atoms with moving grain boundaries (Lueke and Detert, 1957; Cahn, 1962b), the

solute-boundary interaction energy  $G_s$ , being negative or positive, depending on whether there is adsorption or desorption (respectively) of the impurity at the boundary. Under certain circumstances, the solute atoms can be expected to be 'dragged' along ( $G_s < 0$ ) with, or pushed ahead ( $G_s > 0$ ) of the boundary, reducing its rate of migration, relative to that expected in a pure material. In considering solute-drag during transformation, it is useful to begin by emphasizing and briefly reviewing some of the relevant aspects of 'conventional' drag theories which deal with the motion of grain boundaries.

### 8.1. Conventional Solute-Drag Theories

#### 8.1.1. Diffusion coefficients for solute-drag theory

All the conventional theories on solute-drag require the segregation (or desegregation) of solute atoms to the interface (to a level which differs from the bulk solute concentration  $\bar{c}_i$ ). The interface itself is assumed to have a finite width  $\delta_b$ , usually defined as the distance normal to the interface plane, over which the solute-interface interaction free energy  $G_s$  is non-zero. The drag force ( $P$ ) on the boundary is obviously zero when segregation does not occur, or when the composition profile due to the segregation is symmetrical with respect to the centre plane of the interface. For a moving boundary, the existence of a finite drag requires the diffusion of solute atoms in the direction of boundary motion; one of the major difficulties in applying solute-drag theory to real problems is the suitable choice of a diffusion coefficient describing this process.

In his theoretical paper on drag effects, Cahn (1962b) took the diffusivity to be some function of the distance from the centre of the boundary, presumably approaching the value of the bulk diffusivity at large distances normal to the interface. At the centre plane of the boundary, the diffusion coefficient would be given by the grain boundary diffusivity. By referring to the results of Turnbull and Hoffman (1954), Cahn suggested that the diffusivity would increase typically by a factor of  $10^6$  as the centre of the boundary was approached. However, the work of Turnbull and Hoffman was concerned with solute transport along the grain boundary, rather than across it—solute drag on the other hand relies on impurity diffusion in the direction of boundary motion, and across the boundary itself. The diffusivity of an interface must in general be considered to be highly anisotropic, reflecting the nature of its defect structure. Hence, it is not surprising that the movement of atoms along the interface is easier than that in the bulk of matter—interface dislocations should act as pipes for the channelling of atoms. However, the transport of atoms across the interface may be a very different problem (Shewmon, 1965); it is now well established that the boundary structure can in general be described in terms of areas of good fit (and hence little free volume, relative to an ideal crystal) separated by localised regions of higher distortion (e.g. interface dislocations). Under these circumstances (at least for coherent and semi-coherent interfaces), the diffusion coefficient describing the movement of atoms across the interface, must be more closely related to bulk diffusivity. These problems are further emphasized by the fact that the boundary width  $\delta_b$  in the solute-drag theories is usually assumed to be equal to a few interatomic distances. Such a large  $\delta_b$  is probably acceptable when  $\delta_b$  is defined as the region over which  $G_s$  is non-zero. However, it is not obvious that the diffusivity should also vary over the same distance  $\delta_b$ .

Finally, there have been suggestions (Smidoda *et al.*, 1978, 1979) that the diffusivity of a moving boundary is higher than that of a stationary one. It is not at all obvious how this might influence the concepts of the solute-drag theory.

### 8.1.2. *Interaction free energy*

While Cahn's solute-drag theory is general, in the sense that both  $D$  and  $G_s$  can be expressed as functions of the distance ( $z - Z$ ), it is usually necessary to make simplifying assumptions about the forms of these functions. The way in which the drag force  $P$  varies with  $G_s$  has been considered by Hillert and Sundman (1976). For cases where  $G_s$  varies gently from zero (at  $z - Z = \pm(\delta_b/2)$ ) to some other value within the boundary, the drag force  $P$  goes through a maximum as the interface velocity increases. However, if  $G_s$  changes discontinuously from a constant value within the boundary to zero at  $z - Z = \pm(\delta_b/2)$ ,  $P$  never decreases with increasing velocity. As Hillert (1969) pointed out, the former choice of  $G_s$  is probably more realistic, especially when the discrete nature of lattices is taken into account. Nevertheless, it is recognised that in the absence of detailed knowledge on solute/interface interactions, the choice of  $G_s$  must be somewhat uncertain. The form of  $G_s$  also determines the region of the boundary from which the main component of the drag force originates (Cahn, 1962b; Hillert and Sundman, 1976). The value of diffusivity in those particular regions would then control the drag effect (Cahn, 1962b). This complication may be minimised if  $D$  was always close to bulk diffusivity, as suggested earlier for semi-coherent interfaces.

### 8.1.3. *Composition profile at the boundary*

The drag theories either predict (Cahn, 1962b), or are designed (Hillert, 1969; Hillert and Sundman, 1976) so that the solute concentration behind (trailing) the interface, during steady-state motion, is always equal to the bulk solute level  $\bar{c}_b$ , as if the boundary did not exist. The solute concentration at  $z - Z < (-\delta_b/2)$  is thus always  $\bar{c}_i$ . For a stationary boundary, the concentration of solute differs from  $\bar{c}_i$  within the region  $(-\delta_b/2) < z - Z < (\delta_b/2)$ . For a moving boundary, the composition differs from  $\bar{c}_i$  not only within the boundary, but also in front of it, irrespective of whether  $G_s$  is less than or greater than zero. The extent of penetration into the region beyond  $z - Z = (\delta_b/2)$  depends on interface velocity amongst other factors.

### 8.1.4. *Drag at interphase-interfaces*

The theory for solute segregation induced drag on transformation interfaces is not well established and the experimental evidence in this area is all the more difficult to interpret.

Hillert (1969, 1975) and Hillert and Sundman (1976) first extended the concepts of grain boundary drag theory to apply to certain special cases of interphase interfaces. They considered transformations in which the product (ferrite) formed from the parent (austenite) without any change in composition—however, the transformation considered was not martensitic, because substitutional solute atoms were allowed to segregate within the interface, with a solute concentration spike in the austenite adjacent to the interface. The height of this extremely narrow concentration spike was chosen to be consistent with the existence of local equilibrium at the interface. Free energy is thus dissipated in driving the  $X$  atom spike ahead of the interface, and in driving the diffusion of  $X$  atoms which have segregated in the boundary itself. This dissipation of free energy manifests itself as a drag force on the interface.

As the velocity of the interface increases, the height of the solute spike in the austenite deviates from local equilibrium; it follows (Hillert and Sundman, 1976) that less free energy is dissipated in driving this reduced spike and so that its contribution to the total drag force diminishes. Eventually, at high enough velocities, only the atoms segregated within the interface contribute to the drag force.

In many ways, the theory relies heavily on the local equilibrium concept, and in addition, is acknowledged (Hillert and Sundman, 1976) to be restricted in applicability to transformations whose parent and product phases have identical compositions. It is not clear whether interface segregation induced solute-drag would significantly contribute in circumstances where the parent and product phases differ in composition and hence require the long range diffusion and redistribution of solute during transformation.

Recently, there have been suggestions implying the existence of significant interactions between substitutional alloying elements and austenite–ferrite transformation interfaces. These have all been referred to as ‘special’ drag effects, since it is claimed that they operate when the transport of solute atoms in the direction of boundary movement can be ruled out.

## 8.2. *Special Solute-Drag Effects*

### 8.2.1. *Interaction of carbide-forming elements with interfaces*

One of the first special drag effects was proposed by Kinsman and Aaronson (1967) who sometimes found the growth rate of allotriomorphic ferrite (in Fe–Mo–C alloys) to be lower than expected from paraequilibrium theory. The observed interface velocities seemed too large to be consistent with the dragging of Mo atoms “along with the interface” by any “volume diffusion or volume diffusion like process”. On the other hand, steels containing ternary additions of Mn or Si exhibited allotriomorphic ferrite growth kinetics somewhat more consistent with paraequilibrium transformation. This stimulated the suggestion that elements which are strong carbide formers have a tendency to ‘be bound’ to ‘disordered’ austenite–ferrite interfaces, due to the higher carbon concentration that would be expected to exist in the austenite at the transformation interface, during growth involving the partitioning of carbon between the parent and product phases. Presumably, this binding between the Mo atoms in the interface and the C atoms in the adjacent austenite would hinder the transfer of the Mo atoms into the ferrite lattice. Kinsman and Aaronson further suggested that the Mo atoms may be required to diffuse short distances along the interphase-interface before completing their transfer into the ferrite, or alternatively, may simply serve as ‘pinning points’ around which the boundary must bend before it can break away.

Before discussing these ideas in detail, it seems that in the original version of the proposal (Kinsman and Aaronson, 1967), the segregation of Mo (or other substitutional alloying elements) atoms to the interphase-interfaces concerned was not implied (although a later paper (Aaronson, 1969) mentions the “segregation of certain alloying elements to austenite–ferrite interfaces”). However, the time of stay of the Mo atoms in the interface was said to be greater than that of weaker carbide formers, so that the iron atoms in the same alloy can be expected to move relatively more rapidly into the ferrite. This must lead to an enrichment of Mo in the interface. Because of these difficulties of interpretation, it was felt necessary to examine the implications of ‘special drag effects’ both in circumstances where the ratio of substitutional atoms to iron atoms is constant throughout the transforming material (absolutely no segregation anywhere), and for cases where interfacial segregation of *X* atoms is envisaged.

### 8.2.2. *The zero-segregation case*

Conventional solute-drag theories are not applicable in such cases and the special drag effect (Kinsman and Aaronson, 1967) involves the concept that the Mo atoms (or any other carbide forming atoms) should experience a binding force with the high-carbon region in the

austenite at the interface. It might intuitively seem reasonable that a strong carbide-former such as molybdenum should behave in this manner. Nevertheless, such an approach does not take proper account of all the other more subtle interactions that must exist between the Mo atoms and the Fe<sub>α</sub>, Fe<sub>γ</sub> and C<sub>α</sub> atoms, respectively. Bhadeshia (1983a) has shown that despite the high carbon concentration in the γ at the interface, the Mo atoms prefer to be in α for the experiments reported by Kinsman and Aaronson.

### 8.2.3. Special drag with segregation at the interface

More recent developments (Aaronson, 1969; Aaronson *et al.*, 1970; Bradley and Aaronson, 1981) of the original (Kinsman and Aaronson, 1967) special drag theory have definitely involved the segregation of *X* elements at the austenite–ferrite transformation interface. Such segregation is supposed to occur “through a sweeping up” of the *X* atoms, rather than by the diffusion of these atoms through the austenite and/or ferrite to these boundaries. The segregated *X* atoms are then meant to significantly effect the activity of carbon in the austenite which is in contact with these interfaces, thereby altering the carbon concentration profile (and hence the interface migration rate) in the austenite ahead of the interface.

*X* elements which reduce the activity of carbon in austenite are therefore claimed to decrease the carbon concentration gradient in the austenite, leading to a drop in the rate of boundary movement. On the other hand, *X* elements which increase the activity of carbon in austenite would then have the opposite effect on growth kinetics (referred to as an “inverse solute-drag-like effect”; Shiflet *et al.*, 1981a).

There are a number of difficulties with these concepts. Firstly, the proposal that the segregation profile of *X* elements, at the interface, should be solely confined to the interface and not extend into the austenite (since *X* is not supposed to diffuse through the volume of the austenite) may not be correct for a moving interface (for a stationary interface the drag force *P* is zero anyway). Cahn’s theory clearly shows, for the grain boundary case, that the solute profile in the vicinity of the moving interface always extends into the region beyond the interface (i.e. in the region  $z - Z > \delta_b/2$ ). It is interesting that when  $G_s < 0$  in the boundary, there is expected to be a decrease in solute concentration, in the austenite just ahead of the interface (see Fig. 2; Cahn, 1962b).

Secondly, the concept that an *X* element which is segregated into the interface will have an effect on the carbon activity in the adjacent austenite is itself doubtful. The proposal ignores the fact that the segregation of *X* will only occur to the extent that the partial molar free energy of *X* in the interface equals that in the austenite, and it fails to treat the boundary as a thermodynamically separate phase. Even though the concentration of *X* in the interface may be different from that in the bulk of the austenite, its influence on the activity of carbon in austenite will be identical to that of the *X* atoms present in the bulk of the austenite.

There is a further difficulty in the concept that the segregating *X* elements which reduce the activity of carbon in austenite would lead to a decrease in the carbon concentration gradient ahead of the interface and hence reduce the growth rate. The limiting carbon concentrations in each of the phases ( $c_1^{\gamma}$ ,  $c_1^{\alpha}$ ) at the interface during diffusion controlled growth are calculated from the condition that the partial molar free energy of carbon in each phase is equal. If an *X* element reduces the activity of carbon in austenite, then to maintain this equality of partial molar free energies, the concentration (and hence concentration gradient) of carbon (i.e.  $c_1^{\alpha}$ ) must correspondingly increase, in contradiction with Kinsman and Aaronson’s hypothesis.

Finally, it should be noted that the diffusivity of carbon in austenite is influenced by the activity coefficient describing the solution of carbon in austenite, and by the carbon–carbon

interaction energy. Both these factors depend on substitutional alloying element concentrations, so that the rate of growth cannot be discussed simply in terms of concentration gradients ahead of the interface—the effect on diffusivity must also be taken into account.

#### 8.2.4. *Interaction of clusters with interfaces*

Sharma and Purdy (1973) proposed that special solute-drag effects may arise if elements such as Cr or Mo tended to form clusters in the austenite, such that carbon atoms became associated with these clusters. Since ferrite can only accommodate a very limited amount of carbon, the motion of the transformation interface would be hindered by the need to strip these clusters from their carbon atomspheres.

In trying to explain various features of TTT curves, Sharma and Purdy went on to suggest that since the formation of clusters (by volume diffusion in the austenite) would be most difficult at lower temperatures, the proposed drag effect should also be most pronounced at low temperatures. This, however, seems illogical since the less easy formation of clusters at low temperatures should reduce any hinderence to interface motion.

Finally, it is appropriate to note that (for low-alloy steels, at least) the activity coefficient of both Mo and Cr in austenite (Kirkaldy and Baganis, 1978) are less than unity, implying that these elements do not tend to cluster in austenite.

## 9. EXPERIMENTAL MEASUREMENTS OF GROWTH KINETICS

### 9.1. *The Thickening of Ferrite Allotriomorphs*

Aaronson (1962) has exhaustively reviewed the experimental data on the growth rate of allotriomorphic ferrite in low-alloy steels; much of the work prior to 1962 was carried out on rather impure steels, sometimes containing several substitutional alloying elements. This, combined with the indirect techniques used has made the results difficult to theoretically interpret (Aaronson *et al.*, 1970). Nevertheless, much of the early data can be interpreted to imply that the rate of thickening of allotriomorphic ferrite is approximately proportional to the reciprocal of the square root of time (parabolic thickening), indicating diffusion-controlled  $\alpha/\gamma$  interface motion.

Purdy and Kirkaldy (1963) designed an elegant experiment to get around the difficulties associated with the earlier work. The experiment involved the construction of a diffusion-couple, by decarburizing a high-purity plain carbon steel. The resulting polycrystalline layer of ferrite on homogeneous, polycrystalline austenite was subsequently isothermally heat-treated in the  $(\alpha + \gamma)$  phase field, causing the macroscopically planar  $\alpha/\gamma$  interface to move. The movement was monitored metallographically by measuring the thickness of the ferrite layer after quenching the couple to ambient temperature. The same couple was then re-heated to the isothermal transformation temperature to allow the same interface to move again. This procedure permits the continuous monitoring, the same interface and eliminates certain statistical errors. The simple geometry of the diffusion-couple means that the stereological difficulties associated with methods which deal directly with ferrite allotriomorphs (randomly orientated with respect to the plane of polish) are also avoided. Since the macroscopic interface separating the two parts of the diffusion-couple is on a smaller scale composed of many different kinds of  $\alpha/\gamma$  interfaces, the experiment really monitors the properties of a crystallographically averaged interface. If local equilibrium is

assumed, then the parabolic rate constant  $\alpha_1$  can be determined from Wagner's diffusion solution applicable to the motion of a planar interphase-interface in a binary diffusion-couple (Purdy and Kirkaldy, 1963). Purdy and Kirkaldy determined  $\alpha_1 = 0.71 \pm 0.05 \mu\text{ms}^{0.5}$  (at 792°C), in excellent agreement with the value expected theoretically ( $0.73 \mu\text{ms}^{0.5}$ ), proving that at 792°C the  $\alpha/\gamma$  interface motion is controlled by the diffusion of carbon in the austenite ahead of the interface.

Purdy, Weichert and Kirkaldy (1964) applied the above method to diffusion-couples consisting of electroplated layers of pure iron on various Fe–Mn–C alloys (1.52–3.16 Mn, 0.21–0.34 C wt.%), transformed between 725–760°C. The solutions to the diffusion problem for Fe/Fe–Mn–C diffusion-couples were obtained using Kirkaldy's (1959) general solutions for ternary diffusion, for the case where diffusion occurs in both the ferrite and austenite. In all the cases investigated, Purdy *et al.* found the interface position to vary in proportion to the square root of time, indicating diffusion-controlled interface motion. Furthermore, the resulting parabolic rate constants compared well with theoretical values calculated on the basis of local equilibrium at the interface (NPLE). These are important and accurate results, but as will be seen later, the current opinion is that Fe–Mn–C alloys transform by the paraequilibrium mechanism (thermodynamics permitting), since  $z_{2d}$  is usually found to be so small as to appear physically insignificant.

Aaronson and Domian (1966), made a detailed electron microprobe study of the bulk partitioning of substitutional alloying elements during the formation of  $\alpha$  in Fe–X–C alloys ( $X = \text{Si, Mn, Ni, Cr, Mo, Co, Al, Cu}$  or Pt). Their results indicate that bulk redistribution of substitutional elements does not occur during transformation as long as the alloys are not transformed at a high temperature where such redistribution is a thermodynamic necessity. At higher undercoolings, bulk partitioning was not detected, indicating  $\alpha$  growth by the NPLE or paraequilibrium mechanism.

Kinsman and Aaronson (1969, 1973) used a hot-stage thermionic electron emission microscope (THEEM) to study the growth of individual ferrite grain boundary allotriomorphs in high-purity plain carbon steels, and ternary steels containing one of Mo, Mn, Si, Al or Co as the substitutional alloying element. Isothermal transformation experiments were carried out within the temperature range 690–920°C, depending on the alloy concerned. THEEM is a powerful technique allowing particular interfaces to be continuously monitored, as in the diffusion-couple experiments, but unlike the latter, the  $\alpha/\gamma$  interface can be at any arbitrary angle to the plane of observation. Bradley and Aaronson (1977) have shown that this can lead to stereological errors which are difficult to correct, so that absolute values of parabolic rate constants obtained using THEEM can be misleading. Significant information can nevertheless be obtained about the time dependence of interface position; in all of their experiments, Kinsman and Aaronson found the interface to move under diffusion-control, although the actual mechanism (PLE, NPLE, paraequilibrium) cannot be clearly deduced in view of the potentially large stereological errors, which also seem to account for the large scatter in experimental  $\alpha_1$  values obtained using THEEM (Bradley and Aaronson, 1977). In spite of these difficulties, Kinsman and Aaronson were able to show that Al, Si and perhaps Co all increase the growth rate of allotriomorphic ferrite (relative to Fe–C alloys), consistent with the fact that these elements increase the free energy change accompanying the  $\gamma \rightarrow \alpha$  transformation.

Kinsman and Aaronson also suggested that the presence of relatively low interface energy facets on parts of some  $\alpha/\gamma$  boundaries may lead to further scatter in  $\alpha_1$  data. These facets, presumably being less mobile, could hinder the progress of the boundary as a whole. It was also suggested that if the facets are displaced by a ledge mechanism, then circumstances could

arise where the faceted parts of the boundary could be displaced faster than the unfaceted parts, due to the point-effect of diffusion at the ledge corners. While these ideas seem reasonable in principle, it remains to be demonstrated that the presence of facets leads to scatter in the parabolic rate constants. Indeed, the faceting seems to be inconsistent with the observed parabolic kinetics. If the process of atom transfer across the interface becomes restrictive (as in the low mobility facets) then the rate at which an interface moves is generally assumed to be constant with respect to time. This can also be the case when the displacement of the facets occurs by a ledge mechanism if the frequency of ledge nucleation is constant. Under these circumstances, the position of the overall interface should not be proportional to the square root of time, as is observed experimentally.

To avoid the stereological problems of the THEEM method, Bradley *et al.* (1977) used a technique developed by Boswell *et al.* (1968) to study the growth kinetics of ferrite allotriomorphs in plain carbon steels (0.11–0.42 wt.%C), for the temperature range 710–840°C. The technique involves the use of very thin steel specimens ( $\sim 250 \mu\text{m}$  thick), austenitised at 1300°C for 30 min to develop a very large austenite grain structure in which the  $\gamma$  boundaries lie normal to the broad faces of the specimen. If the  $\alpha/\gamma$  boundaries formed on transformation turn out to be parallel to the original  $\gamma/\gamma$  boundaries, then metallographic examination of the broad face of the specimen can yield approximate values of the true allotriomorph thickness. This is assumed to happen and all reported results rely on the assumption that the interface is perfectly normal to the plane of observation. Any errors should certainly be smaller than those using the THEEM method. A disadvantage is that the method does not allow the progress of an individual allotriomorph to be followed, since measurements, as a function of time, are taken on different specimens isothermally transformed for different time periods. In each specimen, it is the thickest allotriomorph that is measured. This could lead to significant errors if the incubation period for the nucleation of  $\alpha$  is relatively large.

Bradley *et al.* (1977) found that in all cases, the experimental  $\alpha_1$  values were significantly lower than those calculated using the Atkinson's method for oblate ellipsoids (Atkinson, 1969). These discrepancies were again attributed to the presence of lower interfacial energy facets.

Bradley and Aaronson (1981a) applied the same experimental technique to Fe–1.73Si–0.40C (725–825°C), Fe–3.28Ni–0.12C (650–715°C), Fe–7.5Ni–0.43C (530–570°C), Fe–3.08Mn–0.12C (550–650°C) and Fe–2.99Cr–0.13C (600–800°C), the concentrations being in wt.%, with the transformation temperature range indicated in the brackets. In all cases, the thickness of the allotriomorphs was found to be approximately proportional to the square root of time ( $0.70 < n < 0.32$ )† with the experimental  $\alpha_1$  values being within an order of magnitude of those calculated assuming paraequilibrium transformation. The Si containing steel was in general found to transform at a rate faster than expected from paraequilibrium theory, the remaining steels generally showing the opposite behaviour. Bradley and Aaronson also compared their experimental data with calculations based on the assumption that growth occurs with local equilibrium at the interface (PLE, NPLE). Their local equilibrium calculations are however, incorrect; the calculations contradict the fact that the PLE and NPLE modes are mutually exclusive and that PLE growth always occurs at a slower rate compared with NPLE growth.

For many of the reaction temperatures and alloys used, the lack of accounting for nucleation time (cf. TTT curves published by Aaronson and Domian, 1966, for

† $n$  is the time exponent in the relation  $Z = \alpha_1 t^n$ .

the same alloys) must lead to significant errors, since the incubation times are sometimes comparable to the time spent by the specimen at the isothermal transformation temperature.

There are significant discrepancies in the data on the Si steel which has poor hardenability (TTT curve in Aaronson and Domian, 1966). The results seem to indicate some transformation during the quench from the isothermal transformation temperature. According to Uhrenius (1978), the specimens transformed at 800 and at 825°C should not contain any ferrite. Fairly thick layers of ferrite were obtained after only 20 s of transformation, whereas TTT curves indicate an incubation period of 100 s at 800°C.

On the basis of their results, Bradley and Aaronson suggest the existence of a "solute-drag-like" effect (somewhat similar to the original proposals of Kinsman and Aaronson, 1967), in which misfitting substitutional alloying elements segregate to  $\alpha/\gamma$  interfaces and then influence the carbon concentration gradient in the austenite ahead of the interface. Those segregated elements which increase the activity of C in the  $\gamma$  (e.g. Si, Ni) are supposed to lead to faster than expected growth kinetics (a negative solute drag-like effect) whereas others which reduce the activity of C in  $\gamma$  (e.g. Mn, Cr) similarly cause a positive drag-like effect, so that transformation kinetics are slower than expected from diffusion-controlled growth theory. These ideas are roughly consistent with Bradley and Aaronson's data, but in view of the uncertainties in the data and technique, and due to the lack of an adequate comparison with local equilibrium theory, the existence of a drag effect cannot be considered established. Bhadeshia (1983a) has recently made a detailed assessment of both the available experimental data and the various theories on solute-drag at interphase interfaces and has concluded that both theory and experiment are far from adequate.

Shiflet *et al.* (1981) found carbide precipitation accompanying the formation of some allotriomorphs of ferrite in the alloys examined by Bradley and Aaronson (1981a). Not all of the allotriomorphs in any given alloy exhibited this precipitation. Precipitation of cementite at the  $\alpha/\gamma$  interface ("interphase precipitation") was occasionally found to occur in the Fe-Si-C and Fe-Ni-C alloys and because this occurs at the transformation front, it was considered to influence the rate of interface motion. The interphase precipitation is supposed to increase the driving force for transformation and the faster than expected  $\alpha_1$  values of some of the alloys studied by Bradley and Aaronson were partly attributed to this effect. These ideas are interesting and need to be quantitatively developed, especially to take proper account of any interface pinning (and hence retardation) due to the presence of the carbides, as observed by Purdy (1978). The presence of interphase carbides must modify the diffusion fields of alloying elements in the proximity of the interface. The long-range substitutional element diffusion necessary for the formation of carbides may also influence transformation kinetics (Bhadeshia, 1983a).

Bradley and Aaronson calculated that for virtually every alloy and transformation temperature examined,  $z_{2d}$  was much less than 1 nm, indicating that the ferrite probably grows by a paraequilibrium mechanism. However, as noted earlier, this may not be a definitive method of identifying the breakdown of local equilibrium (Hillert, 1981).

Romig and Salzbrenner (1981, 1982) carried out high-resolution microanalysis experiments on  $\alpha$  formed by isothermally transforming Fe-1.7Si-0.1V-0.1C wt.% steel. The ferrite was found to form without the bulk partitioning of alloying elements, although significant Si and V concentration gradients were detected in both the austenite and ferrite at the interface. The results were shown to be consistent with the growth of  $\alpha$  by the NPLE mechanism, the concentration gradients in the  $\alpha$  arising due to tie-line shifting resulting from soft-impingement effects.

### 9.2. *The Lengthening of Ferrite Allotriomorphs*

Grain boundary ferrite allotriomorphs acquire their characteristic shape because the transformation rate along the boundary is faster than that in the direction normal to the boundary plane. The initial shape of the allotriomorph is approximately that of an oblate ellipsoid (Bradley *et al.*, 1977). The lengthening of allotriomorphs was initially thought to be linear with time, the process being described in terms of the plate lengthening theory (Mehl and Dubé, 1951; Aaronson *et al.*, 1970) but later work (Kinsman and Aaronson, 1973; Atkinson *et al.*, 1973a) has shown that the lengthening is parabolic with respect to time. The rate constant describing the lengthening process is simply  $\alpha_1$  divided by the thickness to length ratio (the aspect ratio) of the allotriomorph.

Bradley *et al.* (1977) found the approximate aspect ratio to be about 1/3, independent of time at transformation temperature. This is consistent with Horvay and Cahn's (1961) theory for the diffusion-controlled growth of oblate ellipsoids. Bradley *et al.* suggested that the experimentally observed aspect ratio is lower than that expected from the balancing of interfacial tensions at the allotriomorph edges, as calculated using the relative interfacial energy data of Gjostein *et al.* (1966). They suggested that this inconsistency probably arises because the shape of the allotriomorph during growth is not controlled by interfacial energy considerations alone.

### 9.3. *Summary*

The experimental data generally indicate that the thickening and lengthening of ferrite allotriomorphs in low-alloy steels occurs at a rate which is approximately proportional to the reciprocal of the square root of time, even when the transformation temperature is as low as 530°C. This indicates that interface motion is diffusion-controlled and does not seem to be significantly limited by interface processes for  $T > 530^\circ\text{C}$ .

For plain carbon steels, growth is controlled by the diffusion of carbon in the austenite ahead of the interface, although the experimentally determined parabolic rate constants seem consistently smaller than theoretically expected, with the exception of one very accurate value determined using the diffusion-couple method.

In substitutionally alloyed steels, transformed at low-supersaturations, ferrite growth necessarily occurs with the bulk redistribution of alloying elements, presumably by the PLE mechanism. Microanalysis of the parent and product phases clearly demonstrates that there is no bulk partitioning of alloying elements during ferrite growth at high supersaturations, but this could be taken to imply either the NPLE or paraequilibrium transformation mechanisms. Some measurements of parabolic rate constants favour the paraequilibrium mechanism, but diffusion-couple and high-resolution microanalysis methods lend support to the NPLE mechanism. If it is assumed that paraequilibrium growth occurs when the extent of the  $X$  element spike in the  $\gamma$  near the  $\alpha/\gamma$  interface is so small as to be physically unreasonable, then it seems that most reported experimental data conform with paraequilibrium. However, there are doubts about the use of such a criterion for establishing the presence of paraequilibrium.

With the exception of the parabolic rate constants obtained for Fe–Mn–C alloys using the diffusion-couple technique (the results being consistent with the NPLE mode), all other reported rate constants significantly differ from theory, and this has been attributed to the presence of faceting, solute-drag-like effects and interphase carbide precipitation. Further work is needed before the influence of such effects can be properly understood.

It seems that the diffusion-couple method is the most accurate of currently available techniques for the measurement of rate constants. Gokhale (1984) has recently proposed another technique (claimed accuracy  $\sim 25\%$ ) based on stereological counting measurements; this promising technique has yet to be applied.

Finally, we note there are no kinetic data for  $\alpha/\gamma$  interfaces which have been crystallographically or structurally characterised.

## 10. MASSIVE FERRITE

### 10.1. *General Aspects of Massive Transformations*

A massive transformation can be defined as one in which the product phase grows diffusively and has the same bulk composition as the parent phase; an excellent review of the subject has been published by Massalski (1970). Being a diffusional transformation, the product phase is not limited by grain boundaries of the parent phase and the ability of product crystals to cross such boundaries seems particularly pronounced in massive transformations. The transformed microstructure is therefore coarse grained, the grain size sometimes exceeding that of the parent phase.

The product phase was originally thought to bear no rational or reproducible crystallographic orientation relationship with the parent phase (Massalski, 1970). Recent work by Plichta *et al.* (1980) and Plichta and Aaronson (1980) suggests that nucleation would be difficult under these circumstances and that low-energy orientation relationships do exist during massive transformation. The issue is not however settled; Massalski (1984) has pointed out that the products examined by Plichta *et al.* may not have formed by massive transformation, and that there are several systems where no rational orientation relations have been found between the massive transformation products and their respective parent phases. The interface responsible for growth during massive transformation is believed to be incoherent (Massalski, 1958), consistent with the diffusional transformation mechanism and with the fact that there is no IPS shape change as a consequence of the transformation. Because of the lack of a composition change, the massive reaction is sometimes called diffusionless, but this is misleading because reconstructive diffusion is still necessary in order to accomplish the lattice change (Massalski, 1958). The transformation is believed to occur at an interface-controlled rate (Karlyn *et al.*, 1969), the interface velocity being independent of time. The interface sometimes moves continuously, adopting a characteristic ragged contour (Fig. 12a), but there is also evidence that it can migrate by a step mechanism (Aaronson *et al.*, 1968).

In binary alloys, precipitate growth without a composition change can occur below the  $T_0$  temperature (at  $T_0$ , parent and product phases of identical composition have equal free energy). The curve representing  $T_0$  as a function of solute concentration lies within the two-phase field where the parent and product phases co-exist in equilibrium. Massive transformation sometimes seems to occur only when the parent phase is transformed at a temperature within the single-phase field (Massalski, 1984, has pointed out some exceptions to this). This may be because at low undercoolings below  $T_0$ , the massive transformation initiates at nuclei whose composition differs from that of the matrix. As a result, the nuclei become surrounded by a solute enriched or depleted zone; for the nucleus to develop into a massive phase, it has to be able to consume the excess solute and accelerate to the

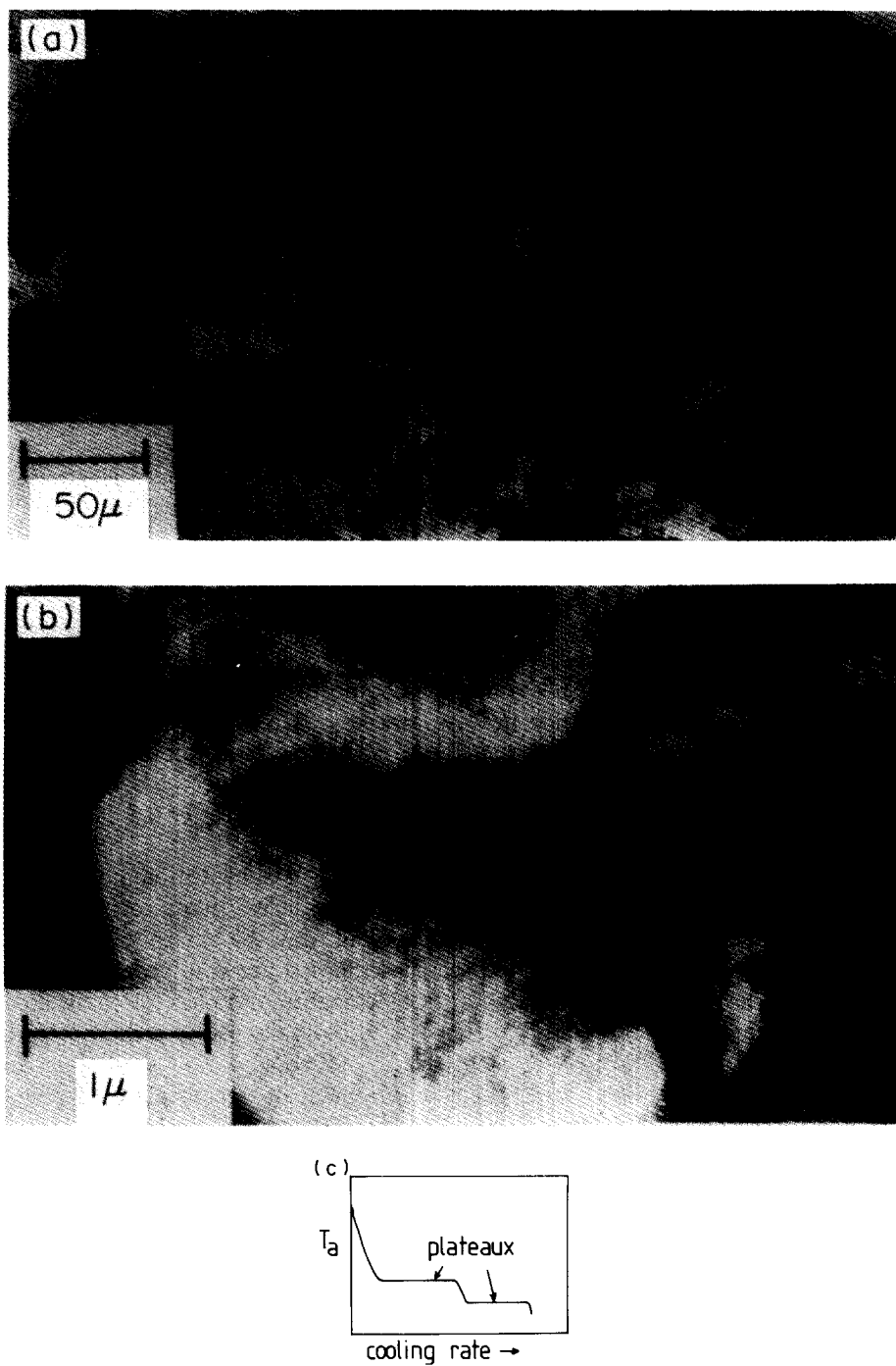


FIG. 12. (a) Optical micrograph showing massive ferrite in Fe-2Mn wt.% alloy, (after Roberts, 1970); (b) transmission electron micrograph of massive ferrite, same alloy as in (a); and (c) schematic plot of  $T_a$  vs. cooling rate, typical of continuous cooling experiments which exhibit just one thermal arrest at a given cooling rate.

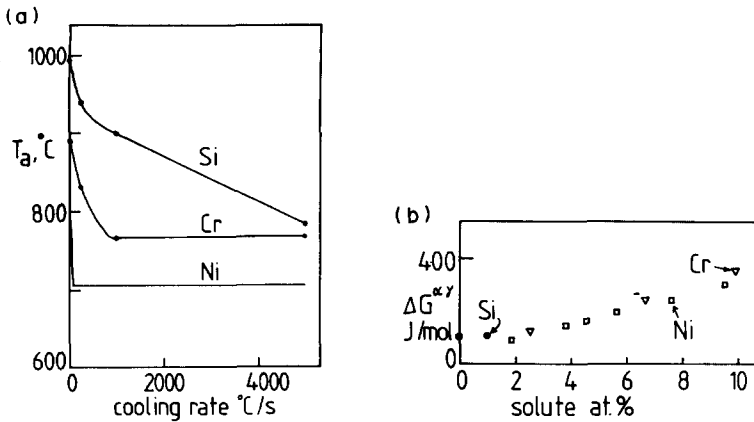


FIG. 13. (a) Results of continuous cooling experiments on Fe- $X$  alloys (the Ni, Si and Cr alloys contain 2.7, 2.7 and 2.6 wt.% of solute respectively); and (b)  $\Delta G^{\alpha\gamma}$  for massive reaction, evaluation at the plateau temperature (after Gilbert and Owen, 1962).

steady-state massive growth rate. Karlyn *et al.* (1969) showed that this can only occur when the alloy is transformed within the single-phase field†.

We note that in ternary alloys, the lack of a bulk composition changes alone is not decisive proof that a diffusional transformation is massive, since the NPLE mechanism of growth also leads to an identical transformation product in the absence of soft-impingement.

### 10.2. Massive Transformation in Iron and its Alloys

Work on the massive transformation in iron ( $\gamma \rightarrow \alpha$ ) and its substitutional alloys is based on continuous cooling experiments, since the rate of reaction is usually too fast to permit isothermal measurements. Transformation during cooling from the austenite phase field can be followed by noting the temperature  $T_a$  at which a thermal arrest appears in the cooling curve. The arrest arises because the enthalpy of transformation modifies the natural cooling curve of the specimen. A linear plot of  $T_a$  vs. cooling rate usually shows a sharp initial drop followed by a plateau region where  $T_a$  is insensitive to cooling rate variations; further increases in cooling rate sometimes lead to the development of further plateaux (Fig. 12c). The highest plateau is usually identified with the massive reaction and the lowest plateau with the formation of martensite although there are differing opinions on the detailed interpretation of cooling curves.

Gilbert and Owen (1962) conducted continuous cooling experiments on "pure" iron (containing  $\sim 0.01\text{C}$  wt.%), Fe-Ni, Fe-Cr and Fe-Si alloys. In pure iron, massive ferrite can form as soon as its nucleation becomes feasible, within the time scale of the experiment; Gilbert and Owen found that the diffusional formation of ferrite is suppressed beyond a cooling rate of about  $5500^\circ\text{C/s}$ , the austenite eventually transforming to martensite at  $545^\circ\text{C}$

†Menon *et al.* (1983) reached this conclusion using thermodynamic arguments, but their treatment relies on the assumption that the nucleus composition is restricted to that giving the largest free energy change. This is incorrect since the nucleus can adopt any composition which leads to a negative free energy change on transformation and nucleation without a composition change is certainly feasible at any temperature below  $T_0$ .

(although martensite formation was not verified by testing for surface relief effects). Some of their results are presented in Fig. 13a which shows that  $T_a$  initially decreases sharply and then levels out at higher cooling rates. In Fig. 13a, the values of  $T_a$  at a zero cooling rate represent transformation temperatures obtained from the relevant binary phase diagrams. It is evident that the influence of alloying elements on  $T_a$  depends on their effect on the equilibrium transformation temperature (i.e. on  $\Delta G^{yz}$ ). Indeed, Gilbert and Owen found  $\Delta G^{yz}$  at the plateau temperature to be independent of the type of alloying element used (Fig. 13b). This is not, however, the whole explanation of alloying element effects, since  $\Delta G^{yz}$  at the plateau temperature gently increases with alloy concentration (though not with alloy type). Gilbert and Owen also demonstrated that the driving force required to initiate massive transformation is always much less than that necessary to induce martensitic reaction.

Bibby and Parr (1964) first used the presence of an IPS shape change to distinguish martensite from massive ferrite in relatively pure iron (<0.01C wt.%). They showed that the  $M_s$  temperature of such iron is sensitive to variations in carbon concentration, increasing to 750°C as the carbon level decreased to <0.0017 wt.%. The critical cooling rate for the transition from massive to martensitic transformation similarly varies from 35000→5000°C as the carbon concentration changes from ~0.005→0.01 wt.%. The reasons for this effect are not clear, but Bibby and Parr suggested that it may have something to do with the association of carbon with substitutional vacancies reducing the self-diffusivity of iron and hence making diffusional transformation more difficult. Later work by Ackert and Parr (1971) has confirmed that the  $M_s$  temperature of low-carbon Fe–C alloys is very sensitive to carbon concentration and this work also indicated that the gap between the massive reaction plateau temperature and the  $M_s$  temperature decreases as the carbon concentration increases, although the reasons for this have not been discussed.

Akert and Parr identified the temperature corresponding to the first plateau with the massive reaction start temperature and this has led Hillert (1975) to conclude that the massive reaction in ferrous alloys starts when the alloys enter the  $\alpha$  single-phase field (as established for a non-ferrous alloy by Karlyn *et al.*, 1969). This cannot be considered established, since massive ferrite may actually form at higher temperatures, before the cooling rate corresponding to the plateau region is reached. Similarly,  $M_s$  temperatures cannot really be identified with the temperature at which the martensite plateau develops in continuous cooling experiments.

Swanson and Parr (1964) similarly showed that the critical cooling rate at the transition from massive to martensitic transformation decreased from 30000→15000°C/s as Ni increased from 1→7 wt.% in pure Fe–Ni alloys. This may be related to the increasing difficulty of nucleating massive ferrite as the stability of the austenite increases with Ni content and as transformation temperatures become depressed.

Parr and his co-workers (Gomersall and Parr, 1965; Wallbridge and Parr, 1966; Parr, 1967) showed that with Fe–Mn, Fe–Cr and Fe–Co alloys, experimental difficulties associated with the fine size of any surface relief effects make the distinction between massive and martensitic reactions difficult to assess, particularly since many of the experimental curves of  $T_a$  vs. cooling rate showed just a single plateau, without the expected discontinuity in  $T_a$  at the critical cooling rate where the transition occurs. The results on these alloys are therefore inconclusive as far as information on the suppression of the massive transformation is concerned.

In view of these difficulties, Pascover and Radcliffe carried out a series of experiments on high-purity Fe–Cr alloys, using the thermal arrest method, for the first time backed by detailed transmission electron microscopy. At very low quench rates, the massive ferrite that

formed consisted of relatively large equiaxed grains containing a low dislocation density, while that formed at higher quench rates had a microstructure of irregular grains with a distinctly higher dislocation density. In both cases, the dislocation distribution resembled that of a recovered microstructure (sub-boundaries, cells, etc.), consistent with the diffusional transformation mechanism. The martensite structure was found to consist of very fine, parallel laths arranged in packets, and Pascover and Radcliffe were able to clearly distinguish between massive ferrite and lath martensite. Their results are interesting in that they observed just one thermal arrest in any given experiment, but that for a given high quench rate, the  $\gamma$  sometimes transformed to massive ferrite but at other times to martensite. This meant that the curves of  $T_a$  vs. cooling rate had, at high cooling rates, two plateaux, the higher one representing massive ferrite and the roughly parallel lower one corresponding to arrests caused by martensite formation. This is consistent with the fact that higher undercoolings are needed to initiate martensitic transformations (Gilbert and Owen, 1962).

Wilson *et al.* (1969) carried out similar experiments on a high-purity Fe-5.1Ni wt.% alloy; they were able to show that the reason why the austenite sometimes transforms to massive ferrite and at other times to martensite is related to the surface roughness of specimens used. Electropolished specimens invariably transformed to martensite whereas those not electropolished transformed to massive ferrite. This suggests that the surface of the thin specimens helps the nucleation of massive ferrite, and Wilson *et al.* (1969) and Wayman (1965) have expressed concern about the use of the thin foil specimens, especially as far as  $M_s$  determinations are concerned. Wilson *et al.* also showed that massive ferrite has a dislocation density of about  $5 \times 10^{-9} \text{ cm}^{-2}$ , irrespective of the quench rate used, and that the dislocation structure is akin to a recovered structure.

The experiments discussed above all yielded just one thermal arrest during cooling from the  $\gamma$  phase field. Wilson and his co-workers (1970, 1984) have reported observing multiple thermal arrests in experiments on pure iron, Fe-Ni and Fe-Cr alloys. As usual, each thermal arrest could, at sufficiently high cooling rates, be associated with a characteristic plateau†. The observation of up to four arrests in a single experiment implies, according to Wilson, the existence of four different transformations in pure iron. The first two plateaux are associated with the formation of "equiaxed ferrite" and massive ferrite respectively, the difference between these arising during nucleation (Wilson, 1978); massive ferrite nuclei are assumed to be more highly strained compared with equiaxed ferrite nuclei, the reasoning being based on the observed high dislocation density of fully grown massive ferrite (Wilson *et al.*, 1969). In Wilson's (1978) interpretation, the two reactions thus follow separate 'C' curves in the TTT diagram, the plateau temperatures of the continuous cooling experiments being taken to correspond to the points on the TTT diagram where the nucleation rate is at a maximum. Christian (1979) has pointed out that with the parameters he uses, Wilson's interpretation predicts incredibly low nucleation rates, inconsistent with experimental data. More significantly, the model identifies the temperature corresponding to the minimum incubation time on the TTT curve (assumed to depend only on nucleation) with the plateau temperature concerned, and this is not correct because the reactions are all supposed to follow C curve kinetics. A 'C' curve necessarily implies that the temperature of maximum reaction rate must decrease with increasing cooling rate, so that the model (Wilson, 1978) does not in fact predict plateaux in plots of  $T_a$  vs. cooling rate. The reasons for the existence of such plateaux are therefore not clear; Bhattacharya *et al.* (1973) have suggested that the plateaux

†Morozov *et al.* (1971, 1972) have found many such plateaux during continuous cooling experiments on high-purity iron, although only a single thermal arrest seems to have been observed in any given experiment.

are artefacts of plotting, but Wilson (1978) showed that the plateaux exist irrespective of the method of plotting the results.

In a TTT diagram, the point corresponding to the fastest isothermal reaction rate on a given C curve is called the 'nose' of the C curve; Wilson's experiments imply that for pure iron (and its binary substitutional alloys), the noses of the C curve for 'equiaxed ferrite', massive ferrite, bainite and martensite occur at progressively shorter times since the cooling rate has to increase in the same order to detect these transformations.

Hillert (1975) has proposed a novel explanation of many of the characteristics of massive reactions in ferrous alloys based solely on growth considerations. His approach relies on the fact that all reported experiments have been conducted on alloys containing traces of interstitials as impurities. It is proposed that even in dilute binary Fe-C alloys, it is possible to obtain ferrite of the same composition as the parent austenite, while maintaining 'local equilibrium' at the interface†. Since  $x_1^{\gamma} \gg \bar{x}_1$ , there exists a narrow carbon concentration spike in the austenite ahead of the interface. With the constraint that  $x_1^{\beta} = x_1^{\gamma}$ , it is only possible to get composition invariant growth when the alloy is transformed within the  $\alpha$  phase field when  $f_1 = 1$  (since  $x_1^{\beta}$  is otherwise less than  $\bar{x}_1$ ), so that the model explains why massive transformations may not occur in the two-phase  $\alpha + \gamma$  phase field even though the  $T_0$  curve lies in this field.

Under these circumstances, the growth of massive ferrite can be expected to occur under mixed diffusion and interface-control, some of the free energy of transformation being dissipated in driving the diffusion of C in the  $\gamma$  ahead of the interface. This loss of free energy can be subtracted from the total driving force and the rate of interface motion obtained by substituting the residue into an equation for interface-controlled growth. The calculated interface velocity was found to initially increase sharply with decreasing temperature, the plot of temperature vs. decreasing growth rate having the form of a 'C' curve. If growth is considered to be the limiting factor in overall transformation kinetics, then this C curve is replicated in the TTT diagram for the alloy. The model therefore predicts the existence of a plateau (at the temperature corresponding to  $x_1^{\beta} = \bar{x}_1$ ) in the relevant 'C' curve of the TTT diagram and hence explains the first plateau in continuous cooling experiments.

The model also predicts that the transition from massive to martensitic transformation occurs at lower cooling rates with increasing carbon content, consistent of the work of Bibby and Parr (1964). However, Hillert found the calculated extent of the carbon concentration spike in the  $\gamma$  to be sometimes unrealistically small and when he took this into account, by ignoring the spike for the region  $z_{1,d} < 0.1$  nm, the transition was found to be independent of carbon concentration. As discussed earlier (in the context of local equilibrium  $\rightarrow$  paraequilibrium), the intuitive feeling that concentration spikes of extents small relative to atomic dimensions are unrealistic may not be justified.

Caretti and Bertorello (1983) recently proposed an alternative explanation for the variation of  $T_a$  with cooling rate, based on evidence (Perepezko and Massalski, 1975; Plichta *et al.*, 1978) that the nucleation time in massive transformations is larger than the growth time, so that it may be more reasonable to assume that the overall transformation kinetics depend mainly on nucleation considerations. They considered the initial sharp fall in the curve to correspond to nucleation occurring at grain boundary sites, while the first plateau begins to

†Local equilibrium is in this case taken to imply that  $x_1^{\beta} = x_1^{\gamma}$ , even though  $x_1^{\beta} = \bar{x}_1$ . The idea of composition invariant growth in a binary alloy, with local equilibrium at the interface can be shown to be thermodynamically incorrect, unless  $x_1^{\beta} = x_1^{\gamma} = \bar{x}_1$ , and this only happens when the alloy composition falls on the  $\alpha/\alpha + \gamma$  phase boundary. On the other hand, it is conceivable that a carbon concentration spike builds up in the  $\gamma$  at the interface, due to some initial transient, although the height of the spike may not equal  $x_1^{\beta}$ .

develop when the cooling rate is sufficiently large to allow massive ferrite nucleation within the bulk of the parent phase to dominate. The model does not seem to explain why  $T_a$  then becomes relatively insensitive to further increases in cooling rate, so giving rise to the characteristic first plateau. Nevertheless, Caretti and Bertorello provided interesting evidence to show that volume nucleation dominates over the plateau region. For several alloy systems, the undercooling ( $\Delta T$ ) below the equilibrium transformation temperature, obtained by extrapolating the plateau to zero cooling rate, was found to increase linearly with the solidification experiments where a similar correlation was ascribed to homogeneous nucleation.

#### 11. ORIENTATION RELATIONSHIP BETWEEN AUSTENITE AND FERRITE

An understanding of the crystallography of any transformation is important since the properties of interfaces depend on the relative dispositions of the crystals that they connect. The development of morphology also depends on crystallography since this determines the orientation dependence of the interface energy.

Perhaps the most interesting experimental observation in this context is that the orientation relationships that are found to develop during phase transformations are usually not random (Ryder and Pitsch, 1966; Ryder *et al.*, 1967; Christian, 1969). The frequency of occurrence of any particular orientation relation usually far exceeds the probability of obtaining it by simply taking two separate crystals and joining them up in an arbitrary way. This indicates that there are favoured orientation relationships, perhaps because it is these which allow best fit at the interface between the two crystals (Johnson *et al.*, 1975; Pitsch and Ryder, 1977). This would in turn reduce the interface energy and hence the activation energy for nucleation. Embryos which by chance happen to be orientated in this manner would find it relatively easy to grow into successful nuclei, giving rise to the non-random distribution mentioned earlier.

On the other hand, it could be the case that nuclei actually form by the homogeneous deformation of a small region of the parent lattice (Ryder and Pitsch, 1966) so that there is a co-ordinated movement of atoms during the nucleation process. The deformation which transforms the parent structure to that of the product (e.g. the Bain strain), would have to be of the kind which minimises strain energy. Of all possible ways of accomplishing the lattice change by homogeneous deformation, only a few might satisfy the minimum strain energy criterion—this would again lead to the observed non-random distribution of orientation relationships. It is a major phase transformations problem to determine which of these factors really determine the existence of reproducible orientation relations. The problem has further complications for diffusional transformations since the product phase grows by the unco-ordinated movements of atoms and its growth is consequently not limited to the grain in which it originally nucleated.

While the idea of a homogeneous deformation of the parent lattice leading to the nucleation of the product phase is quite general as far as the nature of the deformation is concerned, Ryder and Pitsch specifically proposed that a coherent nucleus forms as a small, thin platelet such that the plate plane, and one direction within that plane are unrotated (though not necessarily undistorted) by the homogeneous deformation. A pair of corresponding planes and a pair of corresponding directions within those planes remain parallel in the interface during nucleation. On taking the pure strain part of all such homogeneous deformations as the Bain strain, they found that the residual rigid body rotations were rather small, so that

all  $\gamma/\alpha$  orientation relationships should lie within some  $11^\circ$  of the Bain orientation†. The Kurdjumov–Sachs (1930) orientation relationship (i.e.  $\{111\}_\gamma \parallel \{011\}_\alpha$ , and  $\langle 01\bar{1}\rangle_\gamma \parallel \langle 11\bar{1}\rangle_\alpha$ ) and Nishiyama–Wasserman (1934) orientation relationship (i.e.  $\{111\}_\gamma \parallel \{011\}_\alpha$ , and  $\langle 01\bar{1}\rangle_\gamma$  about  $5.3^\circ$  from  $\langle 11\bar{1}\rangle_\alpha$  towards  $\langle 1\bar{1}1\rangle_\alpha$ ) both lie within the  $11^\circ$  region about the Bain orientation.

Ryder and Pitsch additionally suggested that for precipitates which nucleate homogeneously in the austenite, the unrotated plane and direction should be the closest-packed planes and directions respectively of the two lattices. Alternatively, if the precipitate nucleated heterogeneously at a grain boundary, then the unrotated plane should correspond to the plane of the grain boundary, and that this may not be a close-packed plane.

Arguments have been advanced (Aaronson *et al.*, 1976) which claim that nucleation involving the co-operative movement of atoms (as implied in the Ryder–Pitsch theory) is thermodynamically impossible at the low supersaturations where nucleation occurs, but these are necessarily based on weak assumptions about the nucleus shape, composition and stored energy.

King and Bell (1975) conducted a detailed study of the crystallography of allotriomorphic ferrite in a Fe–0.47C wt.% alloy isothermally transformed above the eutectoid temperature. In almost all the cases they analysed, the  $\alpha$  was found to possess an orientation relationship with at least one adjacent  $\gamma$  grain which approximated to the Kurdjumov–Sachs (KS) or Nishiyama–Wasserman (NW) orientation relationships. In fact, the range of orientations detected was more restricted than the  $11^\circ$  Bain region of Ryder and Pitsch. The orientations tended to cluster at and around the KS and to a lesser extent the NW relations. It was always possible to find a close-packed plane of  $\gamma$  which was within  $2^\circ$  of a closest-packed plane of the  $\alpha$ ; within these planes, a close-packed direction of the  $\gamma$  could always be found within some  $8^\circ$  of a similar direction in the  $\alpha$ .

King and Bell also found that over half of the  $\alpha$  particles examined had a KS/NW type of orientation relationship with both the adjacent  $\gamma$  grains. They showed that this is unexpected since for a random population of  $\gamma$  grain boundaries, about one in three might allow a  $\alpha$  orientation to be chosen which is within the Bain regions of both the adjacent matrix grains. The higher proportion observed was attributed to the presence of texture in the specimens studied, but such texture is likely to be present in most real materials and their results are consistent with the earlier qualitative observations of Aaronson (1962) and Hillert (1962) that  $\alpha$  allotriomorphs often develop into Widmanstätten ferrite on both sides of the grain boundary, given that Widmanstätten ferrite is a displacive transformation product and therefore is confined to the grain with which it has a systematic orientation relationship.

King and Bell (1974, 1976) also measured the orientation relationship between Widmanstätten ferrite and  $\gamma$  and obtained broadly similar results to their work on allotriomorphic ferrite.

It is difficult unambiguously to interpret the above work and to deduce a nucleation mechanism, even though the experimentally determined orientation relations lie within the expected range. Both interfacial energy minimisation and strain energy minimisation could lead to similar non-random distributions of orientation relations. In this respect, Crosky *et al.* (1980) did crystallographic experiments on the nucleation of FCC  $\alpha$ -brass rods from BCC brass, a problem which is the reverse of the  $\gamma \rightarrow \alpha$  transformation in iron. Rods nucleated near free surfaces were found to form with a crystallography which allowed their invariant-lines

†The Bain orientation follows from the nature of the Bain strain:  $\langle 100\rangle_\gamma \parallel \langle 110\rangle_\alpha$ ,  $\langle 001\rangle_\gamma \parallel \langle 001\rangle_\alpha$ . The Bain strain alone does not rotate any plane or direction by more than about  $11^\circ$ , so that any set of corresponding planes and directions can be made parallel after this strain by a rotation of not more than  $11^\circ$  (Crosky *et al.*, 1980).

to lie in the surface plane, indicating that nucleation is dominated by strain energy minimisation, consistent with the existence of co-ordinated atomic displacements during nucleation. They also showed that if interface energy minimisation controls nucleation then other surface nucleation events are expected but not found. Experiments like these may help towards resolving the factors which determine orientation relations in steels.

## 12. INTERPHASE PRECIPITATION

'Interphase precipitation' occurs during the diffusional growth of ferrite from metastable austenite and involves the formation of particles of a third phase at the  $\alpha/\gamma$  interface. The third phase may be cementite, alloy carbides or other phases† which have limited solubility in the austenite and ferrite lattices at the transformation temperature. The ferrite and the third phase do not grow co-operatively during transformation, as in the pearlite reaction or in discontinuous reactions. An example of interphase precipitation is illustrated in Fig. 14, which shows  $\text{Cr}_{23}\text{C}_6$  particles nucleated at the sessile part of the  $\gamma/\alpha$  interface during  $\alpha$  growth by a step mechanism. The carbide particles seem to grow while in contact with the austenite, growth terminating after the carbides become enclosed in ferrite following the passage of a trailing step. The low concentration of carbon in the ferrite then prevents further carbide growth.

Interphase precipitation was first recognised in alloy steels containing ternary additions of strong carbide forming elements (Gray and Yeo, 1968; Davenport *et al.*, 1968). Fine dispersions of alloy carbides were observed as regular rows of particles, all of which usually have the same crystallographic orientation in any given ferrite grain. Electron microscopy of partially transformed specimens revealed that the rows of carbides are actually parts of sheets of carbides in three dimensions, the carbides nucleating at  $\gamma/\alpha$  interfaces during transformation (Davenport and Honeycombe, 1971). The row-like appearance of such precipitation only becomes apparent during transmission electron microscopy (using thin foil specimens) if the planes on which the carbides precipitate are virtually parallel to the beam direction (Davenport and Honeycombe, 1971), particularly if the sheet spacings are small compared with the foil thickness.

Interphase precipitation is for the most part associated with the step mechanism of  $\alpha/\gamma$  interface motion (Fig. 14), the carbides precipitating on the stationary, immobile component of the interface (Campbell and Honeycombe, 1974) because the steps themselves move too rapidly to allow successful precipitate nuclei to develop (Honeycombe, 1976; Aaronson *et al.*, 1978).

Because the precipitates nucleate in contact with both the ferrite and austenite lattices, they tend to adopt a crystallographic orientation which allows good lattice matching with both phases, and this restricts the number of crystallographic variants of carbide that can form (Howell *et al.*, 1979). Tilman and Edmonds (1974) have found more than one variant of carbide due to interphase precipitation in Fe–Mo–C alloys, but the detailed three-phase crystallography has yet to be determined for this system.

Interphase precipitation is also found in cases where the  $\alpha/\gamma$  interface does not move by a step mechanism, but is displaced continuously (Ricks and Howell, 1982, 1983). In these

†The third phase may be cementite (observed in an impure commercial steel by Davenport and Becker, 1971, and in a high-purity Fe–C alloy by Balliger, 1977) or alloy carbides (or carbonitrides) such as VC (Davenport *et al.*, 1962), NbC (Gray and Yeo, 1968), TiC (Freeman, 1971),  $\text{Mo}_2\text{C}$  (Berry and Honeycombe, 1970),  $\text{Cr}_7\text{C}_3$  and  $\text{Cr}_{23}\text{C}_7$  (Mannerkoski, 1964; Campbell, 1971),  $\text{W}_2\text{C}$  (Davenport and Honeycombe, 1971),  $\text{M}_6\text{C}$  (Tilman and Edmonds, 1974). Interphase precipitation of Cu and Au particles has also been observed (Howell *et al.*, 1980; Ricks, 1979).

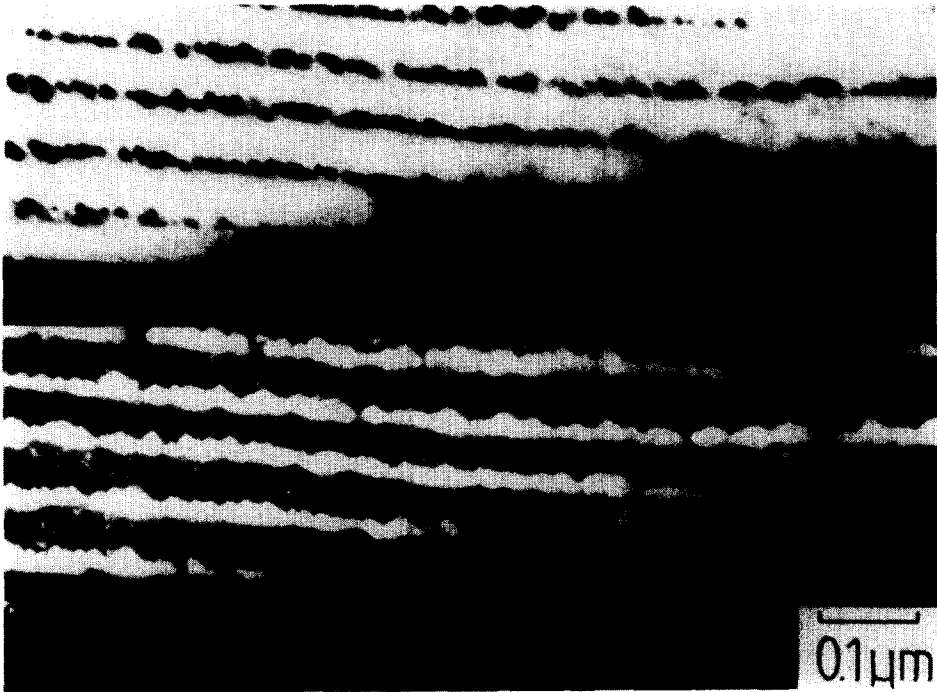


FIG. 14. Bright-field and  $\text{Cr}_{23}\text{C}_6$  corresponding dark-field transmission electron micrographs showing interphase carbide precipitation during the stepped growth of ferrite from austenite (Campbell, 1971).

circumstances, interphase precipitation acts to pin the  $\alpha/\gamma$  interface and the resulting precipitate dispersions in the  $\alpha$  can be random, or in the form of regular, non-planar sheets of carbides. In the former case, where random dispersions of carbides are formed, the  $\alpha/\gamma$  boundary migrates by bowing inbetween coarsely spaced carbide particles. If, on the other hand, the precipitation of carbide particles at the  $\alpha/\gamma$  interface is copious, and interface bowing becomes difficult, then a "quasi-ledge" mechanism operates (Fig. 15). The curved  $\alpha/\gamma$  interface becomes pinned by the finely spaced particles, but at some position where the particle spacing is locally large, an interface bulge develops and subsequently becomes pinned but is able to spread laterally, giving in effect a ledge mechanism even though the interface energy may not be orientation dependent.

### 13. CONCLUSIONS

Major advances have been made in our understanding of the diffusional formation of ferrite in iron and its alloys, and in our knowledge of diffusional transformations in general. The difference between morphology and mechanism is better understood and ferrite can be clearly discussed in the context of the numerous other transformations that occur in steels.

Irrespective of whether there is a composition change during transformation, the very nature of a diffusional reaction requires the unco-ordinated mixing up of atoms during interface motion. Diffusive mixing is responsible for the reconstruction of the parent lattice into that of the product, in a way which minimizes the strain energy of transformation. This

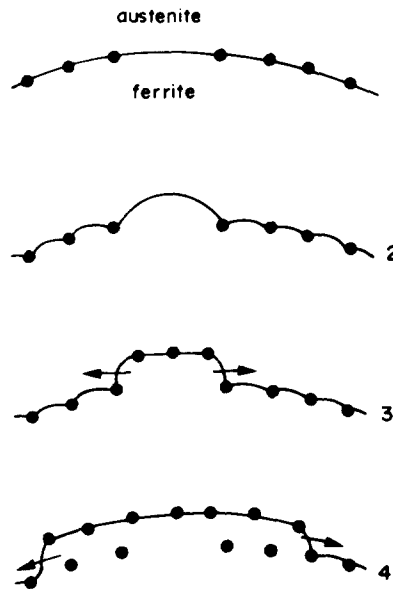


FIG. 15. Schematic diagram showing the operation of a quasi-ledge mechanism resulting in the production of curved rows of interphase precipitates (after Ricks and Howell, 1983). Finely spaced particles first pin the boundary. The boundary then develops a bulge where particle spacing is locally large, only to be re-pinned by further precipitation, so that the bulge is only free to move laterally, giving a quasi-ledge mechanism of growth.

reconstructive diffusion destroys any atomic correspondence between the parent and product phases and this is a major distinction between diffusional and displacive transformations.

Ferrite can under suitable conditions grow by a diffusional mechanism whatever the structure of the  $\alpha/\gamma$  interface. The mobility of the interface must however depend on its structure and often determines the mechanism of interface motion. These conclusions seem reasonable even though there is little evidence on the nature of the  $\alpha/\gamma$  interfaces responsible for the diffusional growth of ferrite.

Interface motion can occur by a step mechanism or by the continuous displacement of every element of the interface. The exact mechanism is determined by the orientation dependence of interface energy (and hence mobility) and by the driving force for interface motion. The rate at which an interface moves can be controlled by the diffusion of solute in the matrix ahead of the interface (diffusion-controlled), by the rate at which atoms transfer across the interface (interface-controlled) or by a mixture of the two processes (mixed-control).

The theory of diffusion-controlled growth is well advanced and sets out the possibilities of ferrite growth with local equilibrium or local paraequilibrium at the moving interface. It is currently not possible to theoretically decide which of these modes is favoured in a particular set of circumstances, and experimental evidence does not help since it is not in general sufficiently precise. The possible existence of solute-drag effects and interface pinning effects may further complicate the interpretation of experimental evidence.

The theory of interface-controlled growth is much less advanced and still relies on important assumptions about the relationship between interface velocity and driving force.

There is little experimental work on the interface-controlled growth of ferrite in steels. Massive ferrite may be an interface-controlled reaction although there are suggestions that its growth involves local equilibrium at the interface.

## APPENDIX

### 14. DIFFUSION-CONTROLLED GROWTH OF WIDMANSTÄTTEN FERRITE

Particle dimensions during diffusion-controlled growth vary parabolically with time when the extent of the diffusion field in the matrix increases with particle size. The growth rate thus decreases with time. The diffusion-controlled lengthening of plates or needles can however occur at a constant rate since solute can be partitioned to the sides of the plates or needles. The purpose of this appendix is to present a treatment of diffusion-controlled linear growth using Widmanstätten ferrite as an example, even though the formation of Widmanstätten ferrite is strictly not within the context of this review. The shape change accompanying Widmanstätten ferrite growth implies the existence of a glissile  $\alpha_w/\gamma$  interface and since carbon is partitioned during growth, the rate of growth can be expected to be controlled by the diffusion of carbon in the austenite ahead of the moving interface, even when the reaction occurs at a low homologous temperature. Iron and substitutional atoms do not diffuse during  $\alpha_w$  growth and there is no reconstructive diffusion during transformation.

#### 14.1. Theory of Diffusion-Controlled Plate Growth

Trivedi (1970) has given a solution for the problem of the diffusion-controlled growth of plates. The shape of the plates is taken to be that of a parabolic cylinder and is assumed to be constant throughout growth. The plate lengthening rate ( $V_1$ ) at a temperature  $T$  for steady-state growth is obtained by solving the equation:

$$f_1 = (\pi)^{0.5} \exp\{p\} \operatorname{erfc}\{p^{0.5}\} [1 + (r_c/r)f_1 S_2\{p\}], \quad (14.1)$$

where the Péclet number  $p$ , which is a dimensionless velocity, is given by

$$p = V_1 r / 2D_{11}. \quad (14.2)$$

The weighted-average diffusion coefficient  $D_{11}$  for carbon in austenite can be determined using eq. 5.10, with the integral evaluated over the range  $\bar{x}$  to  $x_r$ , where  $x_r$  is the carbon concentration in the austenite at the plate tip.  $x_r$  may significantly differ from the equilibrium carbon concentration  $x_1^{\gamma\alpha}$  because of the Gibbs–Thompson capillarity effect (Christian, 1975) which allows for the change in equilibrium concentration as a function of interface curvature;  $x_r$  decreases as interface curvature increases, and growth ceases at a critical plate tip radius  $r_c$  when  $x_r = \bar{x}_1$ . For a finite plate tip radius ( $r$ ),

$$x_r = x_1^{\gamma\alpha} [1 + (\Gamma/r)], \quad (14.3a)$$

where  $\Gamma$  is the capillarity constant (Christian, 1975) given by

$$\Gamma = (\sigma V_m / RT) [(1 - x_1^{\gamma\alpha}) / (x_1^{\gamma\gamma} - x_1^{\gamma\alpha})] / [1 + [d(\ln \Gamma_1) / d(\ln x_1^{\gamma\alpha})]] \quad (14.3b)$$

where  $\sigma$  = interface energy per unit area;  $\Gamma_1$  = activity coefficient of C in  $\gamma$ ; and  $V_m$  = molar volume of ferrite. This assumes that the  $\alpha$  composition is unaffected by capillarity, since  $x_1^{\gamma\gamma}$  is always very small. The function  $S_2\{p\}$  of eq. 14.1 depends on the Péclet number; it corrects for variation in composition due to changing curvature along the interface and has been numerically evaluated by Trivedi.

As pointed out earlier, Trivedi's solution for diffusion-controlled growth assumes a constant shape (parabolic cylinder), but the solution is not really shape-preserving. The capillarity effect implies that  $x_r$  varies over the surface of the parabolic cylinder, and this should lead to a deviation from the parabolic shape. Trivedi claims that the variation in  $x_r$  has a negligible effect provided the tip radius is greater than  $3r_c$ . Equation 14.1 on its own simply provides a relation between velocity and tip radius but does not allow these quantities to be fixed; additional theory is needed to enable the choice of a particular  $r$ , and hence to fix  $V_1$ . Small tip radii favour fast growth due to the point effect of diffusion, but this is opposed by the capillarity effect since the driving force for growth tends to zero as  $r \rightarrow r_c$ . Zener proposed that the plate should tend to adopt a tip radius which allows  $V_1$  to be maximised but there is not fundamental justification nor experimental evidence to support this hypothesis. Recent work (Glicksman *et al.*, 1976; Langer and Muller-Krumbhaar, 1978) on the dendritic growth of solid from liquid (formally an almost identical problem) has conclusively demonstrated that the dendrites do not attain a radius consistent with the Zener maximum velocity hypothesis, the actual tip radius being determined by a shape stability criterion. If these results can be extrapolated to solid-state transformations, then any calculated velocities would be less than those given by the Zener hypothesis.

In the absence of reliable data on plate tip radii, the Zener hypothesis provides an upper limit for  $V_1$ . A comparison with experimental data (Fig. 16) shows that experimental  $\alpha_w$  lengthening rates in Fe-C alloys always *exceed* corresponding maximum calculated lengthening rates; this discrepancy can only increase if the maximum velocity hypothesis is not valid, or if any appreciable part of the free energy is dissipated in interface processes. The shape of  $\alpha_w$  is not really that of a parabolic cylinder but is lath-like (Watson and McDougall, 1973). It is therefore useful to compare experimental data with needle lengthening rates, even though a needle shape is a poor representation of Widmanstätten ferrite, which has a definite habit plane. Trivedi has obtained a steady-state solution for the diffusion-controlled growth of paraboloids of revolution (i.e. needles):

$$f_1 = p \exp\{p\} Ei\{p\} [1 + (r_c/r)f_1 R_2\{p\}], \quad (14.4)$$

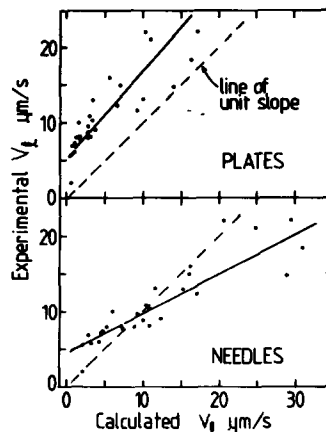


FIG. 16. Plots of experimental vs. calculated lengthening rates for Widmanstätten ferrite. The calculations are based on the maximum velocity hypothesis and the  $\alpha_w/\gamma$  interface energy is taken to be 0.2 J/mol. The details of the calculations are given by Bhadeshia (1985) but the experimental data are due to Hillert (1960), Townsend and Kirkaldy (1968) and Simonen *et al.* (1973).

where the function  $R_2\{p\}$  corrects for the variation in composition due to the changing curvature of the interface and has been numerically evaluated by Trivedi.  $r_c$  is twice as large as that for plates. A comparison of experimental data with maximum calculated needle lengthening rates is presented in Fig. 16; it is evident that the plate model is a somewhat better representation of  $\alpha_w$  lengthening, although neither of the models are perfect.

Finally, we note that Trivedi has also given a slightly more elaborate theory to take account of any free energy dissipated in interface processes. In this, a second set of functions ( $S_1\{p\}$  for plates and  $R_1\{p\}$  for needles) is introduced to allow for the variation in dissipation due to the changing orientation of the interface.

#### ACKNOWLEDGEMENTS

The author is grateful to Professor D. Hull for the provision of laboratory facilities at the University of Cambridge and to Professor J. W. Christian, Dr J. F. Knott and Professor T. B. Massalski for their stimulating comments and advice.

#### REFERENCES

- AARONSON, H. I. (1955) Symposium on the *Mechanism of Phase Transformations in Metals*, p. 47, Institute of Metals, London.
- AARONSON, H. I. (1962) *Decomposition of Austenite by Diffusional Processes* (eds V. F. Zackay and H. I. Aaronson) p. 387, Interscience, New York.
- AARONSON, H. I. (1969) *Mechanics of Phase Transformations in Crystalline Solids*, Monograph 13, p. 270, Institute of Metals, London.
- AARONSON, H. I. and DOMIAN, H. A. (1966) *TMS-AIME* **236**, 781.
- AARONSON, H. I., DOMIAN, H. A. and POUND, G. M. (1966) *TMS-AIME* **236**, 768.
- AARONSON, H. I., LAIRD, C. and KINSMAN, K. R. (1968) *Scr. Metall.* **2**, 259.
- AARONSON, H. I., LAIRD, C. and KINSMAN, K. R. (1970) *Phase Transformations*, p. 313, ASM, Metals Park, Ohio.
- AARONSON, H. I., DOOLEY, D. W. and RUSSELL, K. C. (1976) *Scr. Metall.* **10**, 607.
- AARONSON, H. I., PLICHTA, M. R., FERRANTI, G. W. and RUSSELL, K. C. (1978) *Metall. Trans. A* **9A**, 363.
- ABRAMOWITZ, M. and STEGUN, I. A. (1964) (eds) *Handbook of Mathematical Functions*, National Bureau of Standards, Washington.
- ACKERT, R. J. and PARR, J. G. (1971) *JISI* **209**, 912.
- ATKINSON, C. (1967) *Acta metall.* **15**, 1207.
- ATKINSON, C. (1968) *Acta metall.* **16**, 1019.
- ATKINSON, C. (1969) *TMS-AIME* **227**, 1255.
- ATKINSON, C. (1981) *Proc. R. Soc. (Lond.)* **A378**, 351.
- ATKINSON, C. (1982a) *Proc. R. Soc. (Lond.)* **A384**, 107.
- ATKINSON, C. (1982b) *J. appl. phys.* **53**, 5689.
- ATKINSON, C., AARON, H. B., KINSMAN, K. R. and AARONSON, H. I. (1973a) *Metall. Trans.* **4**, 783.
- ATKINSON, C., KINSMAN, K. R. and AARONSON, H. I. (1973b) *Scr. Metall.* **7**, 1105.
- BAIN, E. C. (1924) *Trans. AIMME* **70**, 25.
- BAKER, J. C. and CAHN, J. W. (1969) *Acta metall.* **17**, 575.
- BAKER, J. C. and CAHN, J. W. (1971) *Solidification*, p. 23, ASM, Ohio.
- BALLINGER, N. K. (1977) PhD Thesis, University of Cambridge.
- BERRY, F. G. and HONEYCOMBE, R. W. K. (1970) *Metall. Trans.* **1**, 3279.
- BHADESHIA, H. K. D. H. (1981) *Metal Sci.* **15**, 477.
- BHADESHIA, H. K. D. H. (1981b) *Acta metall.* **29**, 1117.
- BHADESHIA, H. K. D. H. (1982a) *J. Phys. Colloque C4* **43**, 437.
- BHADESHIA, H. K. D. H. (1982b) *Phys. Stat. Sol. (a)* **69**, 745.
- BHADESHIA, H. K. D. H. (1983a) *J. Mater. Sci.*, **18**, 1473.
- BHADESHIA, H. K. D. H. (1983b) *Scripta Metall.* **17**, 857.
- BHADESHIA, H. K. D. H. (1985) *Mater. Sci. Tech.* **1**, 497.
- BHADESHIA, H. K. D. H. and EDMONDS, D. V. (1980) *Acta metall.* **28**, 1265.
- BHATTACHARYA, S. K., PEREPECKO, J. H. and MASSALSKI, T. B. (1983) *Scr. Metall.* **7**, 485.
- BIBBY, M. J. and PARR, J. G. (1964) *JISI* **202**, 100.
- BOLZE, G., COATES, D. E. and KIRKALDY, J. S. (1969) *Trans. ASM* **62**, 794.

- BOSWELL, P., KINSMAN, K. R. and AARONSON, H. I. (1968) Unpublished work, Ford Motor Co., Dearborn, Michigan.
- BRADLEY, J. R. and AARONSON, H. I. (1977) *Metall. Trans. A* **8A**, 317.
- BRADLEY, J. R. and AARONSON, H. I. (1981a) *Metall. Trans. A* **12A**, 1729.
- BRADLEY, J. R., SHIFLET, G. J. and AARONSON, H. I. (1981b) Proc. Int. Conf. on *Solid→Solid Phase Transformations*, p. 819, *TMS-AIME*, Warrendale, Pennsylvania.
- BROWN, L. C. and KIRKALDY, J. S. (1964) *TMS-AIME* **230**, 223.
- BURTON, W. K., CABRERA, N. and FRANK, F. C. (1950) *Phil. Trans. R. Soc. (Lond.)* **A243**, 299.
- CAHN, J. W. (1960) *Acta metall.* **8**, 556.
- CAHN, J. W. (1961) *Acta metall.* **9**, 795.
- CAHN, J. W. (1962a) *Acta metall.* **10**, 179.
- CAHN, J. W. (1962b) *Acta metall.* **10**, 789.
- CAHN, J. W. (1980) *Bull. Alloy Phase Diagrams* **1**, 27.
- CAHN, J. W. and KALONJI, G. (1981) Proc. Int. Conf. on *Solid→Solid Phase Transformations*, p. 3, *TMS-AIME*, Warrendale, Pennsylvania.
- CAHN, J. W., HILLIG, and SEARS, G. W. (1964) *Acta metall.* **12**, 1421.
- CAMPBELL, K. (1971) PhD Thesis, University of Cambridge.
- CAMPBELL, K. and HONEYCOMBE, R. W. K. (1974) *Metal Sci.* **8**, 197.
- CARETTI, J. C. and BERTORELLO, H. R. (1983) *Acta metall.* **31**, 325.
- CHRISTIAN, J. W. (1965) *Physical Properties of Martensite and Bainite*, Spec. Rep. 93, p. 1, Iron and Steel Institute, London.
- CHRISTIAN, J. W. (1969) *Mechanism of Phase Transformations in Crystalline Solids*, Monograph 13, p. 129, Institute of Metals, London.
- CHRISTIAN, J. W. (1975) *Theory of Transformations in Metals and Alloys*, 2nd edn, Pt. 1, Pergamon Press, Oxford.
- CHRISTIAN, J. W. (1979) *Phase Transformations*, York Conference, p. 1, Institution of Metallurgists, London.
- CHRISTIAN, J. W. and CROCKER, A. G. (1980) *Dislocations in Solids*, (ed. F. R. N. Nabarro) Vol. 3, North-Holland, Amsterdam.
- CHRISTIAN, J. W. and EDMONDS, D. V. (1983) *Phase Transformations in Ferrous Alloys* (ed. A. R. Marder and J. I. Goldstein) p. 293, *TMS-AIME*, Warrendale, Pennsylvania.
- COATES, D. E. (1973a) *Metall. Trans.* **4**, 395.
- COATES, D. E. (1973b) *Metall. Trans.* **4**, 1077.
- COATES, D. E. (1973c) *Metall. Trans.* **4**, 2313.
- CRANK, J. (1975) *The Mathematics of Diffusion*, 2nd edn, p. 209, Clarendon Press, Oxford.
- CROSKY, A., MCDUGALL, P. G. and BOWLES, J. S. (1980) *Acta metall.* **28**, 1495.
- DARKEN, L. S. (1948) *TMS-AIME* **175**, 184.
- DARKEN, L. S. (1949) *TMS-AIME* **180**, 430.
- DARKEN, L. S. and GURRY, R. W. (1953) *Physical Chemistry of Metals*, pp. 146–148, McGraw Hill, New York.
- DAVENPORT, A. T. and BECKER, P. C. (1971) *Metall. Trans.* **2**, 2962.
- DAVENPORT, A. T. and HONEYCOMBE, R. W. K. (1971) *Proc. R. Soc.* **A322**, 191.
- DAVENPORT, A. T., BERRY, F. G. and HONEYCOMBE, R. W. K. (1968) *Metal Sci.* **2**, 104.
- DE HOFF, R. T. (1981) Proc. Int. Conf. on *Solid→Solid Phase Transformations*, p. 503, *TMS-AIME*, Warrendale, Pennsylvania.
- DUBÉ, C. A. (1948) PhD Thesis, Carnegie Inst. of Technology.
- DUNN, W. and MCELLELLAN, R. B. (1970) *Metall. Trans.* **1**, 1263.
- EHRENFEST, P. (1933) *Proc. Acad. Sci. Amsterdam* **36**, 153.
- EINSTEIN, A. (1905) *Ann. Phys.* **17**, 549.
- EONMOTO, M., AARONSON, H. I., AVILA, J. and ATKINSON, C. (1981) Proc. Int. Conf. on *Solid→Solid Phase Transformations*, p. 561, *TMS-AIME*, Warrendale, Pennsylvania.
- FICK, A. (1855) *Ann. Phys.* **170**, 59.
- FRANK, F. C. (1950) *Proc. R. Soc.* **A201**, 586.
- FREEMAN, S. (1971) *The Effect of Second Phase Particles on the Mechanical Properties of Steel*, p. 152, ISI, London.
- FRIDBERG, J., TORNDHAL L. and HILLERT, M. (1969) *Jernkontorets Ann.* **153**, 263.
- GIBBS, J. W. (1961) *The Scientific Papers of J. W. Gibbs*, p. 57, Dover Publications, New York.
- GILBERT, A. and OWEN, W. S. (1962) *Acta metall.* **10**, 45.
- GILMOUR, J. B., PURDY, G. R. and KIRKALDY, J. S. (1972a) *Metall. Trans.* **3**, 1455.
- GILMOUR, J. B., PURDY, G. R. and KIRKALDY, J. S. (1972b) *Metall. Trans.* **3**, 3213.
- GJOSTEIN, N. A., DOMIAN, H. A., AARONSON, H. I. and EICHEN, E. (1966) *Acta Metall.* **14**, 1637.
- GLICKSMAN, M. E., SCHAEFER, R. J. and AYRES, J. D. (1976) *Metall. Trans. A* **7A**, 1747.
- GOKHALE, A. M. (1984) *Metall. Trans. A.* **15A**, 391.
- GOLDSTEIN, J. I. and RANDICH, E. (1977) *Metall. Trans. A* **8A**, 105.
- GOMERSALL, D. W. and PARR, J. G. (1965) *JISI* **203**, 275.
- GRAY, J. M. and YEO, R. B. G. (1968) *Trans. ASM* **61**, 255.
- HARTLEY, G. S. (1931) *Trans. Faraday Soc.* **27**, 10.
- HICKLEY, C. M. and WOODHEAD, J. (1954) *JISI* **176**, 129.

- HILLERT, M. (1951) *Jernkontorets Ann.* **135**, 403.
- HILLERT, M. (1953) Internal Report, Swedish Inst. Met. Res.
- HILLERT, M. (1960) *Growth of Ferrite, Bainite and Martensite*, Internal report, Swedish Inst. for Metals Research.
- HILLERT, M. (1962) *Decomposition of Austenite by Diffusional Processes* (eds V. F. Zackay and H. I. Aaronson) p. 197, Interscience, New York.
- HILLERT, M. (1969) *Mechanism of Phase Transformations in Crystalline Solids*, Monograph 13, p. 231, Institute of Metals, London.
- HILLERT, M. (1975) *Metall. Trans. A* **6A**, 5.
- HILLERT, M. (1981) Proc. Int. Conf. on *Solid→Solid Phase Transformations*, p. 789, TMS-AIME, Warrendale, Pennsylvania.
- HILLERT, M. and SUNDMAN B. (1976) *Acta metall.* **24**, 731.
- HONEYCOMBE, R. W. K. (1976) *Metall. Trans. A* **7A**, 915.
- HORVAY, G. and CAHN, J. W. (1961) *Acta metall.* **9**, 695.
- HOWELL, P. R., SOUTHWICK, P. D. and RICKS, R. A. (1979a) *J. Microsc.* **116**, 151.
- HOWELL, P. R., BEE, J. V. and HONEYCOMBE, R. W. K. (1979b) *Metall. Trans. A* **10A**, 1213.
- HOWELL, P. R., RICKS, R. A., BEE, J. V. and HONEYCOMBE, R. W. K. (1980) *Phil. Mag. A* **41**, 165.
- HOWELL, P. R., SOUTHWICK, P. D., ECOB, R. C. and RICKS, R. A. (1981) Proc. Int. Conf. on *Solid→Solid Phase Transformations*, p. 591, TMS-AIME, Warrendale, Pennsylvania.
- HULTGREN, A. (1951) *Jernkontorets Ann.* **135**, 403.
- JOHNSON, W. C., WHITE, C. L., MARTH, P. E., RUF, P. K., TUOMINEN, S. M., WADE, K. D., RUSSELL, K. C. and AARONSON, H. I. (1975) *Metall. Trans. A* **6**, 911.
- JONES, G. J. and TRIVEDI, R. K. (1971) *J. appl. Phys.* **42**, 4299.
- JONES, G. J. and TRIVEDI, R. K. (1975) *J. Cryst. Growth* **29**, 155.
- KARLYN, D. A., CAHN, J. W. and COHEN, M. (1969) *TMS-AIME* **245**, 197.
- KAUFMAN, L., RADCLIFFE, S. V. and COHEN, M. (1962) *Decomposition of Austenite by Diffusional Processes* (eds V. F. Zackay and H. I. Aaronson) p. 313, Interscience, New York.
- KING, A. D. and BELL, T. (1974) *Metal Sci.* **8**, 253.
- KING, A. D. and BELL, T. (1975) *Metall. Trans. A* **6A**, 1419.
- KING, A. D. and BELL, T. (1976) *Metallography* **9**, 397.
- KINSMAN, K. R. and AARONSON, H. I. (1967) *Transformation and Hardenability in Steels*, p. 39, Climax Moly, Ann Arbor, Michigan.
- KINSMAN, K. R. and AARONSON, H. I. (1973) *Metall. Trans.* **4**, 959.
- KIRKALDY, J. S. (1958) *Can. J. Phys.* **36**, 907.
- KIRKALDY, J. S. (1959) *Can. J. Phys.* **37**, 30.
- KIRKALDY, J. S. (1962) *Decomposition of Austenite by Diffusional Processes* (eds V. F. Zackay and H. I. Aaronson) p. 387, Interscience, New York.
- KIRKALDY, J. S. (1970) *Adv. Mater. Res.* **4**, 55.
- KIRKALDY, J. S. and BAGANIS, E. A. (1978) *Metall. Trans. A* **9A**, 495.
- KIRKALDY, J. S. and PURDY, G. R. (1962) *Can. J. Phys.* **40**, 208.
- KIRKENDALL, E. O. (1942) *Trans. Am. Inst. Min. metall. Engrs* **147**, 104.
- KURDJUMOV, G. and SACHS, G. (1930) *Z. Phys.* **64**, 325.
- LANGER, J. S. and MULLER-KRUMBHAAR, H. (1978) *Acta metall.* **26**, 1681.
- LANGER, J. S. and MULLER-KRUMBHAAR, H. (1978) *Acta metall.* **26**, 1689.
- LUEKE, K. and DETERT, K. (1957) *Acta metall.* **5**, 628.
- MACHLIN, E. S. (1953) *Trans. Am. Inst. Min. metall. Engrs* **197**, 437.
- MANNERKOSKI, M. (1964) *Acta polytech. scand.* Ch. 26.
- MASSALSKI, T. B. (1958) *Acta metall.* **6**, 243.
- MASSALSKI, T. B. (1970) *Phase Transformations*, p. 433, ASM, Metals Park, Ohio.
- MASSALSKI, T. B. (1984) *Metall. Trans. A* **15A**, 421.
- MAZANEC, K. and CADEK, J. (1958) *Revue Métall.* **212**, 501.
- MCLELLAN, R. B. and DUNN, W. (1969) *J. phys. Chem. Solids* **30**, 2631.
- MEHL, R. F. and DUBÉ, C. A. (1951) *Phase Transformations in Solids*, p. 545, John Wiley, New York.
- MENNON, E. S. K., PLICHTA, M. R. and AARONSON, H. I. (1983) *Scr. Metall.* **17**, 1455.
- MILLER, D. G. (1960) *Chem. Rev.* **60**, 15.
- MOROZOV, O. P., MIRZAYEV, D. A. and SHTEYNBERG, M. M. (1971) *Fiz. Metall. Metalloved.* **32**, No. 6, 1290.
- MOROZOV, O. P., MIRZAYEV, D. A. and SHTEYNBERG, M. M. (1972) *Fiz. Metall. Metalloved.* **34**, No. 4 795.
- MULLER-KRUMBHAAR, H. and LANGER, J. S. (1978) *Acta metall.* **26**, 1708.
- NISHIYAMA, Z. (1934) *Sci. Rep. Tohoku Univ.* **23**, 638.
- NOLFI, F. V., SHEWMON, P. G. and FOSTER, J. S. (1969) *TMS-AIME* **245**, 1427.
- ONSAGER, L. (1931) *Phys. Rev.* **37**, 405; (1931) **38**, 2265.
- ONSAGER, L. (1945-46) *Ann. N.Y. Acad. Sci.* **46**, 241.
- PARR, J. G. (1967) *JISI* **205**, 426.
- PASCOVER, J. S. and RADCLIFFE, S. V. (1968) *TMS-AIME* **242**, 673.
- PEREPEZKO, J. M. and MASSALSKI, T. B. (1975) *Acta metall.* **23**, 621.

- PHILIP, J. R. (1960a) *Aust. J. Phys.* **13**, 1.  
PHILIP, J. R. (1960b) *Aust. J. Phys.* **13**, 13.  
PHILIP, J. R. (1969) *Adv. Hydrosci.* **5**, 215.  
PITSCH, W. and RYDER, P. L. (1977) *Scr. Metall.* **11**, 431.  
PLICHTA, M. R. and AARONSON, H. I. (1980) *Acta metall.* **28**, 1041.  
PLICHTA, M. R., PEREPEZKO, J. H., AARONSON, H. I. and LANGE, W. F. (1980) *Acta metall.* **28**, 1031.  
PURDY, G. R. (1978) *Acta metall.* **26**, 487.  
PURDY, G. R. and KIRKALDY, J. S. (1963) *TMS-AIME* **227**, 1255.  
PURDY, G. R., WEICHERT, D. H. and KIRKALDY, J. S. (1964) *TMS-AIME* **230**, 1025.  
RANDICH, E. and GOLDSTEIN, J. I. (1975) *Metall. Trans. A* **6A**, 1553.  
RICKS, R. A. (1979) PhD Thesis, University of Cambridge.  
RICKS, R. A. and HOWELL, P. R. (1982) *Metal Sci.* **16**, 317.  
RICKS, R. A. and HOWELL, P. R. (1983) *Acta Metall.* **31**, 853.  
RIGSBEE, J. M. (1979) Proc. Int. Conf. on *Martensitic Transformations*, p. 381, M.I.T., Boston.  
ROBERTS, M. J. (1970) *Metall. Trans.* **1**, 3287.  
ROMIG, A. D. and SALZBRENNER, R. (1981) Proc. Int. Conf. on *Solid→Solid Phase Transformations*, p. 849, TMS-AIME, Warrendale, Pennsylvania.  
ROMIG, A. D. and SALZBRENNER, R. (1982) *Scr. Metall.* **16**, 83.  
ROSENTHAL, D. (1946) *Trans. ASME* **68**, 849.  
RUDBERG, E. (1952) *Jernkontorets Ann.* **136**, 91.  
RYDER, P. L. and PITSCH, W. (1966) *Acta metall.* **14**, 1437.  
RYDER, P. L., PITSCH, W. and MEHL, R. F. (1967) *Acta metall.* **15**, 1431.  
SAHAY, S. K. (1985) Unpublished work, University of Cambridge.  
SHARMA, R. C. and PURDY, G. R. (1973) *Metall. Trans.* **4**, 2303.  
SHEWMON, P. G. (1965) *TMS-AIME* **233**, 419.  
SHIFLET, G. J., AARONSON, H. I. and BRADLEY, J. R. (1981) *Metall. Trans. A* **12A**, 1743.  
SILLER, R. H. and MCLELLAN, R. B. (1969) *TMS-AIME* **245**, 697.  
SILLER, R. H. and MCLELLAN, R. B. (1970) *Metall. Trans.* **1**, 985.  
SIMONEN, E. P., AARONSON, H. I. and TRIVEDI, R. (1973) *Metall. Trans.* **4**, 1239.  
SMIDODA, K., GOTTSCHALK, C. and GLEITER, H. (1978) *Acta metall.* **26**, 1833.  
SMIDODA, K., GOTTSCHALK, C. and GLEITER, H. (1979) *Metal Sci.* **13**, 146.  
SMITH, R. P. (1946) *J. Am. Chem. Soc.* **68**, 1163.  
SMITH, R. P. (1953) *Acta metall.* **1**, 578.  
SWANSON, W. D. and PARR, J. G. (1964) *JISI* **202**, 104.  
TANZILLI, R. A. and HECKEL, R. W. (1968) *TMS-AIME* **242**, 2313.  
TILMAN, C. J. and EDMONDS, D. V. (1974) *Metals Tech.* **1**, 456.  
TOWNSEND, R. D. and KIRKALDY, J. S. (1968) *Trans. ASM* **61**, 605.  
TRIVEDI, R. (1970) *Metall. Trans.* **1**, 921.  
TRIVEDI, R. and POUND, G. M. (1967) *J. appl. Phys.* **38**, 3569.  
TURNBULL, D. (1950) *J. appl. Phys.* **21**, 1022.  
TURNBULL, D. and HOFFMAN, R. E. (1954) *Acta metall.* **2**, 419.  
UHRENIUS, B. (1978) *Hardenability Concepts with Applications to Steel* (eds D. V. Doane and J. S. Kirkaldy) p. 28, TMS-AIME.  
WAGNER, C. (1952) *Thermodynamics of Alloys*, p. 53, Addison-Wesley, Reading, Mass.  
WALLBRIDGE, J. M. and PARR, J. G. (1966) *JISI* **204**, 119.  
WATSON, J. D. and MCDUGALL, P. G. (1973) *Acta metall.* **21**, 961.  
WAYMAN, C. (1965) Spec. Rep. 93, p. 37, Iron and Steel Institute, London.  
WELLS, C., BATZ, W. and MEHL, R. F. (1950) *TMS-AIME* **188**, 533.  
WILSON, E. A. (1970) *Scr. Metall.* **4**, 309.  
WILSON, E. A. (1984) *Metal Sci.* **18**, 471.  
WILSON, T. L., JACKSON, J. K. and MINER, R. E. (1969) *TMS-AIME* **245**, 2185.  
ZENER, C. (1949) *J. appl. Phys.* **20**, 950.